PHYSICAL AND FUNCTIONAL INTERACTION OF p53 and p110α and IMPLICATIONS IN OVARIAN CARCINOGENESIS

By

AREZOO ASTANEHE

B.Sc., The University of British Columbia, 2002

A THESIS SUBMITTED IN PARTIAL FULFILMENT OF THE REQUIREMENTS FOR THE DEGREE OF

MASTER OF SCIENCE

In

THE FACULTY OF GRADUATE STUDIES

(Reproductive and Developmental Sciences)

THE UNIVERSITY OF BRITISH COLUMBIA

July 2005

ABSTRACT

In approximately 40% of ovarian cancers, PIK3CA, which encodes the p110α catalytic subunit of phosphatidylinositol 3-kinase (PI3K) is amplified. This amplification correlates with increased PIK3CA transcription, p110α protein expression, and PI3K activity. Moreover, PIK3CA is implicated as an oncogene in ovarian cancers. Another common mutation in ovarian cancer leads to loss of p53 function. Alterations to p53 are known to be involved in tumour development and progression. Previous studies have shown that in benign cells, the p53 and PI3K pathways are connected through the regulation of PTEN by p53. Therefore, in the presence of p53, PTEN levels increase and exert their effect through decreasing P-AKT levels, and thereby pro-survival activities. In addition, it has been suggested that in cancer cells, p53 down-regulates the pro-survival pathway, independent of PTEN, by negatively regulating p110α levels. However, it has not been shown whether the p53 effect on p110α levels is direct or indirect and whether this interaction exists in benign cells. Our studies show, for the first time, a direct relationship between p53 and PI3K pathways. We used temperature sensitive cells, in which p53 function was regulated through the shift in temperature. We showed that p53 negatively regulates PIK3CA transcript and p110α levels through direct binding to the PIK3CA promoter. Moreover, we determined that the regulation of p110α levels by p53 is also present in ovarian cancer cells where overexpression of p53 significantly reduced p110α levels. In addition, for the first time, we identified two alternate promoters (promoter1a and promoter1b) upstream of two alternate first exons (exon1a and exon1b) that transcribe into two alternate transcripts with different 5' untranslated regions (5' UTRs). Our results determined direct binding of p53 to PIK3CA promoter1a, and studies to determine whether this direct binding is responsible for the suppression of the promoter and the down-regulation of PIK3CA transcript and p110α levels are currently in progress. Our studies suggest that the loss of p53 in ovarian

cancers may result in loss of transcription suppression of PIK3CA and therefore increased p110α levels and PI3K activity, which may in turn lead to increase in proliferation and resistance to apoptosis.

TABLE OF CONTENTS

LIST OF TABLES

LIST OF FIGURES

LIST OF ABBREVIATION

ATM	Ataxia Telangiectasia Mutated
α	Alpha
°C	Degree Celsius
4EBP1	4E Binding Protein 1
5' UTR	5 Prime Untranslated Region
A	Adenine
AAP	Abridged Anchor Primer
ANOVA	Analysis Of Variance between groups
AUAP	Abridged Universal Amplification Primer
BLAT	BLAST-Like Alignment Tool
BRCA	Breast Cancer gene
BSA	Bovine Serum Albumin
C	Cytosine
cDNA	Complementary Deoxyribose Nucleic Acid
ChIP	Chromatin Immunoprecipitation
CO2	Carbon Dioxide
DMEM	Dulbecco's Modified Eagle Medium
DNA	Deoxyribose Nucleic Acid
DNK-PK	double-stranded DNA-dependent Protein Kinase
dNTP	Deoxyribosenucleotide Triphosphate
EGF	Epidermal Growth Factor
EGFR	Epidermal Growth Factor Receptor
EOC	Epithelial Ovarian Carcinoma
EST	Expressed Sequence Tag
FAK	Focal Adhesion Kinase
FBS	Fetal Bovine Serum
G	Guanine
GAPDH	Glyceraldehyde 3-Phsophate Dehydrogenase
GFP	Green Fluorescent Protein
GSP1	Gene Specific Primer 1
GSP2	Gene Specific Primer 2
GSP3	Gene Specific Primer 3
GTP	Guanosine Triphosphate
HA	Haemagglutinin
HEK	Human Embryonic Kidney
HPV	Human Papilloma virus
HRP	Horseradish Peroxidase
hTERT	Human Telomerase Reverse Transcriptase
IGF-IR	Insulin-like Growth Factor-I Receptor
ILK	Integrin Linked Kinase
IOSE	Immortalized Ovarian Surface Epithelium
IRS-1	Insulin Receptor Substrate-1
iSH2	Inter-Src Homology 2

MAPKAP kinase-2	Mitogen-Activated Protein Kinase-Activated Protein Kinase-2
MDM-2	Mouse Double Minute-2
MK2	Mitogen-activated protein kinase-activated protein Kinase-2
mRNA	Messenger Ribose Nucleic Acid
Myr	Myristoylated
NES	Nuclear Export Signal
NGS	Normal Goat Serum
NLS	Nuclear Localization Signal
Non-ts	Non-Temperature Sensitive
OSE	Ovarian Surface Epithelium
OSEC2	Ovarian Surface Epithelium Colony 2
p85BD	P85 Binding Domain
P-AKT	Phosphorylated AKT
PBS	Phosphate Buffered Saline
PC	Post Crisis
PDE3B	Phosphodiesterase 3B
PDK	Phosphoinositide Dependent Kinase
PH	Pleckstrin Homology
PI3K	Phosphatidylinositol-3-Kinase
PIK3CA	Phosphatidylinositol-3-Kinase Catalytic Alpha
PKB	Protein Kinase B
PKCα	Protein Kinase C Alpha
PKCβ	Protein Kinase C Beta
pRb	Protein Retinoblastoma
PtdIn	Phosphatidylinositol
PtdIns(3,4,5)P_3	Phosphatidyl Inositol (3, 4, 5) Tri-Phosphate
PtdIns(4,5)P_2	Phosphatidyl Inositol (4, 5) Bis-Phosphate
PTEN	Phosphatase and Tensin Homolog
Pu	Purine
pY	Phosphorylated Tyrosine
Pyr	Pyrimidine
RACE	Rapid Amplification of cDNA Ends
RBD	Ras Binding Domain
RNA	Ribose Nucleic Acid
rRNA	Ribosomal Ribose Nucleic Acid
RT-PCR	Reverse Transcriptase-Polymerase Chain Reaction
S473	Serine 473
SDS-PAGE	Sodium Dodecyl Sulphate-Polyacrylamide Gel Electrophoresis
SELEX	Systematic Evolution of Ligands by Exponential Enrichment
SH2	Src-Homology 2
SH3	Src-Homology 3
SV40 T Ag	Simian Virus 40 Large T Antigen
SV40 t Ag	Simian Virus 40 Small t Antigen
T	Thymine
T308	Threonine 308

Tag	**Large T Antigen**
T-AKT	**Total AKT**
TBP	**TATA Box Binding Protein**
TBS	**Tris Buffered Saline**
TdT	**Terminal Deoxynucleotidyl Transferase**
Temp	**Temperature**
Ts	**Temperature Sensitive**
UCSC	**University of California Santa Cruz**
μ	**Micro**
WT	**Wild-type**

PREAMBLE

This thesis comprises a main section discussing the main hypothesis, which looks at functional and physical interactions of p53 and PI3K. Appendix 1 includes results that were obtained during the first year of my master's studies looking at the role of PIK3CA as an oncogene. Appendix 2 outlines a side project that resulted in the establishment of a permanent cell line.

ACKNOWLEDGEMENTS

My deepest gratitude and appreciation goes to my supervisor, Dr. Nelly Auersperg. I would like to offer my appreciation to Michelle Woo and Takayo Ota for their kindness and constant support during the past two years. My special thanks goes to Clara Salamanca, Sarah Maines-Bandiera and Roshni Nair for all their help. I would like to thank my committee members and chair, Dr. Sandra Dunn, Dr. Calvin Roskelley, and Dr. Keith Choi. My sincere thanks go to Dr. Sandra Dunn and Dr. Wyeth Wasserman for critical reading of my thesis. A special thank you goes to Dr. Wyeth Wasserman and Dave Arenillas for helping me with the promoter analysis. I could not have achieved this without your help. I would like to thank Dr. Barry Davies for providing us with the OSEC2 cells. I also would like to thank Dr. Gordon Mills for providing us with the AKT-PH-GFP constructs. I would like to show my appreciation to Dr. Peter Schlosshauer for going through so much trouble in order to send us the ovarian tissue section. I would also like to acknowledge Dr. David Huntsman and Janine Senz for their kindness and for allowing me to use their reagents and instruments for real-time PCR. I would also like to thank the BC Research Institute for the graduate studentship. Last but certainly not least, I would like to thank my family for their constant support.

CHAPTER 1:

INTRODUCTION

1.1 Epithelial Ovarian Carcinoma

Ovarian cancer is the fifth most common cause of death from cancer among Canadian women, and the leading cause of death from gynaecological malignancies. The incidence rate of ovarian cancer is one ninth of that of breast cancer, however, the death rate from breast cancer is only 3.5 times greater than that of ovarian cancer (Canadian Cancer Statistics, 2005). Symptoms of ovarian cancers generally appear after the cancers have spread, and screening tests are available only for the detection of advanced cases and for patient follow-ups. Therefore, more than 75% of ovarian cancers are discovered in late stages when disease is spread beyond the pelvis (Gordon et al., 2002). However, when women are diagnosed with an early stage of ovarian cancer, the survival rate is close to 90% (Wong and Auersperg, 2003). Introduction of cisplatin and paclitaxel therapy has made some improvements in the duration of survival. However, success in the treatment of women with advanced, recurrent or persistent ovarian cancer has remained largely unchanged (Dunton, 1997; Harries and Gore, 2002a; Harries and Gore, 2002b; Parmar et al., 2003). To improve the survival outcome of women affected by ovarian cancer, it is critical to detect disease at earlier stages. In order to develop effective therapies and to detect disease at an early stage, improvements in our understanding of the processes leading to the initiation and progression of ovarian cancer are required.

Over 85% of human ovarian cancers are epithelial ovarian carcinomas (EOC). Based on histological resemblance to normal tissues, EOC is classified into several subtypes including serous (most common), endometrioid, mucinous, clear cell, and transitional cell. These EOC are believed to arise in the ovarian surface epithelium (OSE). OSE, a single layer of squamous-to-

cuboidal epithelium, is a simple mesothelium that covers the outer surface of the ovary. The remainder of the ovarian carcinoma cases originates from the stroma or germ cells (Auersperg et al., 2001). Ovarian tumours in most species other than human arise in stromal components of the ovary or germ cells, and not in the OSE. Animal models to investigate the molecular mechanisms underlying ovarian epithelial carcinogenesis are limited to genetically engineered mice and xenograft models. Therefore, the etiology and early events in epithelial ovarian carcinogenesis are among the least understood of all major human malignancies (Katso et al., 1997).

The first tissue culture systems for OSE from human were developed twenty years ago (Auersperg et al., 1984; Siemens and Auersperg, 1988). OSE are generally difficult to work with since they are few in number and have a short life span. Introduction of SV40 large T antigen (Tag) (Maines-Bandiera et al., 1992) and HPV genes P6 and P7 (Nakamura et al., 1994; Tsao et al., 1995; Wan et al., 1997) into OSE cells extends the population doubling capacity of these cells, while maintaining some but not all of the properties of the OSE cells. p53 and pRb are sequestered and become inactivated through interaction with SV40 Tag (Wright et al., 1989). Through this interaction, SV40 Tag can regulate and limit normal proliferation of cells (Cowell, 1990). SV40 Tag regulates the function of p53 by direct binding to the DNA binding domain of p53, which results in loss of transcriptional activity of p53 (Pipas and Levine, 2001).

1.2 PI3K Enzyme Family

Phosphatidylinositol-3-kinase (PI3K) is a dual specificity protein. It has protein kinase activity, but in addition, it has the unique ability to phosphorylate membrane phosphatidylinositols (PtdIns) on the 3-hydroxyl group of the inositol head group (Luo et al., 2003). The primary function of 3-phosphorylated inositol lipids (3-phosphatidylinositols) is to serve as membrane targeting signals to mediate membrane recruitment of selected proteins that

contain pleckstrin homology (PH) domains (Cantley, 2002). PH domains function as lipid binding constituents and thus recruit proteins to the inner leaflet of the plasma membrane (Lemmon et al., 1996). Phosphorylation of membrane PtdIns by PI3K plays an essential role in the control of cell proliferation, differentiation, senescence, cytoskeletal organization, motility, angiogenesis, and cell survival (Toker and Cantley, 1997; Vanhaesebroeck et al., 1997; Wymann and Pirola, 1998).

There are three classes of PI3Ks categorized as class I, II, or III, depending on the structure, regulation, and substrate selectivity of their subunits (Fruman et al., 1998; Vanhaesebroeck et al., 2001). Two subgroups, A and B, of the class I PI3Ks exist. Class I PI3Ks are heterodimers and consist of a catalytic and a regulatory subunit. There are multiple isoforms of class IA catalytic subunits (p110α, p110β, and p110δ) and regulatory subunits (p85α, p85β, p55γ, p55α, and p50α). Distinct genes encode all these different isoforms (Foster et al., 2003). These class IA PI3Ks are activated primarily by growth factor–responsive tyrosine kinases such as epidermal growth factor receptor (EGFR) (Wymann and Pirola, 1998) and integrin-responsive kinases such as focal adhesion kinase (FAK) (Chen and Guan, 1994). In contrast to class IA, class IB PI3K is activated by βγ subunits of heterotrimeric G proteins (Katso et al., 2001). Class I PI3Ks reside in the cytoplasm in resting cells. However, their substrates, PtdIns, are localized on the cell membrane (Fruman et al., 1998; Vanhaesebroeck et al., 2001). Class I PI3Ks are the only enzymes capable of converting PtdIns(4,5)P_2 to the critical second messenger PtdIns(3,4,5)P_3. In quiescent cells, PtdIns(3,4,5)P_3 is essentially absent. However, extracellular stimulation transiently increases its level at the plasma membrane. The production of PtdIn is linked with proliferation and survival in many cell types (Vanhaesebroeck et al., 2001; Vivanco and Sawyers, 2002). The focus of our studies is the p110α catalytic subunit of the class IA

PI3Ks, because as will be further discussed below, the PIK3CA gene that codes for p110α is frequently amplified in serous EOC (Shayesteh et al., 1999).

1.3 Activation, Regulation and Targets of Class IA PI3Ks

The PIK3CA gene (GenBank NM_006218) is located on chromosome 3q26.32 and codes for the p110α catalytic subunit of PI3K (Wang et al., 2005). Functional domains of p110α include: p85 binding domain (p85BD), Ras binding domain (RBD), C2 domain, helical domain and catalytic domain (Samuels et al., 2004). The helical domain (the 'PIK domain') found only in lipid kinases, connects the C2 domain to the catalytic domain (Walker et al., 1999). The C2 domain of PI3K binds phospholipids and may be involved in recruiting PI3K to membrane fractions (Wymann and Pirola, 1998). The p110α catalytic subunit forms a heterodimer with the p85 (α or β) regulatory subunit. p85 (α or β) regulatory subunits of class IA PI3Ks contain one Src-homology 3 (SH3) domain, two Src-homology 2 (SH2) domains, and an inter-SH2 (iSH2) domain. The iSH2 domain mediates the interaction of p85 with p110α, and this interaction is shown to be required for maximal enzymatic activity of p110α (Klippel et al., 1994). However, the p110α catalytic subunit is constitutively active, and studies by Klippel et al. (1996) have demonstrated that targeting the p110α subunit to the membrane either by N-terminal myristoylation, or by C-terminal prenylation is sufficient to allow for catalytic activity (Klippel et al., 1996). The iSH2 domain of p85 is not necessary, but is required for maximal activation of PI3K. In addition, the SH2 domain of p85 is required to recruit the p110α to the membrane where the PI3K substrates, PtdIns, reside. The two SH2 domains of p85 bind to phosphorylated tyrosines (pY) within the sequence context pY-X-X-M where X can be any amino acid. p85 has been identified as a downstream effector of both receptor and non-receptor tyrosine kinases (Wymann and Pirola, 1998). Upon tyrosine phosphorylation of tyrosine kinases, PI3K is

recruited to the membrane and its PtdIn targets via interaction of the p85 SH2 domains with the pY (Toker and Cantley, 1997; Vanhaesebroeck et al., 1997; Wymann and Pirola, 1998). It has also been suggested that the p110α catalytic subunit can interact directly with GTP-bound Ras and so may be recruited to the membrane and its targets (Rodriguez-Viciana et al., 1996a; Rodriguez-Viciana et al., 1996b). Therefore, the PI3K lipid kinase activity converts PtdIns(4,5)P_2 to PtdIns(3,4,5)P_3, which acts to recruit its downstream targets to the membrane via their PH domains (Cantley, 2002).

In addition to its lipid kinase activity, PI3K also has a serine kinase activity. The p110α catalytic subunit autophosphorylates as well as phosphorylates the p85 regulatory subunit at serine 608 (Beeton et al., 2000; Carpenter et al., 1993; Dhand et al., 1994; Foukas et al., 2004). This phosphorylation of p85 subunit causes an 80% decrease in PI3K activity. It has also been reported that PI3K targets exogenous protein substrates including IRS-1 (Lam et al., 1994), PDE3B (Rondinone et al., 2000), 4EBP1 and H-Ras (Foukas and Shepherd, 2004).

A well-known regulator of the PI3K activity is PTEN, a phosphatase that can dephosphorylate many membrane PtdIns. PtdIns(3,4,5)P_3 is the major substrate for PTEN. Because of its role to negatively regulate PI3K activity, PTEN has been implicated to function as a tumour suppressor (Maehama and Dixon, 1998). Mutations in PTEN are common in different types of cancers. Interestingly, mutations of PTEN rarely occur in serous types of ovarian carcinoma, while somatic mutations of PTEN are very common in endometrioid ovarian carcinoma (Obata et al., 1998).

There are several downstream targets of PI3K. However, the most studied target of PI3K is AKT, a serine-threonine kinase that consists of three highly homologous members, AKT1 (PKBα), AKT2 (PKBβ) and AKT3 (PKBγ). It has been shown that AKT2 is overexpressed (Bellacosa et al., 1995) and is activated (Liu et al., 1998) in ovarian carcinomas. The PI3K/AKT pathway is believed to be a critical signalling pathway regulating cell growth, proliferation, and

apoptosis (Coffer et al., 1998). Translocation of AKT to the inner surface of the plasma membrane is induced through binding of PtdIns(3,4,5)P_3 to the PH domain of AKT (Franke et al., 1997b; Klippel et al., 1997). Upon membrane localization due to PI3K activity, AKT is activated through phosphorylation on two residues, T308 and S473, by the PI3K-dependent kinases, PDK1 and PDK2 (Franke et al., 1997a; Stokoe et al., 1997). These PDKs also possess PH domains and are recruited to the membrane as a result of PtdIns phosphorylation by PI3K activity (Alessi et al., 1997; Vanhaesebroeck and Alessi, 2000). There is controversy surrounding the identity of PDK2 (Dong and Liu, 2005). Several kinases that have been suggested to be PDK2 are: mitogen-activated protein kinase-activated protein kinase-2 (MAPKAP kinase-2 or MK2) (Alessi et al., 1996), integrin-linked kinase (ILK) (Delcommenne et al., 1998), p38 MAP kinase (Rane et al., 2001), protein kinase Cα (PKCα) (Parker and Murray-Rust, 2004), PKCβ (Kawakami et al., 2004), the double-stranded DNA-dependent protein kinase (DNK-PK) (Hill et al., 2002), and the ataxia telangiectasia mutated (ATM) gene product (Viniegra et al., 2005). Whether any or all of these kinases act to phosphorylate AKT on S473 remains to be established.

1.4 Phosphatidylinositol-3-kinase and Epithelial Ovarian Carcinoma

It has previously been demonstrated using comparative genomic hybridization that in approximately 40% of ovarian cancers, there is an increase in copy number at 3q26, which contains the PIK3CA gene (Iwabuchi et al., 1995; Shayesteh et al., 1999). Suzuki et al. (2000) suggested that this gain may be an early event in ovarian cancer development, since it occurs frequently in low grade and low stage tumours (Suzuki et al., 2000). The PIK3CA gene encodes the p110α catalytic subunit of PI3K and maps to the center of the 3q26 amplicon. Shayesteh et al. (1999) implicated PIK3CA as an oncogene in EOC. They demonstrated that in addition to

increased copy number, PIK3CA transcription, p110α protein expression, and PI3K activity are increased in ovarian cancer cell lines as well as in cells from ovarian tumour ascites and primary uncultured cancer cells. They also demonstrated that inhibition of PI3K by LY294002, a specific PI3K inhibitor, decreased proliferation and increased apoptosis. This overexpression of p110α does not accompany any change in levels of p85 in the cells, yet Shayesteh et al. (1999) demonstrated that the p85 levels are not limiting and are present in excess since the increase in p110α protein expression corresponds with increase in p85-p110α heterodimerization (Shayesteh et al., 1999).

In addition to PIK3CA gene amplification, somatic activating mutations of this gene have been detected in several types of cancers. More than 75% of mutations in the PIK3CA gene are in exon9 and exon20, the helical and kinase domains of PI3K protein respectively (Samuels and Velculescu, 2004). Wang et al. (2005) studied 109 advanced ovarian carcinomas and concluded that mutations in exons 9 and 20 are more common in the rare histological types of ovarian cancer, clear cell and mucinous types (Wang et al., 2005). Furthermore, Campbell et al. (2004) showed that somatic changes in PIK3CA either through mutation or gene amplification are extremely common and occur in approximately 30% of all ovarian cancers. They also observed that somatic mutations occur when PIK3CA amplification is not present and therefore, suggested that mutations and amplifications of PIK3CA in ovarian cancer are two mutually exclusive events (Campbell et al., 2004). Levine et al. (2005) demonstrated that the mutations of PIK3CA play an oncogenic role in ovarian and breast carcinomas (Levine et al., 2005).

1.5 The p53 Tumour Suppressor Protein

In 1979, TP53 that codes for the p53 protein was identified as one of the first tumour suppressor genes (Lane and Crawford, 1979; Linzer and Levine, 1979; Linzer et al., 1979). The

human p53 protein is made up of 393 amino acids. p53 protein has three functional domains: N-terminal transcriptional activity domain (amino acids 1-95), central DNA-binding domain (amino acids 102-292), and a C-terminal regulatory domain (amino acids 300-393) responsible for tetramerization, DNA damage recognition and non-specific DNA binding (Powell et al., 2000). p53 has three nuclear localization signals (NLS) that enable its import to the nucleus (Liang and Clarke, 1999a; Liang and Clarke, 1999b; Roth et al., 1998). Moreover, it has two nuclear export signals (NES) that enable its export from the nucleus (Stommel et al., 1999; Zhang and Xiong, 2001). In the case of DNA damage, p53 is imported into the nucleus via its NLS and forms a tetramer. This tetramer binds to target genes and effect their transcription (el-Deiry et al., 1992). In the tetramer state, the NES is masked and thus nuclear export is blocked (Stommel et al., 1999).

p53 is a transcription factor and its activation regulates genes involved in cell cycle arrest and apoptosis. The p53 function is regulated through p53 transcription, translation, protein stability and post-translational modifications (Gu and Roeder, 1997; Gu et al., 1997; Rodriguez et al., 1999). In response to cellular stress, p53 is stabilized and thus accumulates in the nucleus where it can regulate transcription of genes. One way to stabilize p53 is through phosphorylation on Serines 15 and 20 of the N-terminus (Chehab et al., 1999; Shieh et al., 1999; Unger et al., 1999). Phosphorylation at these positions inhibits interaction with MDM-2 as well as masks the NES, which leads to nuclear accumulation of p53. MDM-2 is a negative regulator of p53 with E3 ubiquitin ligase function that promotes p53 degradation. There is an autoregulatory feedback where p53 activates transcription of MDM-2, its negative regulator (Kubbutat et al., 1997). In some cancers where p53 protein is wild-type, the p53 pathway is disrupted through overexpression of MDM-2 levels, which lead to degradation of p53 and its loss of function (Cuny et al., 2000). Interestingly, the PI3K/AKT pathway regulates nuclear import of MDM-2. AKT phosphorylates MDM-2 on serines 166 and 168, which leads to nuclear import of MDM-2,

and in turn degradation of p53 and a decrease in p53 transcriptional activity (Mayo and Donner, 2001). It has been shown that constitutively active PI3K and AKT can delay the onset of p53-mediated apoptosis (Sabbatini and McCormick, 1999).

1.6 p53 Mechanism of Transactivation or Transrepression

El-Deiry identified the consensus p53-binding site in 1992 (el-Deiry et al., 1992). This consensus site was defined as two copies of the sequence 5'-PuPuPu-C(A/T)(T/A)G-PyrPyrPyr-3', separated by 0-13 base pairs. This consensus binding site forms four repeats of the pentamer 5'-PuPuPu-C(A/T)-3' alternating between the positive and negative strands of the DNA duplex (Halazonetis and Kandil, 1993). This arrangement is consistent with the concept that p53 binds DNA as a homotetramer (Friedman et al., 1993). Although the p53 binding site originally identified by el-Deiry in 1992 was said to contain 0-13 spacer nucleotides, the p53 sites in p53-induced genes typically contain spacer elements less than two nucleotides (Deng et al., 1995). It has previously been shown that increasing the spacer from 1 to 4 nucleotides can eliminate the ability of p53 to activate transcription, while increasing the spacer to 10 nucleotides can restore transcription activation (Deng et al., 1995).

In contrast to our knowledge regarding the role of p53 as a transcriptional activator, the subject of transrepression by p53 remains to be relatively unknown due to lack of a p53 consensus binding site within a number of repressed promoters (May and May, 1999). In these promoters the repression is mediated through physical interaction of p53 with activating transcription factors (Iotsova and Stehelin, 1996; Kanaya et al., 2000; Kubicka et al., 1999; Ohlsson et al., 1998; Subbaramaiah et al., 1999; Sun et al., 1999; Yun et al., 1999). Ohlsson et al. (1998) provided data supporting an interaction between p53 and Sp1 transcription factor in the regulation of the promoter activity of the insulin-like growth factor-I receptor (IGF-IR) (Ohlsson et al., 1998). Moreover, Kanaya et al. (2000) demonstrated that interaction of p53 with Sp1 is

responsible for the hTERT transcription downregulation (Kanaya et al., 2000). In addition, It has been demonstrated that repression can occur through interaction of p53 with the basal machinery, as p53 has been shown to directly interact with TATA-binding protein (TBP) (Farmer et al., 1996; Seto et al., 1992; Subbaramaiah et al., 1999; Truant et al., 1993). However, there are few promoters that are repressed by direct binding of p53 to the p53 consensus sequence of the promoter (Budhram-Mahadeo et al., 1999; Hoffman et al., 2002; Johnson et al., 2001; Lee et al., 1999; Ori et al., 1998). In the case where p53 interacts directly with the consensus site, the repression is suggested to be mediated through loss of activation by adjacent factors and not actively due to the p53 binding. Budhram-Mahadeo et al. (1999) demonstrated that Brn-3a and p53 bind to adjacent sites in the p2 promoter of Bcl-2. This p53 binding inhibits the Brn-3a transactivation of the Bcl-2 p2 promoter (Budhram-Mahadeo et al., 1999). Moreover, Hoffman et al. (2002) demonstrated that p53 binds directly to the Survivin promoter on a site that overlaps with a binding site for E2F transcription factors. This binding was shown to repress the Survivin gene transcription. It was proposed by Hoffman et al. (2002) that increasing the size of the spacer changes the orientation of the p53 dimers. Transactivation can occur only if the dimers are on the same face of the DNA helix. If this orientation changes then p53 binds without activating transcription. However, it is suggested that this passive binding interferes with the binding of other transcription factors and thereby causes transcriptional repression (Hoffman et al., 2002).

1.7 p53 and Cancer

The most common genetic alteration found in human cancers is mutation of the p53 gene. As in other cancers, overexpression of the p53 protein in ovarian cancer appears to correlate closely with the presence of mutation in the p53 gene (Marks et al., 1991). Nuclear accumulation of the p53 protein is significantly correlated with p53 gene inactivating mutations in cancers

including epithelial ovarian carcinoma (Kihana et al., 1992). However, many tumour types that contain wild-type p53 have lost its activity through cytoplasmic sequestration of p53. This nuclear exclusion of p53 occurs through its active exportation from the nucleus. Cytoplasmic localization inhibits the tumour suppressing activity of p53 and is a poor prognostic factor in cancer (Moll et al., 1992; O'Brate and Giannakakou, 2003). Moreover, the p53 pathway can also be inhibited through mutations in other proteins that regulate activity of p53, such as MDM-2 (Cuny et al., 2000).

Alterations to p53 are known to be involved in tumour development and progression. p53 mutations commonly occur in ovarian serous carcinomas (Kupryjanczyk et al., 1993). It is believed that p53 mutations are an early step in ovarian carcinogenesis. OSE lined inclusion cysts and invaginations are common sites of benign metaplasia as well as early neoplastic progression (Deligdisch et al., 1995; Scully, 1995a; Scully, 1995b). It has been demonstrated that overexpression of p53, indicative of loss of p53 function, is present in inclusion cysts with normal or atypical cytology, adjacent to malignant lesions (Hutson et al., 1995). Moreover, p53 expression, although weak and focal, has been shown in the ovarian epithelium lining inclusion cysts and deep invaginations that are hyperplastic or dysplastic, in ovaries removed prophylactically from women (Schlosshauer et al., 2003).

1.8 p53 Regulation of the PI3K Pathway

Stambolic et al. (2001) demonstrated that the PTEN tumor suppressor, a negative regulator of the PI3K pathway, is positively regulated by p53. They revealed a p53 binding site on the PTEN promoter and determined through deletions and mutations of the region that this binding site is necessary for inducible transactivation of PTEN by p53. Moreover, they demonstrated that PTEN is required for p53-mediated apoptosis in immortalized mouse

embryonic fibroblasts. The findings of Stambolic et al. (2001) demonstrated that transcriptional activation of PTEN by p53 is one way to maintain low levels of PI3K activity. They suggest that in cancers with loss of p53 or mutated PTEN there is an increase in PI3K activity due to loss of positive regulation (Stambolic et al., 2001). In addition, Singh et al. (2002) suggested that p53 may negatively regulate transcription of PIK3CA in cancer. They used EB1, a colon cancer derived cell line carrying a wild-type p53 gene with an inducible metallothionein promoter, and found progressive down-regulation of p110α expression as a result of p53 induction (Singh et al., 2002).

1.9 Hypotheses and Aims

Loss of function mutations in p53 as well as increases in p110α levels have been shown to occur early in ovarian carcinogenesis. Based on observations by Singh et al. (2002), and the importance of PIK3CA and p53 in ovarian cancer, our aim was to determine whether a relationship between p53 and PI3K pathways exists in benign ovarian surface epithelium as well as ovarian cancer cells. In addition, we wanted to determine whether the regulation of p110α levels by p53 is direct via interaction of p53 with the PIK3CA promoter, or indirect via other signalling mediators. In order to look at physical interaction of p53 and the PIK3CA, it was necessary to characterize the PIK3CA promoter, since it had not been identified. We studied the functional and physical interaction of p53 and PIK3CA in order to provide insights into the process of ovarian carcinogenesis. We hypothesize that in addition to PIK3CA gene amplification in EOC, p110α levels are increased due to loss of negative regulation by p53. Therefore, we suggest a novel mechanism for neoplastic progression of EOC through loss of p53 function.

CHAPTER 2:

MATERIALS AND METHODS

2.1 Cell Culture:

This study was initiated with two temperature sensitive cell lines, IOSE 166a and IOSE 166h. These cells were previously established in our laboratory through infection of cells with the tsSV40Tag A209, a chimeric virus containing an origin-defective adenovirus plus a temperature-sensitive SV40 large T antigen (Chou et al., 1974). The mutation at amino acid residue 209 causes the temperature sensitivity. The temperature sensitive model is outlined in Figure 1. At 34°C, the permissive temperature, the Tag binds to p53 and conditionally immortalizes the cells. This in turn, like many of the common missense mutations that occur in TP53, leads to posttranslational stabilization and relative overexpression of the inactive p53, which allows for its detection by immunohistochemistry and western blot analysis. After a shift to 39°C, the non-permissive temperature, the Tag can no longer bind p53 and thus the cells revert back to normal. However, these cells have a finite growth potential even when cultured at 34°C, which limits the number of experiments that may be carried out. Therefore, for most of our experiments we used OSEC2 cells, which were kindly provided by Dr. Barry R Davies (University of Newcastle, UK). These human OSE-derived cells, in addition to the tsSV40Tag, express telomerase and are thus truly immortalized at the permissive temperature, 34°C. A more detailed description and characteristics of OSEC2 cells are described by Davies et al. (Davies et al., 2003). In brief, after about 4 population doublings, OSE cells were exposed to supernatants from the retroviral packaging lines TEFLY-A and PA317 producing high-titre full-length pBabehygro-hTERT (O'Hare et al., 2001) and pS/tsA58-U19/8 (Stamps et al., 1994), respectively. The cells were then selected with 0.5 mg/ml of G418 or 25 mg/ml of hygromycin B

until the uninfected cells were killed. The pS/tsA58-U19/8 contains the SV40 Tag with two point mutations that make the protein thermosensitive. At 39°C, the SV40 Tag becomes inactive, and thus cannot bind to p53 (Figure 1). At 34°C, the cells remain immortalized since the Tag binds to p53 (Figure 1). By shifting the temperature to 39°C the immortalization is reversed and normal characteristics of cells are restored (Davies et al., 2003). These temperature sensitive cells were maintained at 34°C, while experiments were carried out at both 34°C and 39°C.

IOSE 397, IOSE 80pc, and WI38 cells were used as control cells. Both IOSE 397 and IOSE 80pc are immortalized with the SV40 Tag. However, IOSE 80pc cells have gone through crisis and have become a permanent line. Both of these cells lack functional p53. WI38 cells are lung fibroblast cells with wild-type p53. These control cells were maintained at 37°C, while experiments were performed at 34°C, 37°C, and 39°C.

WI38, SKOV3 and OVCAR3 were purchased from American Type Culture Collection (ATCC). CaOV3, OVCAR5, OVCAR8, and A2780 were obtained from Dr. Hamilton (Fox Chase Cancer Center, Philadelphia, PA), and MCF-7 cancer lines were obtained from Dr. Roskelley (University of British Columbia, Vancouver, BC).

A2780 and MCF-7 cells were maintained in Dulbecco's modified Eagle's medium (DMEM; Gibco) supplemented with 5% fetal bovine serum (FBS; Hyclone Laboratories Ltd). All other cancer lines were maintained in 1:1 mixture of 199:105 medium (Sigma) supplemented with 5% FBS. The ts and non-ts IOSE, OSEC2 and WI38 cells were grown in 1:1 mixture of 199:105 medium supplemented with 10% FBS. All cells were maintained in a 5% CO2/air atmosphere, and passaged using 0.06% trypsin/0.01%EDTA in EDTA in Ca/Mg-free Hanks' basal salt solution.

FIGURE 1

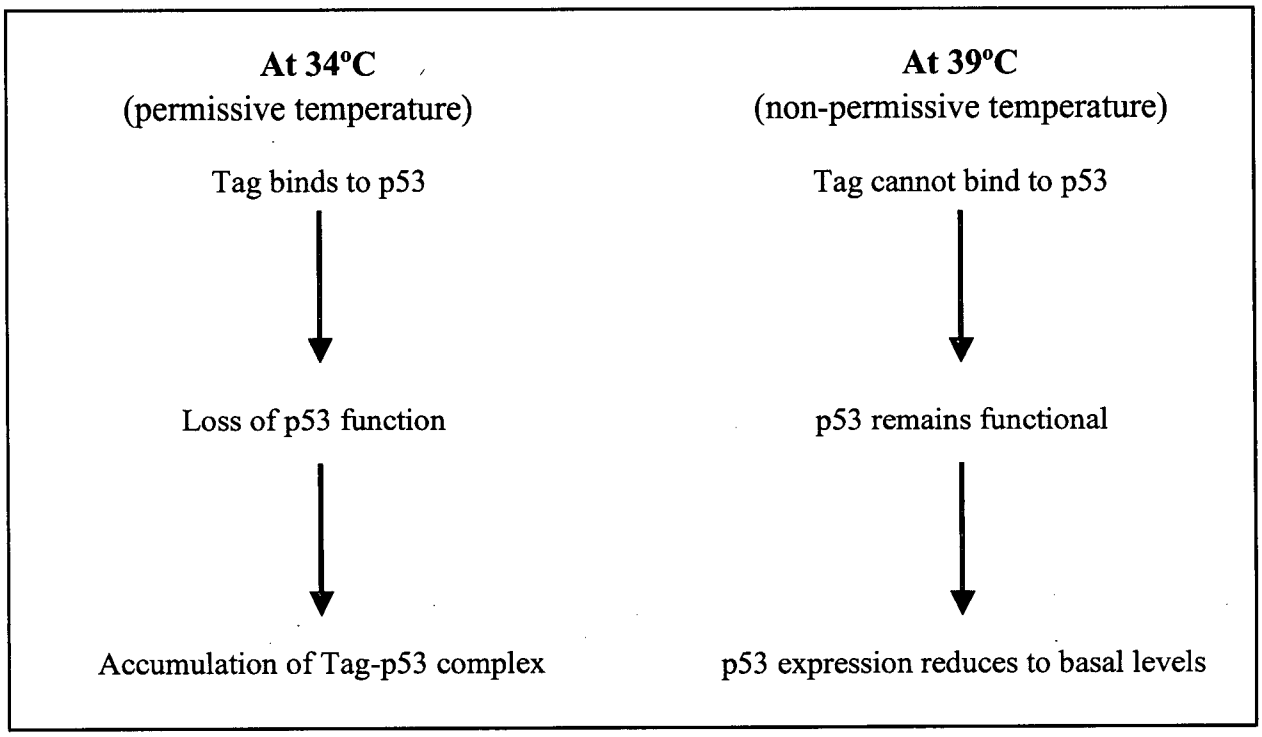

Figure 1: The Temperature Sensitive Model. At 34°C, the permissive temperature, the SV40 Tag binds to p53, which results in its loss of function. Cells make more p53 in order to compensate for loss of p53 function. As a result, p53 is overexpressed and accumulates in the nucleus, yet is functionally inactive because it is bound to Tag. At 39°C, the Tag has an amino acid mutation that prevents its binding to p53. Therefore, at the non-permissive temperature, p53 remains functional and its expression reduces to basal levels.

2.2 Determination of Protein Levels After the Temperature Shift:

Temperature sensitive cells and IOSE 80pc, IOSE 397 and WI38 control cells were grown to approximately 70% confluency. On day 0, a dish of each of the cell lines was maintained at 34°C and the rest moved to 39°C. For the control cells a dish was also maintained at 37°C. On day 1, the cells at 34°C, 37°C and a dish of cells at 39°C were rinsed with ice-cold PBS and lysed with lysis buffer (PBS pH 7.4, 1% Triton x100, 0.5% sodium deoxycholate, 0.1% SDS). Protease inhibitor cocktail (Sigma) was added to the lysis buffer prior to cell lysis. The lysates were maintained at -70°C until all the cell lysates at different time points were collected. Cells at 39°C were lysed on days 3 and 5. Western blot analysis was used to detect levels of proteins in these cell lysates. All experiments were repeated at least three times.

2.3 Western Blot Analysis:

Cell lysates were sonicated on ice for 10-15 seconds and centrifuged at 20817 xg for 10 minutes at 4°C. The supernatants were carefully collected and protein concentrations were determined using the Bio-Rad Dc Protein Assay (Bio-Rad). The cell lysates were mixed with 4x SDS sample buffer (3 parts cell lysates plus one part 4x SDS sample buffer), boiled for 5 minutes and stored at -70°C for later use. The 4x SDS sample buffer was made up of 50% glycerol, 4% SDS, 0.08% Bromophenol Blue, 125mM Tris-HCl, pH 6.8, and 5% β-mercaptoethanol added fresh. Before SDS-PAGE the samples were boiled for 5 minutes. A 20μg aliquot of total cellular protein per sample was subjected to SDS-PAGE and transferred to a supported nitrocellulose (Bio-Rad) membrane. The membranes were incubated in blocking buffer (1xTBS (10x TBS: 24.2g Tris-Base, 80g NaCl, 1L H20, pH 7.6), 0.1% Tween-20 with 5% non-fat dry milk) for 1 hour at 23°C, and washed three times for 5 minutes in TBS-T (1xTBS and 0.1% Tween-20). The membranes were incubated with the primary antibody diluted in (1x TBS-T with 5% BSA

(Sigma)) overnight at 4°C, washed three times for 5 minutes with TBS-T, and incubated with HRP-conjugated secondary antibody diluted in blocking buffer for 1hour at 23°C. The membranes were washed three times for 5 minutes with TBS-T, incubated with SuperSignal West Pico Chemiluminescent Substrate (Pierce), and exposed to x-ray film. Antibodies used were: anti-p110α polyclonal rabbit antibody (1:500) (Cell SignallingTechnologies catalog #4254), anti-p53 monoclonal (1C12) mouse antibody (1:2000) (Cell Signalling Technologies catalog #2524), anti-Phospho-AKT (Ser473) monoclonal (1:1000) (193H12) rabbit antibody (Cell Signalling catalog #4058), anti-Total-AKT polyclonal rabbit antibody (1:1000) (Cell Signalling Technologies catalog #9272), anti-PTEN monoclonal (138G6) rabbit antibody (1:1000) (Cell Signalling Technologies catalog #9559), and anti-actin polyclonal goat antibody (1:1500) (Santa Cruz, #SC1615).

2.4 Determination of PIK3CA Transcript Levels After the Temperature Shift:

OSEC2 temperature sensitive cells and IOSE 397 and WI38 control cells were grown to approximately 70% confluency. On day 0, two dishes of cells were placed at 34°C and the rest moved to 39°C. On day 1, a dish at 34°C and a dish at 39°C were lysed with the RNeasy Mini Kit (Qiagen) lysis buffer. The lysates were mainained at -70°C until all the cell lysates at different time points were ready for RNA extraction. Cells at 39°C were lysed on days 3 and 5, and at 34°C on day 5. Quantitative Real-Time RT-PCR was used to detect levels of PIK3CA transcript in the cells.

2.5 Quantitative Real-Time RT-PCR:

For quantification of mRNA levels, total RNA was isolated from cells with the RNeasy Mini Kit (Qiagen). Genomic DNA was digested with Deoxyribonuclease I, Amplification Grade

(Invitrogen). cDNA was synthesized with the First-strand cDNA Synthesis Kit (Amersham Bioscences) by use of random hexamers as primers. For quantitative real-time PCR, the TaqMan Universal Master Mix (Applied Biosystems) was used according to the manufacture's instructions. TaqMan Gene Expression Assay (Applied Biosystems, HS00180679) for human PI3K, p110α (PIK3CA) was used that contained the appropriate primers and probes. The expression level of the ribosomal RNA (rRNA) gene was used as control according to the manufacturer's instructions (TaqMan® Ribosomal RNA Control Reagents; Applied Biosystems). The TaqMan assay was performed on a Gene Amp 5700 Sequence Detector (Applied Biosystems), a combined thermocycler and fluorescence detector. Optimal cycling conditions were as follows: Initial step: 50°C for 2 min; 95°C for 10 min; 40 cycles: 95°C for 15 sec, 60°C for 1 min. The expression levels of rRNA were used to normalize the expression level of PIK3CA RNA. All determinations were performed in triplicates, and repeated at least three times.

2.6 PI3K Activity:

OSEC2 temperature sensitive cells and IOSE 397 and WI38 control cells were grown to 70% confluency, and moved to 39°C or maintained at 34°C. A concentration dependent response to serum was studied by serum starvation of all cells in 199:105 medium containing 0.5% FBS for 18 hours. The cells were stimulated for 1 hour with 199:105 medium containing either 0.5%, 1%, 5%, 10%, and 15% FBS. In addition, the cells at both 34°C and 39°C were treated with 20μM of LY294002 (Biomol Research Laboratories), a specific PI3K inhibitor, for 1 hour prior to serum stimulation. The cells were then lysed and prepared for western blot analysis to determine P-AKT levels.

A time dependent response to serum was studied in OSEC2 cells by serum starvation in 199:105 medium with 0.5% FBS for 18 hours, stimulation with 10% FBS 199:105 medium for 15, 30, and 60 minutes, and subsequent cell lysis for western blot analysis of the P-AKT levels.

To furthur investigate the difference in PI3K activation at the two temperatures, a set of OSEC2 cells were maintained at 34°C while another set was moved to 39°C (day 0). 10 hours after the switch in temperature, the cells were serum starved as explained above and either stimulated with 10% FBS medium for one hour, or maintained with 0.5% FBS. The cells were lysed on day 1 at 34°C and 39°C, and on day 3 at 39°C. IOSE 397 and WI38 cells served as controls.

For a more direct look at PI3K activity, AKT-PH-GFP plasmids were obtained from Dr. Gordon Mills (MD Anderson Cancer Center, Houston, TX). AKT-PH-GFP construct contains the sequence of the PH domain of AKT, with the modified C-terminus through addition of a GFP tag sequence. This construct was amplified in DH5α E.coli in LB medium containing 50μg/ml of kanamycin. The bacteria were harvested and purified using the HiSpeed Plasmid Midi Kit (Qiagen). OSEC2 cells were cultured on coverslips to approximately 90% confluency in 35mm dishes, and transfected with 4μg of the AKT-PH-GFP construct using 5μl of Lipofectamine 2000 (Invitrogen). Medium was changed after overnight incubation, and the cells were incubated at 34°C for a total of 24 hours after transfection. The cells were then transferred to 39°C or maintained at 34°C. 24 hours after the shift in temperature, the cells were serum starved (0.5% FBS in 199:105) for 4 hours and subsequently either stimulated with 10% FBS or maintained in the low serum medium. A dish of cells at 34°C was treated with 20μM of LY294002 in the last hour of the serum starvation, and then stimulated with 10% serum for 1 hour. The coverslips were fixed on days 1, 3 and 5 in 4% formaldehyde for 60 minutes at 23°C, stained with Hoechst 33258 (Sigma) (0.5μg/ml) for 10 minutes, rinsed in PBS, mounted with gelvatol, and examined

using a Zeiss Axiophot microscope equipped with a digital camera (Q imaging). Digital images were analyzed using Northern Eclipse 6.0 (Empix Imaging). Three coverslips for each condition were examined at and the cells counted, photographed and analyzed for AKT localization. The cells were grouped by percentage into three categories: cells with strong membrane localization, cells with weak membrane localization, and cells with no membrane localization. A one-way ANOVA test (Tucky) on the GraphpadPrism software was used for statistical analysis.

2.7 Proliferation/ Immunofluorescence:

The temperature sensitive OSEC2 cells and IOSE 397 and WI38 control cells were grown on coverslips to approximately 70% confluency at 34°C and 37°C respectively. Two dishes were mantained at 34°C, while the rest were moved to 39°C. A dish at 34°C was treated with 20μM of LY294002 for 1 hour prior to fixation. On days 1, 3, and 5 the cells were fixed in methanol at -20°C and maintained until all coverslips at different time points were collected. Cells on coverslips were permeablized with 1:1 methanol:acetone for 5 minutes at -20°C, dried, washed in PBS, and blocked with Dako Protein Block (Dako) for 30 minutes. Coverslips were incubated overnight at 4°C with primary Ki-67 monoclonal mouse anti-human antibody (1:50) (Dako, #M0722), diluted in Dako Protein Block. Coverslips were rinsed with PBS, and incubated in secondary Alexa 594-labeled goat anti-mouse IgG (Cedarlane) diluted in Dako Protein Block for one hour at 23°C. The coverslips were rinsed in PBS and mounted with gelvatol. At least six representative fields for each case were photographed and analyzed for Ki-67 staining.

2.8 Apoptosis:

To visualize nuclear morphology, cells were grown on glass coverslips, and fixed in methanol at -20°C, dried, washed in PBS, and stained with Hoechst 33258 at 500ng/ml for 5 minutes, rinsed with PBS, and mounted with gelvatol. At least six representative fields for each case were photographed and analyzed for nuclear morphology and presence of apoptotic figures.

For a quantitaive readout of levels of apoptosis, OSEC2 temperature sensitive cells and IOSE 397 and WI38 control cells were grown to 70% confluency. On day 0, the cells were moved to 39°C or maintained at 34°C. On day 1, the cells at 34°C and 39°C, and on days 3 and 5 the cells at 39°C were trypsinized. In addition, a dish of OSEC2 cells at 34°C was treated with 20μM of LY294002 for 1 hour prior to trypsinization. The cells were centrifuged for 4 minutes, the supernatant discarded, and the cell pellets resuspended in 1ml of medium. 250μl aliquots were centrifuged for 1 minute at 5000 xg, and the supernatants removed. The cell pellets were subsequently lysed in 500μl of incubation buffer (component of Cell Death Detection ELISA kit) for 30 minutes at 23°C, and centrifuged for 10 minutes at 18000 xg. The top 400μl was separated and stored at -20°C until the day of the assay. The assay was performed using the Cell Death Detection ELISA kit (Roche) once samples from days 1, 3 and 5 were collected. Measurements were done with the Microplate Autoreader EL311 (Bio-TEK instruments) at 405nm against substrate solution as blank. The remaining 750μl aliquot of cells was centrifuged, supernatant removed and the pellet maintained at -70°C until all samples were collected. The pellets were lysed with protein lysis buffer, as per protocol for cell lysis, and used for protein quantification using the Bio-Rad Dc Protein Assay. The protein concentration for each sample was used to normalize the readings of the ELISA assay.

2.9 p53 Adenovirus:

p53 cDNA cloned into the XhoI/EcoRI regions of pOTB7 vector was purchased (ATCC). The bacteria were cultured overnight on appropriate growth medium (LB + 25μg/ml Chloramphenicol). Colonies were picked and grown overnight in appropriate growth medium. Miniprep (Qiagen) on the bacterial cultures were performed according to manufacturer's protocol. The vector was then cut with XhoI and EcoRI restriction enzymes, and cloned into pShuttle2 vector (Clonetech). The BD Adeno-X Expression System 1 (BD Bioscience) was used to clone the insert of interest into the Adenoviral construct following the recommendations of the manufacturer. The expression cassette was excised from pShuttle2 by using PI- Sce I and I- Ceu I restriction enzymes, and subsequently ligated into BD Adeno-X Viral DNA. After transformation and selection for ampicillin resistant clones, the purified recombinant adenoviral DNA containing the gene of interest was linearized with Pac I digestion. HEK 293 cells were transfected using 5μl of Lipofectamine 2000 with 10μl of Pac I digested p53 Adeno DNA. The cultures were checked for cytopathic effects periodically after the transfection. A week later, the cells were gently dislodged into medium, transferred into a 15ml centrifuge tube, centrifuged, and the supernatant discarded. The pellet was resuspended in 500μl of filtered sterile PBS (Dulbecco's PBS, Gibco), and the cells were lysed by three consecutive freeze-thaw cycles (-70°C freezer and 37°C waterbath). A fresh 60mm dish of HEK 293 cells were infected with half of the lysate from the third feeze-thaw cycle. When greater than 50% of the cells detached from the plate due to cytopathic effects, the cells and the medium were collected, centrifuged, and resuspended in 500μl of filtered sterile PBS. After three freeze-thaw cycles this viral stock was used to infect the target cells.

SKOV3 cells were infected with varying titrations of the p53 adenovirus diluted in 1ml of medium. After 4 hours, the virus-containing medium was replaced with 2 ml of fresh medium,

and 48 hours after infection, the cells were lysed for western blot analysis. In addition, the SKOV3 cells were infected with the Adeno-GFP construct as control to account for the cytopathic effects of the infection and to check for infection efficiency.

Other cancer cells with mutant and wild-type p53 status (Table 1, results) were infected with either 100μl of the p53 adenovirus or 1ml of the control GFP adenovirus. The 100μl of virus was diluted in 1ml of medium and added onto cells for 4 hours. The virus was removed and 2ml of fresh medium was added to the cells. The cells were lysed 48 hours after infection, and western blot analysis was performed to detect the levels of p53 and p110α in the various ovarian cancer cells with and without infection.

2.10 Immunohistochemistry:

Serial sections of the paraffin blocks were cut at 5μm, de-paraffinized with xylene and rehydrated through a series of graded alcohols (3x 5 minutes in xylene, 2x 3 minutes in 100% ethanol, 1x 3 minutes in 95% ethanol, 1x 3 minutes in 70% ethanol, 2x 2 minutes in dH_2O). Antigen retrieval was performed in a steamer (Black and Decker) for 25 minutes in citrate buffer at pH 6.0, and cooled for 30 minutes at 23°C. The slides were washed in dH_2O three times for five minutes, blocked with 3% H_2O_2 for 30 minutes, rinsed with dH_2O for 1 minute and with PBS three times for 5 minutes. 5% Normal Goat Serum (NGS) was used for blocking for 30 minutes at 23°C. Sections were incubated with anti-p110α polyclonal rabbit antibody (1:25) (Cell SignallingTechnologies catalog #4254), and anti-p53 monoclonal (1C12) mouse antibody (1:500) (Cell Signalling Technologies catalog #2524), diluted in 1% NGS, overnight at 4°C. The sections were washed three times for 5 minutes with PBS, incubated in labelled polymer, HRP (Envision System, K1491, DakoCytomation) for 30 minutes, rinsed with PBS three times for 5 minutes, developed in DAB substrate (Dako) for 10 minutes, washed with dH_2O for 5 minutes,

counterstained in hematoxylin for 5 minutes, and rinsed in running water for 10 minutes. The sections were placed in lithium carbonate for 1 minute, rinsed in running water for 10 minutes, dehydrated through a series of graded alcohols and xylene (2x 10 seconds 95% ethanol, 1x 10 seconds in 100% ethanol, 1x 1 minute, 2x 30 seconds in xylene, 1x 3 minutes in xylene), and coverslips mounted with Permount (Fisher).

The double staining procedure was as above with some exceptions. The cells were stained first with anti-p53 antibody and secondary goat anti-mouse labelled polymer, and developed in DAB/Nickel substrate for 12 minutes. The reaction was stopped in dH_2O, washed in PBS for 5 minutes, incubated with anti-p110α antibody and secondary goat anti-rabbit labelled polymer (Envision plus, K4003, DakoCytomation), and developed with NovaRed substrate for 5 minutes.

2.11 Primer Design:

Primers for PCR experiments were designed using the Primer3 software (http://frodo.wi.mit.edu/cgi-bin/primer3/primer3_www.cgi).

2.12 Bioinformatics:

Wasserman (2004) reviewed a comprehensive set of algorithms and online resources available to identify transcriptional regulatory regions (Wasserman and Sandelin, 2004). The University of California Santa Cruz (UCSC) Genome Browser Database found on the UCSC Genome bioinformatics website (http://genome.ucsc.edu) was used for qualitative promoter analysis studies. The genome browser was used to display the PIK3CA gene in graphical and text-based views. Cross-species homology is computed by UCSC through alignment of genome, mRNA and EST (expressed sequence tag) sequences (Karolchik et al., 2003). Transcripts (ESTs

and cDNAs) for human genes are aligned against the genome sequence by the UCSC annotation pipeline. The exon positions were examined to determine potential promoter locations within the PIK3CA gene. In addition, CpG island locations, as annotated by the UCSC system were reviewed, as they are predictive of promoter positions.

The ConSite web based tool (http://mordor.cgb.ki.se/cgi-bin/CONSITE/consite/) was used to analyze the evolutionary conserved (mouse to human) regions on the PIK3CA gene for putative p53 binding sites. As described, the p53 consensus binding site consists of two palindrome half sites separated by 0-13 nucleotide spacers. The p53 consensus binding site (Figure 2) used by ConSite to search for putative p53 binding sites was based on the in vitro SELEX assay (Shultzaberger and Schneider, 1999). Using this search for p53 binding sites is very strict and ignores the binding sites that have variable spacing. Therefore, in addition to the ConSite search of the consensus p53 binding site without spacer regions, the position frequency matrix (a table of probabilities for observing each nucleotide at each position) of each half of the palindrome was used to search for putative p53 binding sites that include spacer regions. Figure 2 shows the position frequency matrix of the p53 binding site. Each half of the palindrome was analyzed separately and then reviewed together to find p53 binding sites that have 1 to13 nucleotides spaces between the two palindromic sequences. In addition, the conservation of these sequences with the mouse sequence was analyzed by comparing orthologous pairs of genomic sequences in the ConSite website.

FIGURE 2

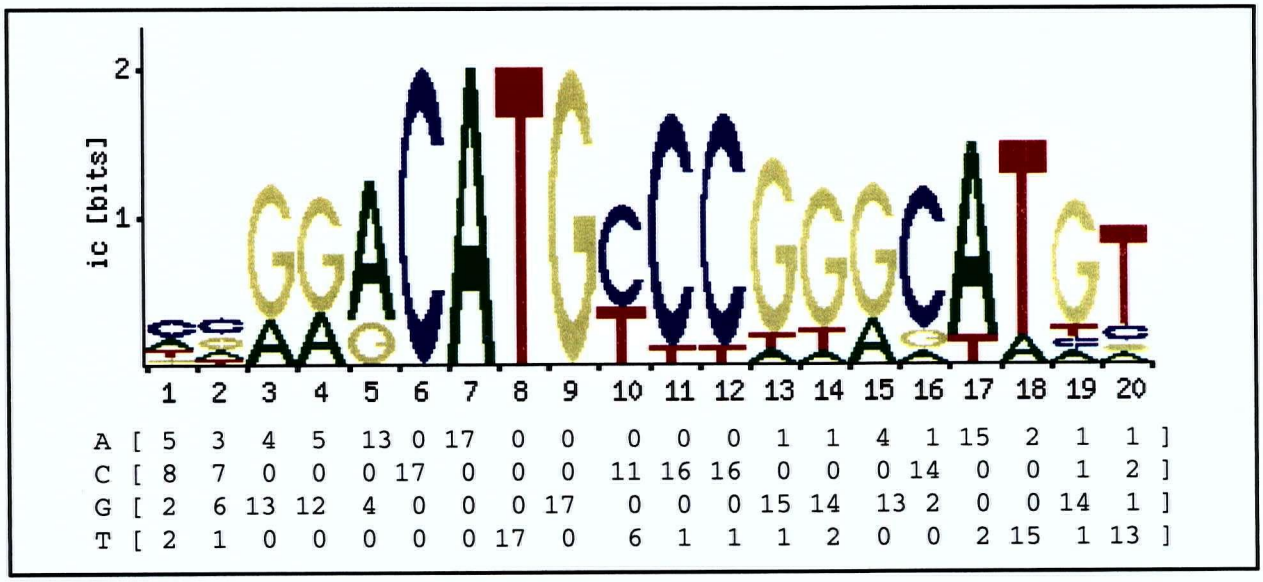

Figure 2: Position Frequency Matrix of the p53 binding site. The p53 consensus binding site consists of two palindrome half sites separated by 0-13 nucleotide spacers. This position frequency matrix is based on the in vitro SELEX assay. The ConSite web based tool uses this matrix to identify putative p53 binding sites on the PIK3CA promoter. This sequence contains 20 nucleotides consisting of two palindromes, and does not take into account spacer nucleotides between the two palindromes. The matrix on the bottom of the graph represents the probability for observing each nucleotide (A, C, G, T) at each of the 20 positions. For example, at position 6 only C is observed, while at position 7 only A is observed.

2.13 5' Rapid Amplification of cDNA Ends (5' RACE):

Total RNA was isolated from OSEC2 cells with RNeasy Mini Kit (Qiagen) using the manufacturer's protocol. Optical densitometry (A260/A280) was used to determine RNA concentration obtained from the cell extracts. 5' RACE was performed with the 5' RACE System for Rapid Amplification of cDNA ends Kit (Invitrogen) as recommended by the manufacturer. The design of gene specific primers (GSP) used for RACE is described in Figure 3 and the primer sequences are listed in Table 1. GSP1 and GSP2 were designed to overlap parts of two exons in order to eliminate amplifcation from genomic DNA instead of mRNA.

PIK3CA mRNA (5μg) was specifically converted to first strand cDNA using GSP1 and SuperScript II RT. Following cDNA synthesis, RNA was degraded with RNase mix and the first strand product was purified from unincorporated dNTP's and GSP1 using GlassMax Spin Cartridges. A homopolymeric tail was added to the 3' ends of the cDNA using terminal deoxynucleotidyl transferase (TdT) and dCTP. This tailed cDNA was amplified by PCR using a nested primer (GSP2), and a combination of anchor and adapter primers (AAP) that allow amplification from the homopolymeric tail. A 1:100 dilution of this primary PCR product was reamplified using a nested primer (GSP3) and Abridged Universal Amplification Primer (AUAP). The PCR conditions used were as follows: initial step: 94°C for 4 minutes; 35 cycles: 94°C for 1 minute, 55°C for 1 minute, 72°C for 1.5 minutes; final extension: 72°C for 5 minutes. Aliquots (10μl) of PCR products were analyzed using agarose gel electrophoresis, ethidium bromide staining, and the 100 bp molecular size standards. The appropriate sized DNA fragment on the gel was excised, and purified using the QIAquick Gel Extraction Kit (Qiagen) as recommended in the manufacturer's protocol. For direct characterization of the 5' end of PIK3CA, this purified RACE product was subjected to DNA sequencing.

FIGURE 3

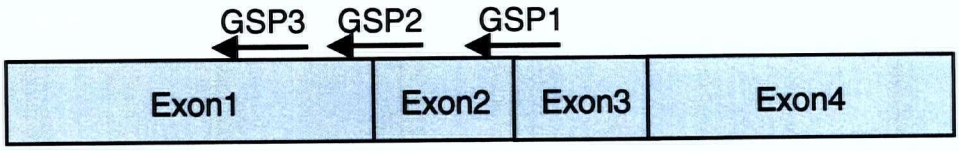

Figure 3: Primer Design for RACE analysis. The first 4 of 20 identified exons of the PIK3CA mRNA are displayed in this figure. Gene specific primers (GSP) were designed to determine presence of upstream exons. Translational start site (ATG) is within exon1. The GSP1 was designed for cDNA synthesis. GSP1 was designed to span a region of exon3 and a region of exon2 in order to eliminate reverse transcription from genomic DNA rather than mRNA. Similarly GSP2 for the PCR amplification of tailed cDNA was designed to span a region of exon2 and a region of exon1. GSP3 was designed internal to exon1 and was used for nested amplification of the first PCR product.

Table 1: Schematic diagram of oligonucleotide primers for RACE analysis of PIK3CA gene

mRNA		Primer 5'-3'
Human PIK3CA	Reverse gene specific primer 1 (GSP1)	TCACCACTATTATTTGCCCTTT
	Reverse gene specific primer 2 (GSP2)	ATGCCGATAGCAAAACCAAT
	Reverse gene specific primer 3 (GSP3)	CGGTTGCCTACTGGTTCAAT
	Forward gene specific primer 4 (GSP4)	TGCTTTGGGACAACCATACA
	Forward gene specific primer 5 (GSP5)	GACCCGATGCGGTTAGAG
	Forward gene specific primer 6 (GSP6)	GGGGAAGAGTTCGTTGTTTG

2.14 Chromatin Immunoprecipitation:

Chromatin Immunoprecipitation was performed using the EZ-ChIP kit (Upstate) as recommended by the manufacturer. The cells were cultured at 80-90% confluency in a 100mm culture dish with 10ml of growth medium. The cells were fixed with 37% formaldehyde to crosslink proteins to DNA. The cells were lysed and chromatin harvested. A 50-watt sonicator was used to shear the chromatin to pieces between 200-1000 base pairs. A separate dish of OSEC2 cells at 39°C were used to determine the optimum shearing condition by using 4, 8, or 12 fifteen second pulses, with 15 seconds in between each pulse. NaCl was used to reverse the DNA-protein crosslink, overnight at 65°C. An unsheared aliquot and the sheared samples were subsequently run on a 2% agarose gel to visualize shearing efficiency. The optimum shearing was achieved with 8 pulses. The chromatin harvested from OSEC2 cells at 39°C and 34°C were then sheared using 8 fifteen second pulses. A 100μl aliquot of the sheared DNA was used for each immunoprecipitation. Mouse Anti-IgG (1μg) and Anti-RNA Polymerase II (1μg) were used for immunoprecipitation of negative and positive controls respectively. Segments of chromatin bound by p53 were immunoprecipitated with 6μg of anti-p53 monoclonal (1C12) mouse antibody (Cell Signaling Technologies catalog #2524). The protein/DNA complexes were reverse crosslinked using 5M NaCl incubated overnight at 65°C. The DNA was purified using spin columns and subsequently eluted with 50 μl of elution buffer. Primers were designed around the putative p53 binding sites to give products approximately between 150 and 200 bps in length (Table 2). The PCR conditions were as followed: initial step: 94°C for 3 minutes; 34 cycles: 94°C for 20 seconds, 59°C for 30 seconds, 72°C for 30 seconds; final extension: 72°C for 2 minutes. For promoter1b with a high GC content, mixtures G and J of the FailSafe kit (EpiCentre Technologies) were used to improve PCR conditions. A 10 μl aliquot of each PCR reaction was used for analysis on a 3% agarose gel with a 100 bp DNA ladder.

Table 2: Schematic diagram of oligonucleotide primers for ChIP Analysis

Primer Name	Primer Sequence 5' to 3'	Product Size (bp)
Forward promoter 1a 1 Reverse promoter 1a 1	CAGACTTCTAAGGTACGCAGCA TGATTCGAAGCAGCTTGTAGG	150
Forward promoter 1a 2 Reverse promoter 1a 2	GGCATAGCAAAAGGTCTCCA CCAGCGTGGTTATGGATTCT	166
Forward promoter 1a 3 Reverse promoter 1a 3	AACCATGTCGGCAGAAGAAC TGGGAGCAAGTGGGTTATTT	180
Forward promoter 1a 4 Reverse promoter 1a 4	ATAAACTTCGGGCGGAAAAG CCGGCAGAAGAGGGTAAGAG	168
Forward promoter 1b Reverse promoter 1b	GAAGTAGAAAGCGGCAGTTCC GCCGAGGGAGAGGAGAGC	192
Forward enhancer 1 Reverse enhancer 1	TCCAGGTTATCTCAGGGGATT AACACGCAATCCAGCACATA	152
Forward enhancer 2 Reverse enhancer 2	CGATTGACAGCATAGATCTCCA CCAACACACACACACACACAC	154
Forward p21 Reverse p21	GTGGCTCTGATTGGCTTTCTG CTGAAAACAGGCAGCCCAAG	125

CHAPTER 3:

RESULTS

3.1 p53 negatively regulates p110α protein levels

To investigate whether a relationship between p53 and p110α protein levels exists in benign ovarian surface epithelium cells, temperature sensitive IOSE cell lines were used to perform western blot analysis. At 34°C, SV40 Tag is functional and binds to and inhibits p53 (Figure 1). SV40 Tag binds to p53 and prevents it from binding to MDM-2, therefore, p53 cannot be degraded by MDM-2 and becomes stable (Reihsaus et al., 1990; Tiemann et al., 1995). Moreover, cells make more p53 in order to compensate for the loss of p53 function. As a result, p53 becomes overexpressed and accumulates in the nucleus. However, p53 binds to Tag and thus becomes functionally inactive. Therefore, overexpression of p53 at 34°C confirms the loss of p53 function in these temperarture sensitive cells. On the other hand, at 39°C because of an amino acid mutation, the Tag is unable to bind to p53. Therefore, p53 is functional and its quantity is maintained at low basal levels (Figure 1). The western blot analysis of three temperature sensitive cells (OSEC2, IOSE 166a, and IOSE 166h) using an anti-p53 antibody showed overexpression of p53 at 34°C, which indicates that p53 is not functional (Figure 4A). Moreover, the p53 levels dramatically decreased in cells at 39°C, showing that p53 became functional at 39°C, and thus its amounts decreased to basal levels. In Figure 4A, representative western blots of the three temperature sensitive cells showed highest p110α protein levels at 34°C where p53 is not functional. Only one day after the shift in temperature to 39°C, where p53 becomes functional, levels of p110α protein significantly decreased, and subsequently, after 5 days at 39°C the p110α protein levels were hardly detectable. Two IOSE lines with non-

functional p53 (IOSE 80pc and IOSE 397) due to immortalization with non-ts SV40 Tag, and a lung fibroblast cell line (WI38) with wild-type p53 were used as controls to rule out the effects of temperature in the observed decrease in levels of p110α protein. In IOSE lines (80pc and 397) without functional p53, p110α levels increased after the shift to the higher temperature. Interestingly, in IOSE 80pc and IOSE 397 control cells, it appears that this increase in p53 levels correlates with simultaneous increase in p110α levels. In addition, WI38 cells with wild-type p53 expressed low levels of detectable p110α protein and these levels did not change in response to an increase in temperature (Figure 4B). PTEN levels were also examined, as it was previously shown that p53 positively regulates PTEN levels (Stambolic et al., 2001). In the temperature sensitive cells, the PTEN levels increased slightly upon the shift in temperature to 39°C. Between the three temperature sensitive cells tested, the increase in PTEN levels is least obvious in the ts OSEC2 cells. In the non-ts control lines IOSE 397and WI38 cells the PTEN levels decreased concurrently with the increase in temperature, while the levels did not change in the IOSE 80pc cells.

FIGURE 4

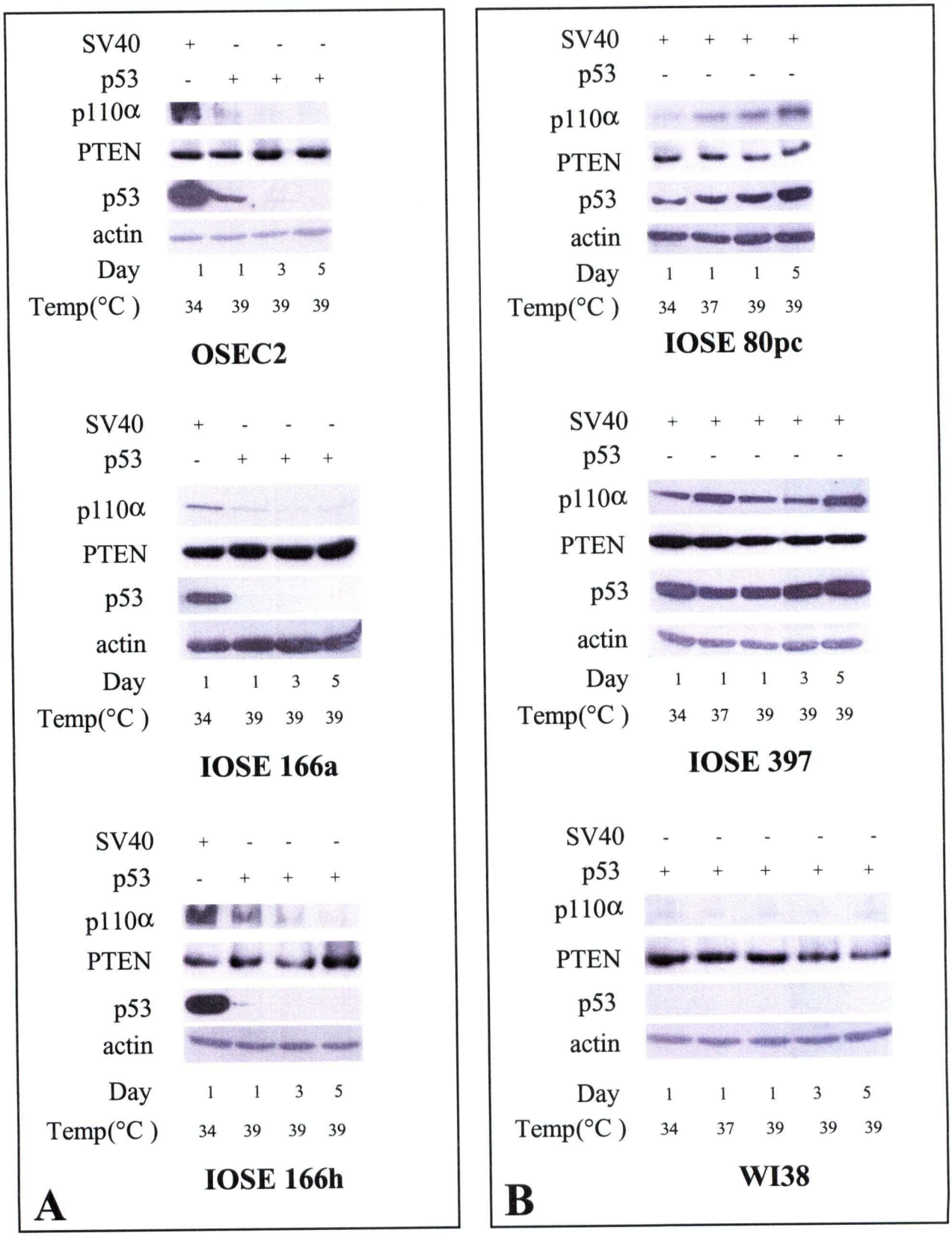
SV40 + - - -
p53 - + + +
p110α
PTEN
p53
actin
Day 1 1 3 5
Temp(°C) 34 39 39 39
OSEC2
SV40 + - - -
p53 - + + +
p110α
PTEN
p53
actin
Day 1 1 3 5
Temp(°C) 34 39 39 39
IOSE 166a
SV40 + - - -
p53 - + + +
p110α
PTEN
p53
actin
Day 1 1 3 5
Temp(°C) 34 39 39 39
IOSE 166h
A
SV40 + + + +
p53 - - - -
p110α
PTEN
p53
actin
Day 1 1 1 5
Temp(°C) 34 37 39 39
IOSE 80pc
SV40 + + + + +
p53 - - - - -
p110α
PTEN
p53
actin
Day 1 1 1 3 5
Temp(°C) 34 37 39 39 39
IOSE 397
SV40 - - - - -
p53 + + + + +
p110α
PTEN
p53
actin
Day 1 1 1 3 5
Temp(°C) 34 37 39 39 39
WI38
B

Figure 4: Effect of p53 function on p110α protein levels. Temperature sensitive cells were maintained at 34°C. Non-ts cells were maintained at 37°C. On day 0 cells were transferred to 34°C or 39°C, and lysed for protein on days 1, 3, and 5. **(A)** At 34°C, p53 levels were high indicative of non-functioning p53. After the shift to 39°C, p53 decreased to basal levels. At 34°C, the p110α levels were high and decreased after a shift in temperature to 39°C where p53 becomes functional. In addition, PTEN levels increased upon the shift in temperature from 34°C to 39°C. **(B)** Western blot analyses of non-ts control cells demonstrated that there is no decrease in the p110α levels with the increase in temperature. In these control cells, the PTEN levels remained unchanged (IOSE 80pc) or decreased (IOSE 397 and WI38) after the shift in temperature to 39°C.

3.2 p53 negatively regulates PIK3CA transcript levels

Real time quantitative RT-PCR was performed to investigate whether p53 regulates PIK3CA transcript levels. In OSEC2 temperature sensitive cells, PIK3CA transcript levels were highest at 34°C where p53 is not functional (Figure 5). Upon gain in p53 function, after a single day at 39°C, PIK3CA transcript levels decreased. Subsequently, after 5 days at 39°C the PIK3CA transcript levels significantly decreased. As a control to show that the decrease in PIK3CA transcript levels by day 5 at 39°C was not due to the lack of cell proliferation, a dish of cells was maintained at 34°C for 5 days. These cells had significantly higher PIK3CA transcript levels compared to cells at 34°C on day 1. This suggests that on day 5 the cells were still proliferating and that the decrease in PIK3CA levels observed in cells at 39°C was not due to overcrowding and contact inhibition. In fact it was observed that at the permissive temperature of 34°C, OSEC2 cells grew steadily, while after the shift in temperature to 39°C, the number of OSEC2 cells did not appear to significantly change until approximately 3 days after the switch in temperature when the number of cells rapidly declined. IOSE 397 cells with non-functional p53 and WI38 cells with wild-type p53 were used as controls to rule out the effects of temperature in the observed drop of the PIK3CA transcript levels. At the higher temperature, PIK3CA transcript levels dramatically increased, ruling out the effect of temperature alone on the observed decline in PIK3CA transcript levels. Therefore, the decrease in PIK3CA transcript levels in OSEC2 cells was due to the function of p53 and not to the increase in temperature. Moreover, the diminishing PIK3CA transcript levels were reversible. OSEC2 cells that were at 39°C for 3 days, were placed back at 34°C for another 2 days. The PIK3CA transcript levels of these cells increased to higher levels than the PIK3CA transcript levels of OSEC2 cells at 34°C on day1 (data not shown). These cells increased in cell number and reached confluency after few days at 34°C.

FIGURE 5

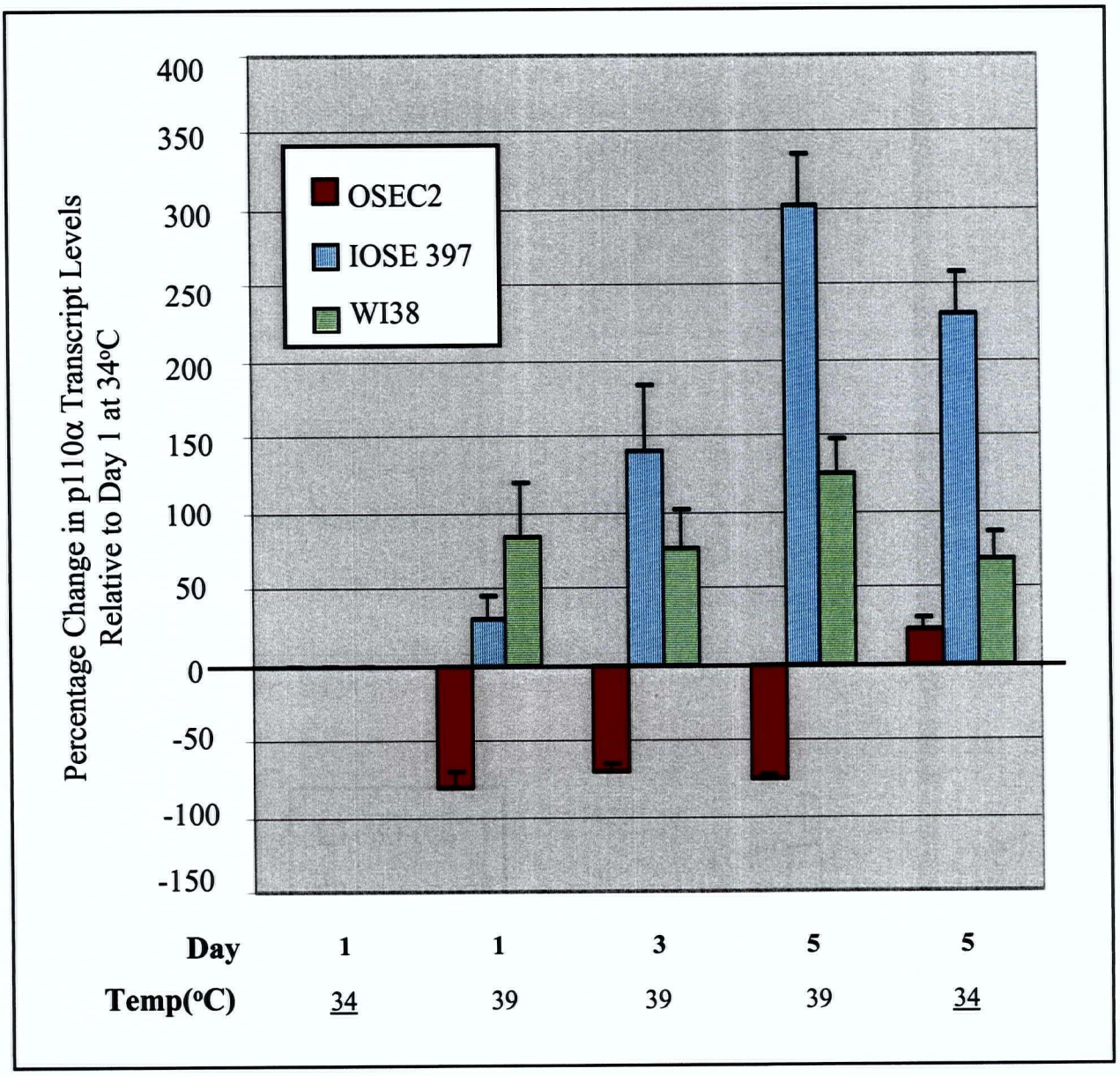

Figure 5: Effect of p53 function on PIK3CA transcript levels. Real Time Quantitative RT-PCR demonstrated that upon shift in temperature to 39°C where p53 is functional, PIK3CA transcript levels significantly decreased in the ts OSEC2 cells (solid red bars). In non-ts control cells, IOSE 397 and WI38 (vertical blue and horizontal green bars respectively), PIK3CA transcript levels increased with an increase in temperature. All the cell lines had higher PIK3CA transcript levels on day 5 at 34°C compared to day 1 at 34°C.

3.3 p53 negatively regulates PI3K activity

To investigate whether the observed decrease in p110α protein and PIK3CA transcript levels had an effect on the PI3K activity, levels of phosphorylated AKT were determined by Western Blot. OSEC2 cells were stimulated with varying concentrations of FBS for 1 hour. Western blot analysis showed that OSEC2 cells had the highest level of P-AKT with 15% serum stimulation (Figure 6A top blot). Moreover, OSEC2 cells at 39°C, even though they had higher P-AKT levels after stimulation with 15% FBS, they had lower levels of P-AKT compared to cells at 34°C. As controls, IOSE 397 and WI38 cells were placed under the same conditions as OSEC2 cells. IOSE 397 and WI38 cells showed an increase in P-AKT levels with 15% serum stimulation, however the cells at 39°C showed an increase in P-AKT levels relative to cells at 34°C (bottom two blots of Figure 6A). Furthermore, a 1 hour treatment with 20μM concentration of the specific PI3K inhibitor, LY294002, prior to serum stimulation blocked phosphorylation of AKT at both temperatures in all cell lines.

To determine treatment time that results in maximal phosphorylation of AKT, OSEC2 cells were stimulated with 10% serum for 15, 30 and 60 minutes. Western blot analysis (Figure 6B) of the cell lysates, showed that phosphorylated AKT levels increased with an increase in stimulation time. The cells at 39°C, although they have increased P-AKT levels after 60 minutes of treatment, had lower levels of P-AKT compared to cells at 34°C. These findings show that there is less phosphorylation of AKT when p53 is functional.

The effect of p53 function on P-AKT levels was studied in more detail, by looking at OSEC2 cells on days 1 and 3 after the shift in temperature from 34°C to 39°C with either 10% serum stimulation or no (0.5%) serum stimulation. Western blot analysis of OSEC2 cells shows that at 39°C, where p53 is functional, cells had lower P-AKT levels after serum stimulation (Figure 6C). Total AKT levels did not change; therefore, the decrease in P-AKT levels at 39°C

suggests that AKT is not as readily phosphorylated. IOSE 397 and WI38 cells were used as controls to rule out the effect of temperature alone on the decrease in P-AKT levels. In these cells, levels of P-AKT did not decrease, but actually increased with the shift in temperature to 39°C. The western blot analysis for P-AKT levels showed decreased PI3K activity concomitant with the gain in p53 function, the decrease in p110α, and the increase in PTEN protein levels.

FIGURE 6(A and B)

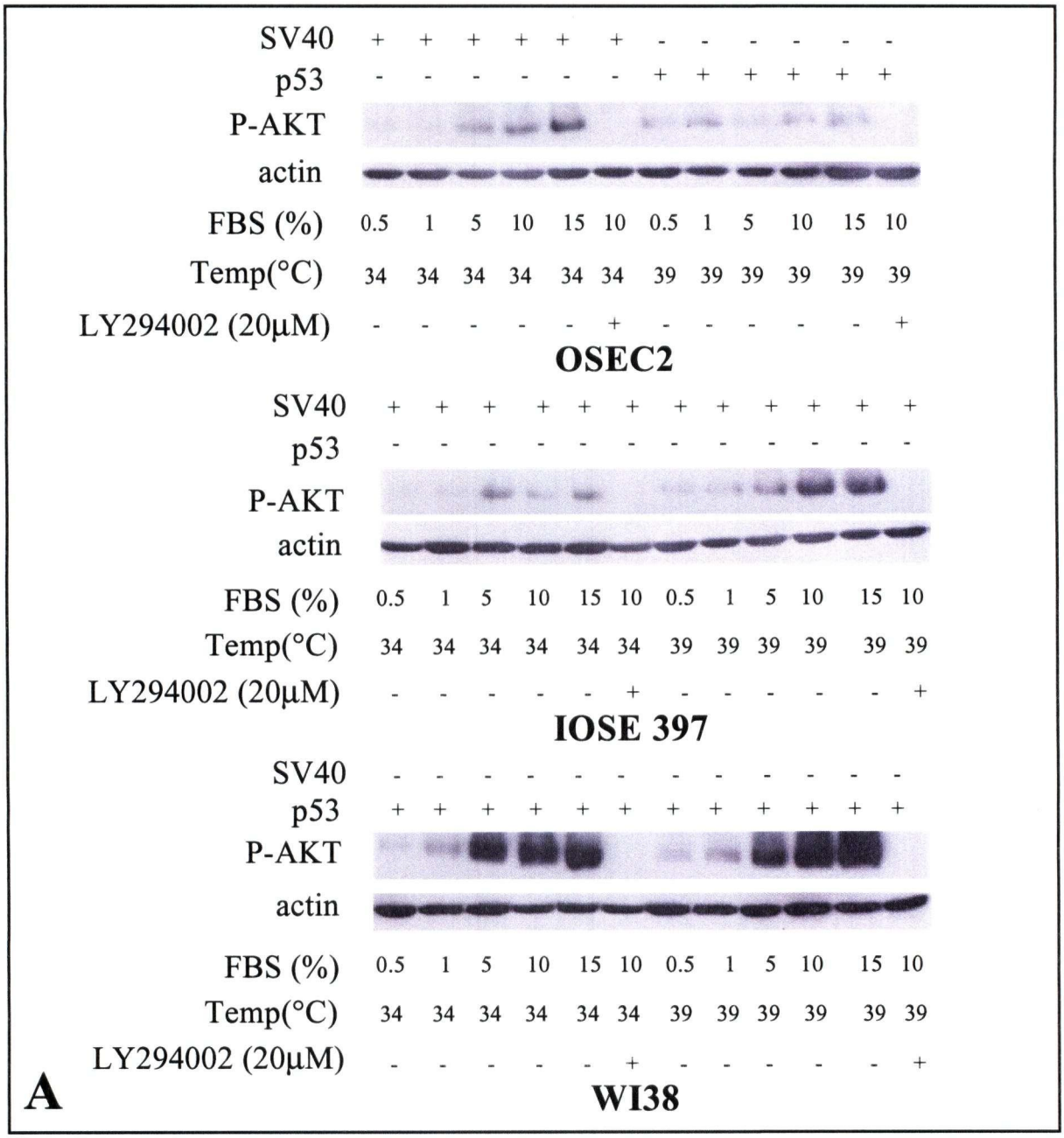

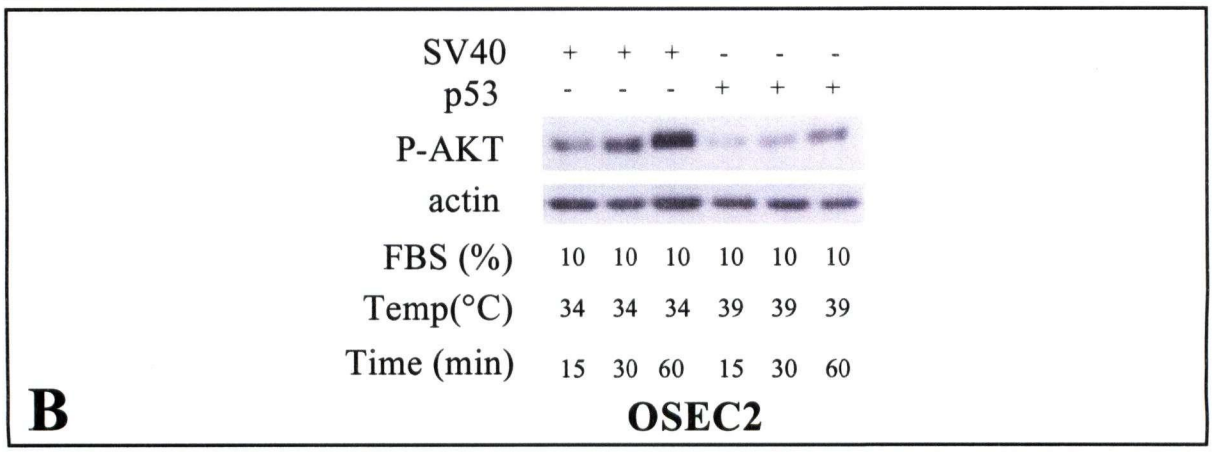

FIGURE 6(C)

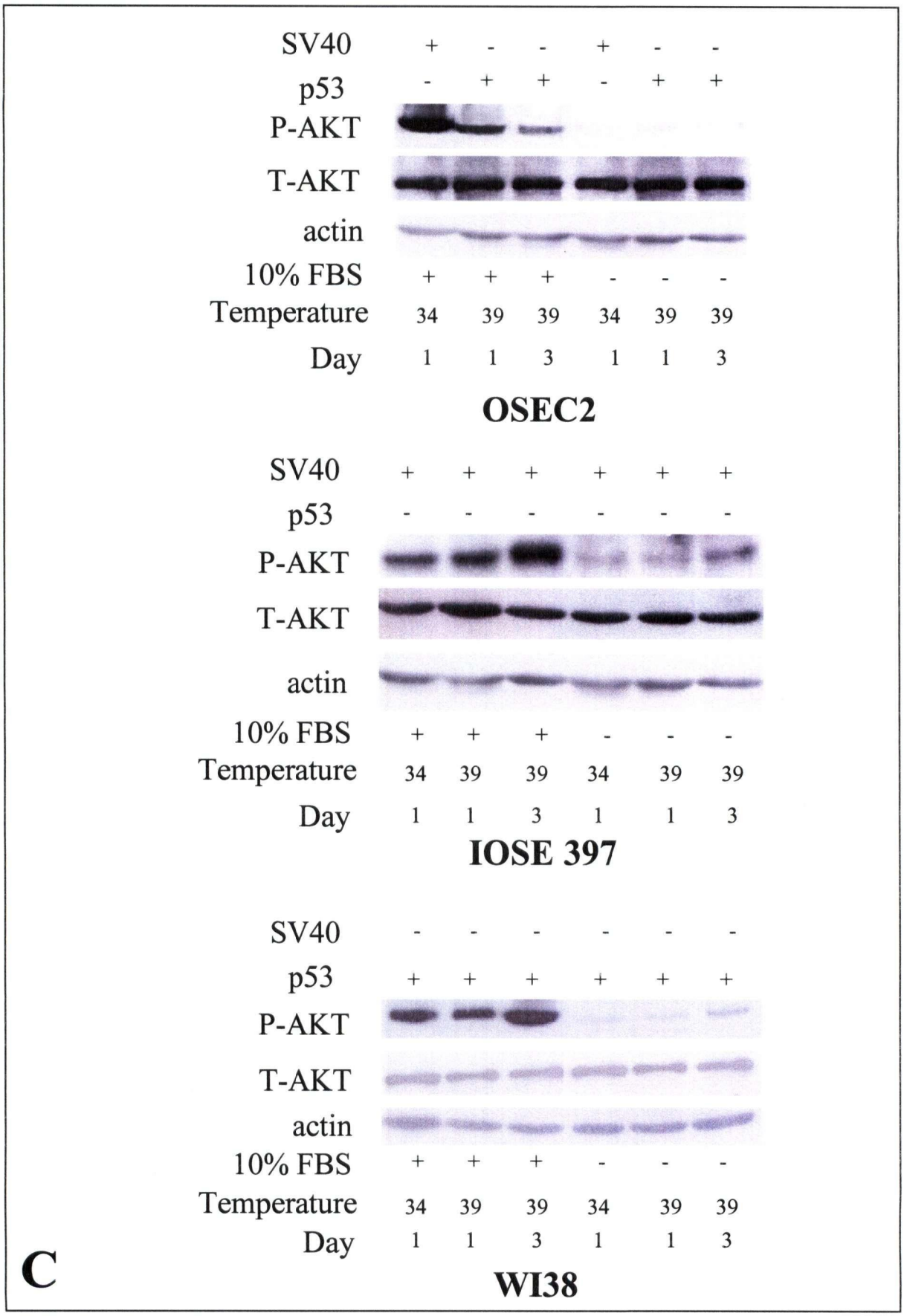
SV40 + - - + - -
p53 - + + - + +
P-AKT
T-AKT
actin
10% FBS + + + - - -
Temperature 34 39 39 34 39 39
Day 1 1 3 1 1 3
OSEC2
SV40 + + + + + +
p53 - - - - - -
P-AKT
T-AKT
actin
10% FBS + + + - - -
Temperature 34 39 39 34 39 39
Day 1 1 3 1 1 3
IOSE 397
SV40 - - - - - -
p53 + + + + + +
P-AKT
T-AKT
actin
10% FBS + + + - - -
Temperature 34 39 39 34 39 39
Day 1 1 3 1 1 3
C
WI38

Figure 6: Effect of p53 function on PI3K activity/AKT phosphorylation. (A) At both the permissive and non-permissive temperatures, P-AKT levels were maximal after 15% FBS stimulation for 1 hour. Temperature sensitive OSEC2 cells at 39°C with functional p53 had lower P-AKT levels compared to cells at 34°C. Control IOSE 397 and WI38 cells did not show decreasing P-AKT levels after an increase in temperature. **(B)** Maximum AKT phosphorylation was observed after 60 minutes of stimulation with 10% FBS. P-AKT levels were lower at 39°C where p53 is functional compared to at 34°C where p53 was bound to Tag and not functional. **(C)** After a shift in temperature to 39°C, less AKT was phosphorylated in the OSEC2 cells while the total AKT levels remained unchanged. In control non-ts IOSE 397 and WI38 cells, the P-AKT levels actually increased after a shift in temperature to 39°C.

For a more direct read out of PI3K activity, an AKT-PH-GFP construct obtained from Dr. Gordon Mills (Houston ,Texas) was used to transiently transfect OSEC2 cells at 34°C. This construct encodes the PH domain of AKT linked to a GFP tag. When active, PI3K phosphorylates PtdIns(4,5)P_2 to PtdIns(3,4,5)P_3. AKT protein is recruited to the membrane through binding of its PH domain to PtdIns(3,4,5)P_3 (Klippel et al., 1997). Once at the membrane, AKT is phosphorylated by PDKs to become activated. Membrane localization of the GFP tag would indicate localization of AKT-PH domain to the membrane where it can bind to PtdIns(3,4,5)P_3 . This membrane localization in turn demonstrates PI3K activity. On the other hand, cytoplasmic localization of the fusion AKT-PH-GFP protein indicates the absence of PI3K activity. After 60 minutes of stimulation with 10% serum, OSEC2 cells at 34°C had brightly stained spots indicating strong membrane localization of the AKT-PH-GFP (Figure 7A, top middle). In comparison, the AKT-PH-GFP was not targeted to the membrane in the non-stimulated OSEC2 cells at 34°C (Figure 7A, top left). Moreover, the OSEC2 cells at 39°C after serum stimulation had significantly less membrane localization. On days 3 and 5 at 39°C, the OSEC2 cells were also tested for AKT-PH-GFP localization, however, by this time the expression of the protein was very low, and thus the level of localization could not be determined accurately. Therefore, localization of the AKT-PH construct via its GFP tag was only studied on day1 at the two different temperatures. In the OSEC2 cells treated with 20μM of LY294002 for 1 hour before serum stimulation, there was no membrane localization in the majority of the cells, but weak localization in some cells (Figure 7A, top right). The percentage of cells with strong membrane localization was significantly higher in stimulated OSEC2 cells at 34°C compared to serum starved cells at 34°C and the OSEC2 at 39°C with or without serum stimulation (Figure 7B). The decrease in membrane localization at 39°C showed that there are lower levels of PI3K activity when p53 is functional.

FIGURE 7 (A)

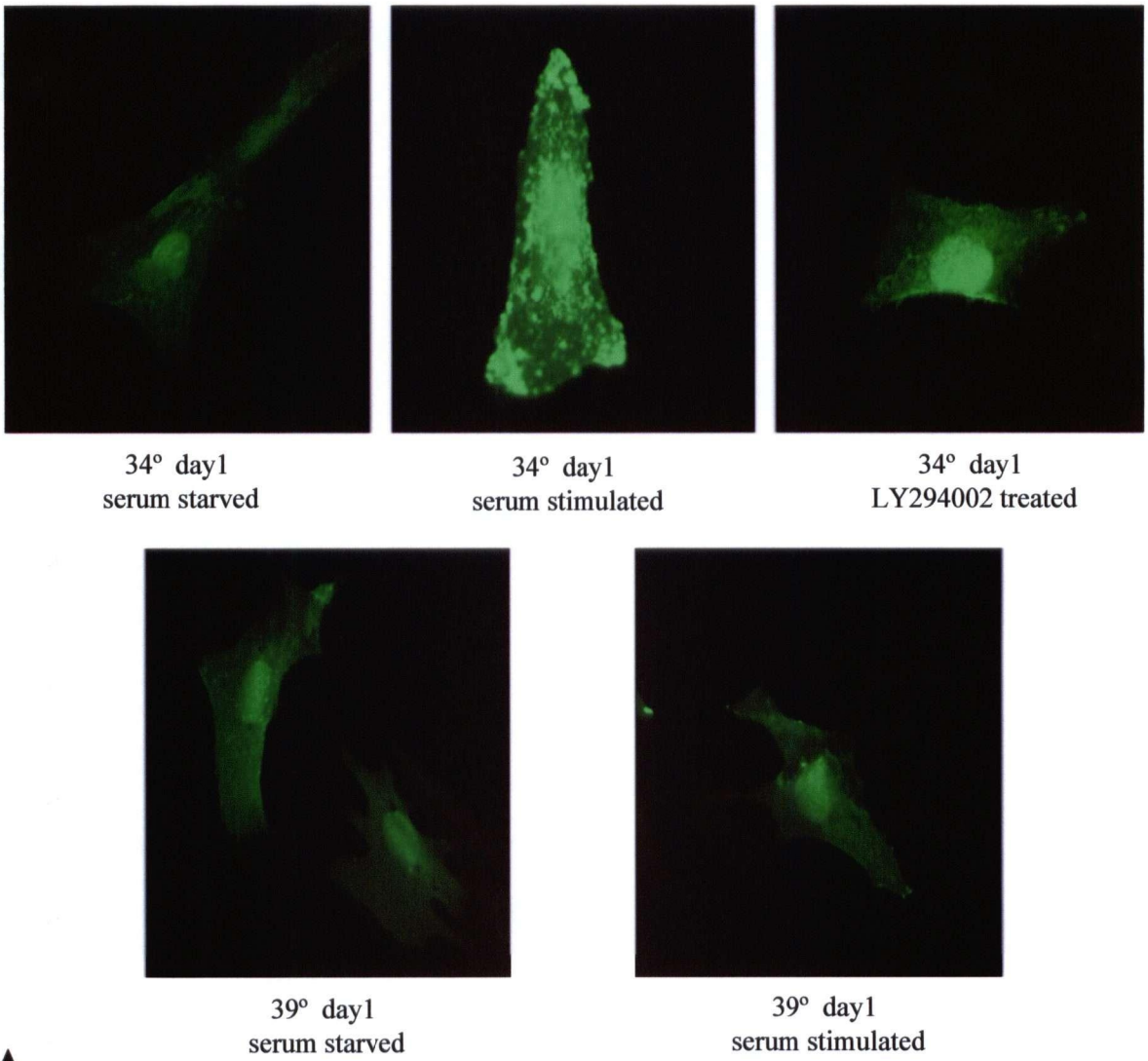
34° day1
serum starved
34° day1
serum stimulated
34° day1
LY294002 treated
39° day1
serum starved
39° day1
serum stimulated
A

FIGURE 7 (B)

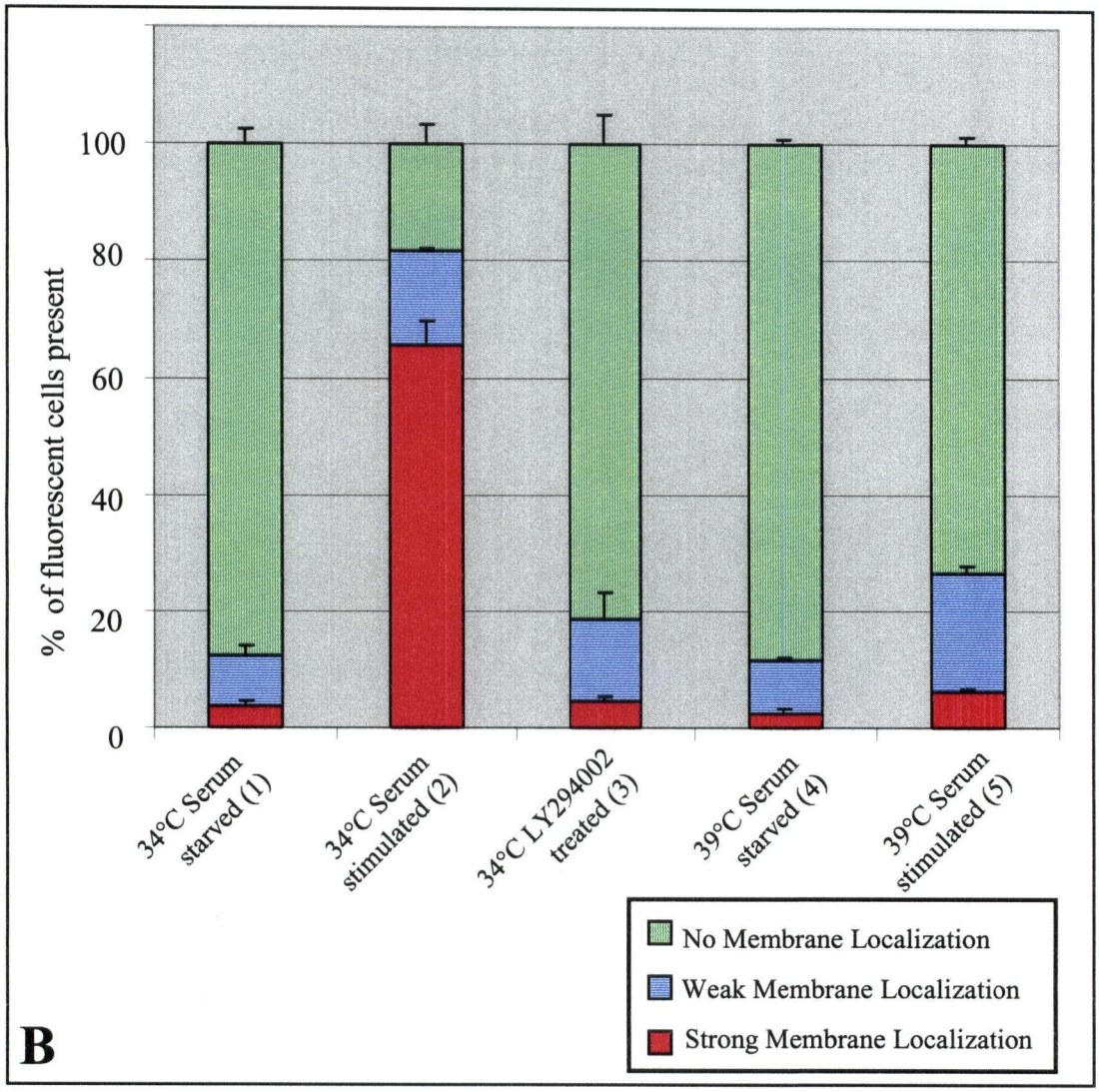

Figure 7: Effect of p53 function on PI3K activity/AKT-PH-GFP membrane localization. A GFP tagged AKT-PH domain construct was transiently transfected into OSEC2 cells at 34°C. 24 hours after transfection the cells were moved to 39°C or maintained at 34°C. 24 hours after the shift in temperature, the cells were serum starved for 4 hours and subsequently either stimulated with 10% serum for 1 hour, or maintained without serum. For the LY294002 treated cells, 20μM of the drug was added the last hour of the serum starvation, and then the cells were stimulated with 10% FBS for 1 hour. **(A)** At 34°C where p53 is non-functional, the AKT-PH-GFP protein was targeted to the membrane after serum stimulation (top middle), indicating that there is PIP3 at the membrane for the AKT-PH domain to bind. In the absence of serum stimulation, the staining in the OSEC2 cells at 34°C (top left) and 39°C (bottom left) was not localized to the membrane. There was some localization of AKT-PH domain to the membrane in the cells treated with LY294002 for 1 hour (top right), and in the OSEC2 cells at 39°C after serum stimulation (bottom right). **(B)** The percentage of cells with strong, weak and no membrane localization under the various conditions tested are illustrated. After serum stimulation the cells at 34°C had the highest percentage of cells with strong membrane localization.

3.4 Decrease in proliferation upon gain in p53 function

PI3K plays a role in cell proliferation and cell cycle regulation. Because p110α protein levels and PI3K activity decrease upon gain in p53 function, we wanted to investigate the effect of this on proliferation. Ki-67 is a proliferative marker present in all active parts of the cell cycle, and absent when the cells enter G0 (Scholzen and Gerdes, 2000). Figure 8A demonstrates OSEC2 cells stained for Ki-67. After only a day at 39°C, coincident with the decline in p110α protein levels, PIK3CA transcript levels, and PI3K activity, there was a significant drop in number of Ki-67 positive nuclei. After 5 days at 39°C, there were almost no proliferating cells present. In addition, treatment of OSEC2 cells at 34°C with 20μM of LY294002 for 1 hour, resulted in a decrease in the number and intensity of proliferating cells, although not to the same extent as the change in p53 function. In addition, IOSE 397 and WI38 cells were used as controls to rule out the effect of temperature on the observed drop in proliferation in the OSEC2 cells. At 39°C, IOSE 397 (Figure 8B) and WI38 (Figure 8C) cells did not show decreased levels of Ki-67 staining. These studies suggest that when p53 becomes functional, and p110α levels and PI3K activity decrease, the cells are less proliferative.

FIGURE 8 (A)

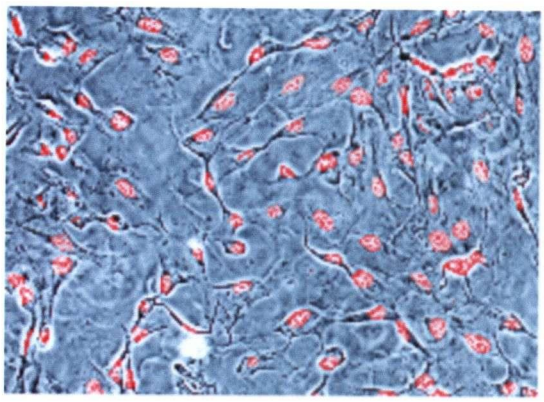

OSEC2 day 1 at 34°

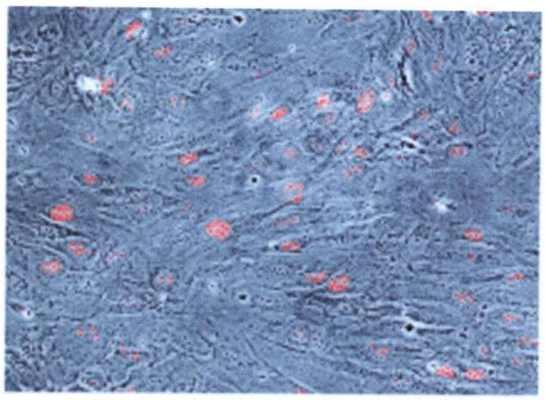

OSEC2 day 1 at 39°

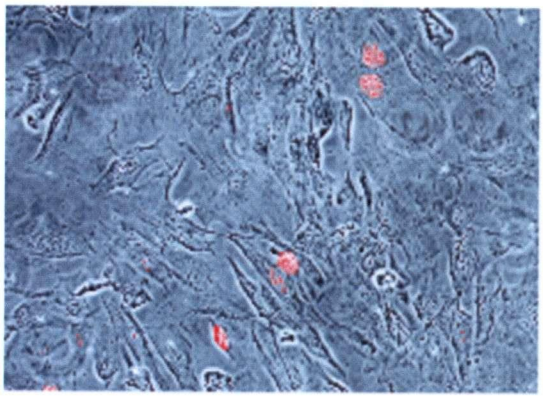

OSEC2 day 3 at 39°

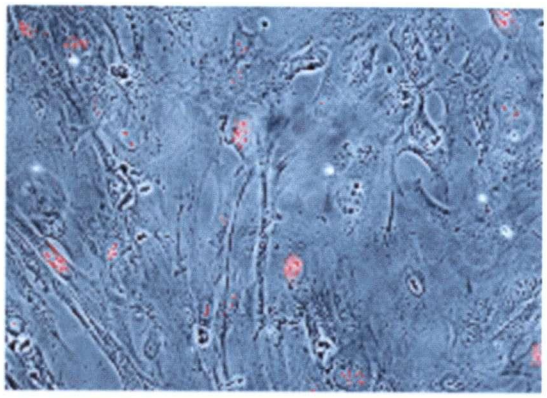

OSEC2 day 5 at 39°

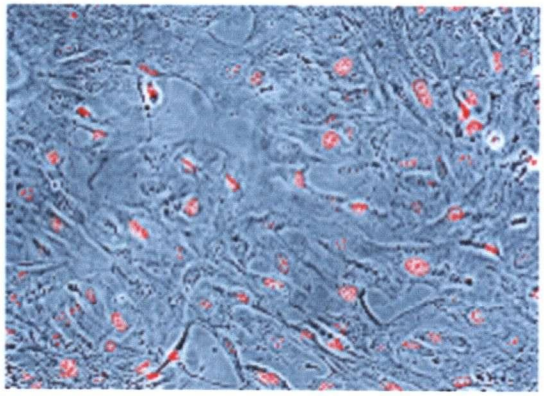

OSEC2 day 1 at 34°
LY294002 (20μM) treatment for 1 hour

A

FIGURE 8 (B and C)

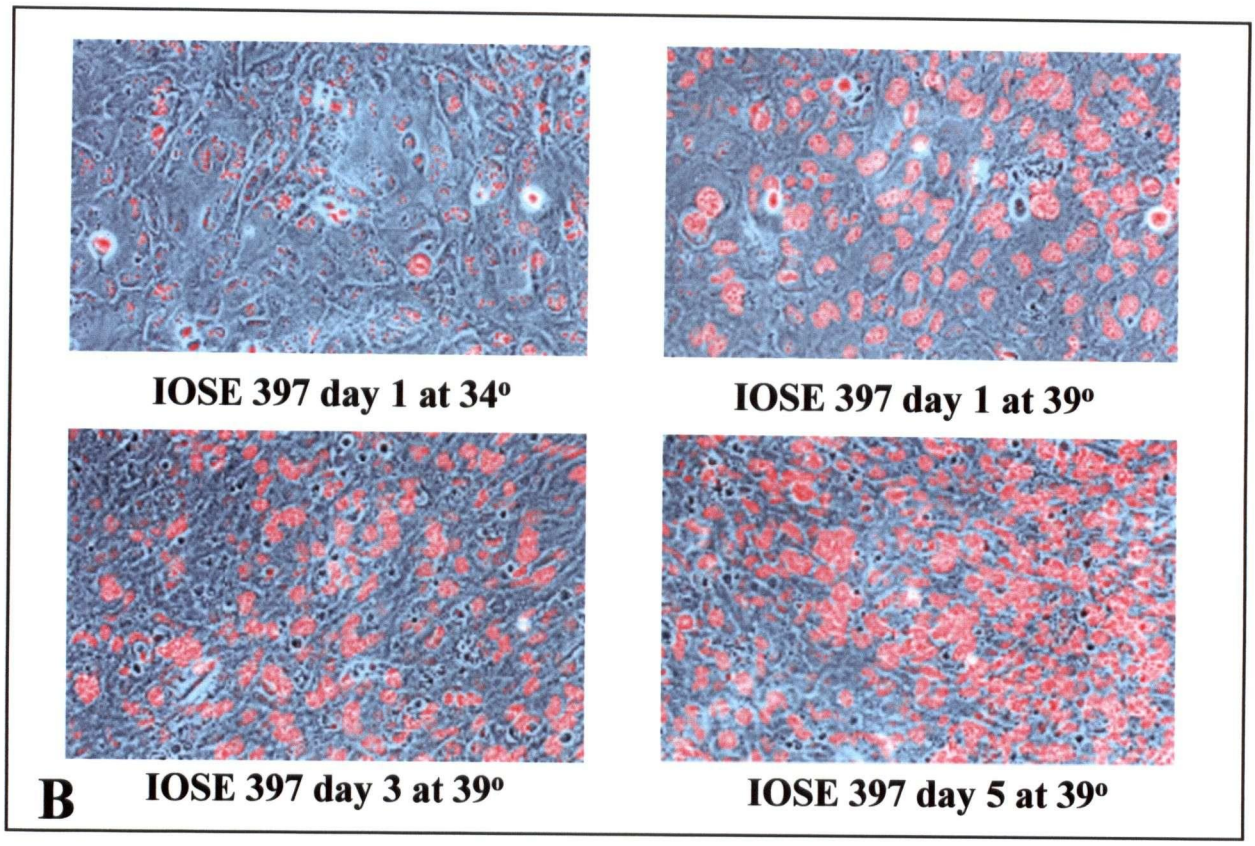

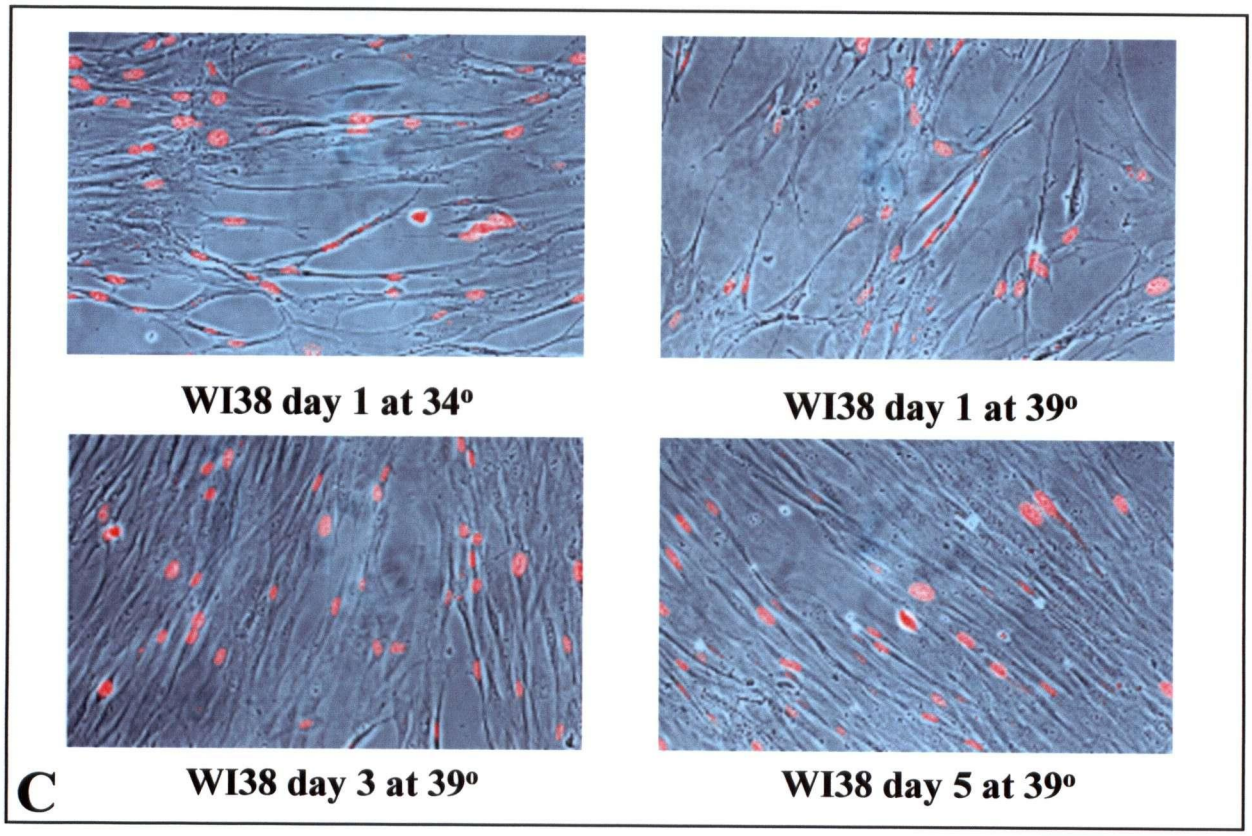

Figure 8: Effect of p53 function on proliferation. (A) At 34°C, 100% of the nuclei of OSEC2 cells stained positive (red) for Ki-67 antigen, indicating that the cells were proliferating. At 39°C, where p53 becomes functional, the number and intensity of the positive Ki-67 nuclei decreased dramatically. OSEC2 cells treated with LY294002 for 1 hour, had reduced number of positively stained nuclei although not as dramatically as after the gain in p53 function. Ki-67 staining of non-temperature sensitive IOSE 397 **(B)** and WI38 **(C)** cells did not indicate a decrease in the number of proliferating cells with the shift in temperature to 39°C.

3.5 Increase in apoptosis upon gain in p53 function

Since AKT is an important regulator of apoptosis, we investigated whether the decrease in PI3K activity and the subsequent decrease in P-AKT levels upon gain in p53 function plays a role in apoptosis. The cells were grown on coverslips and fixed on day 1 at 34°C and days 1, 3 and 5 at 39°C. The nuclear morphology of the cells was observed after Hoechst 33258 staining (Figure 9A). The OSEC2 cells had more apoptotic figures at 39°C than at 34°C. In addition, a quantitative assay confirmed that levels of apoptosis were significantly higher in OSEC2 cells at 39°C, with functional p53, compared to OSEC2 cells at 34°C with non-functional p53 (Figure 9C). OSEC2 cells at 34°C treated with 20μM of LY294002, also had high levels of apoptosis. These studies show that when p53 becomes functional there was more apoptosis, coincident with the drop in p110α protein, PIK3CA transcript, and P-AKT levels. Compared to OSEC2 cells at 34°C, the percentage of apoptotic cells was significantly higher in OSEC2 cells at 39°C. However, percentage of apoptotic cells, on days 3 and 5 after the shift in temperature decreased relative to cells on day 1 at 39°C (Figure 9C). In addition, nuclear morphology of WI38 cells was analyzed. However, there was no apparent apoptotic nuclear morphology in the WI38 cells (Figure 9B). The IOSE 397 cells had an irregular nuclear morphology and thus could not be used for this analysis. Moreover, the quantitative cell death detection ELISA of the IOSE 397 and WI38 cells at 34°C and 39°C determined that levels of apoptosis in IOSE 397 and WI38 cells at 34°C and 39°C were not significantly different. This indicates that the increase in apoptosis observed in OSEC2 cells was not an effect of an increase in temperature alone, but due to the gain in p53 function.

FIGURE 9 (A and B)

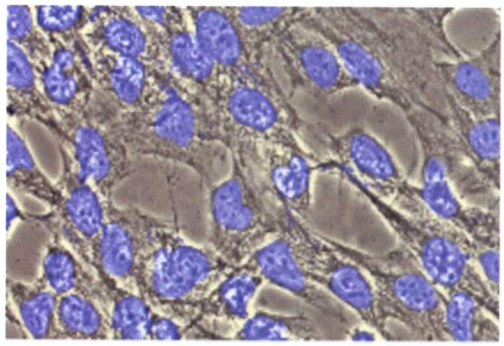

OSEC2 day 1 at 34°

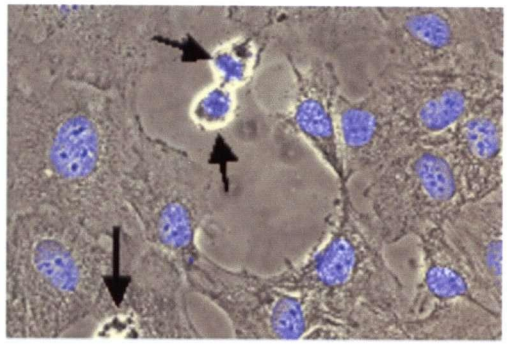

OSEC2 day 1 at 39°

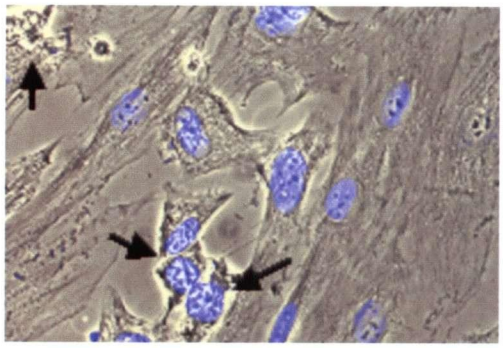

OSEC2 day 3 at 39°

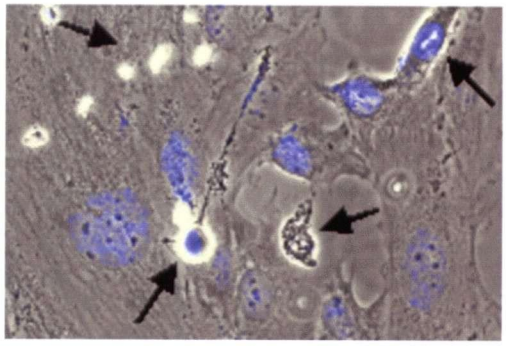

OSEC2 day 5 at 39°

A

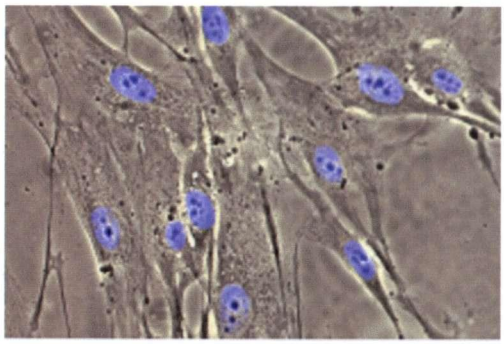

WI38 day 1 at 34°

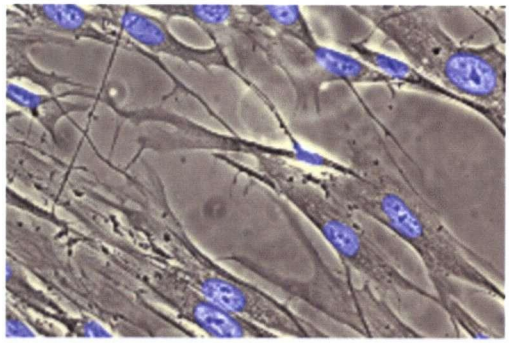

WI38 day 1 at 39°

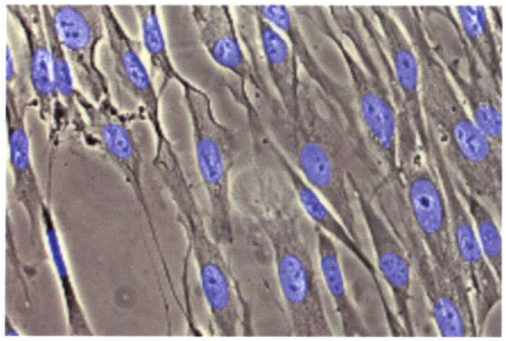

WI38 day 3 at 39°

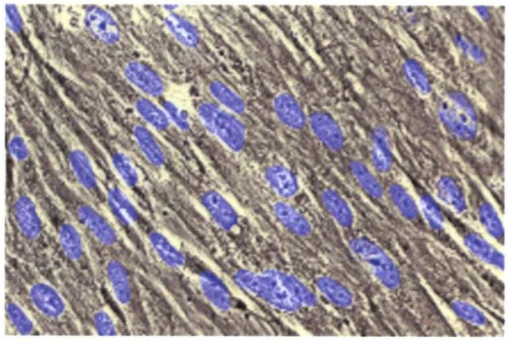

WI38 day 5 at 39°

B

FIGURE 9 (C)

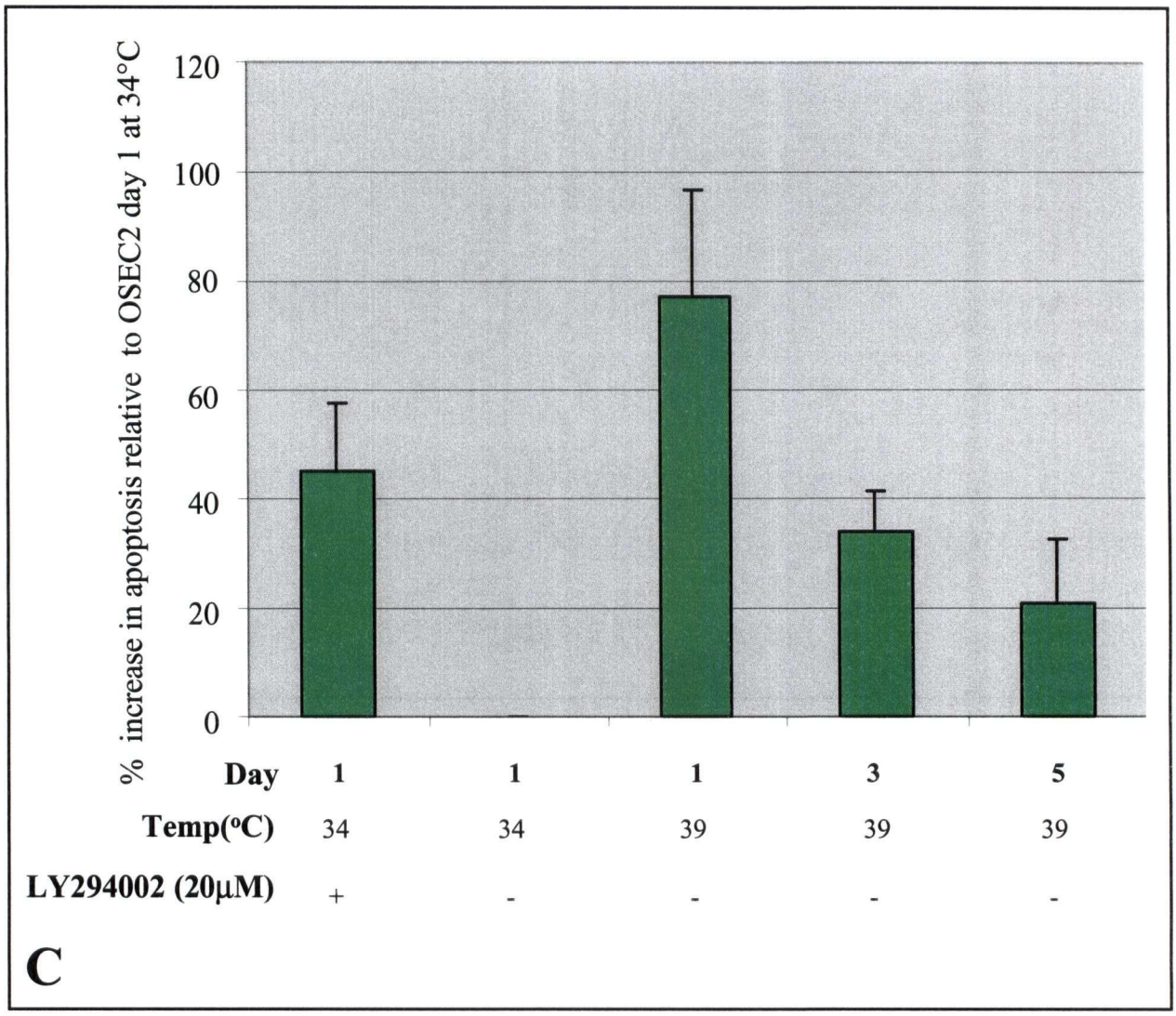

Figure 9: Effect of p53 function on apoptosis. Nuclear morphology was analyzed after Hoechst 33258 staining of cells grown on coverslips under different conditions. **(A)** OSEC2 temperature sensitive cells at 39°C had increased numbers of apoptotic nuclei, indicated with black arrows. **(B)** WI38 non-temperature sensitive control cells did not show any apoptotic nuclei after the shift in temperature from 34°C to 39°C. **(C)** Cell death detection ELISA was performed to quantify levels of apoptosis of the cells. The percentage of apoptotic cells in OSEC2 cells at 39°C was significantly higher than OSEC2 cells at 34°C. However, the percentage of apoptotic OSEC2 cells at 39°C decreased after 3 and 5 days compared to only one day at 39°C. In addition, treatment with LY294002 resulted in increased apoptosis.

3.6 Infection of wild-type p53 into cancer cells reduced the p110α protein levels

SKOV3 cells are Null for the p53 gene, and thus do not express the p53 protein. To determine the optimum titre of the p53 adenovirus for infection, SKOV3 cells were infected with varying amounts of the p53 adenovirus. GFP adenovirus was used as control to determine efficiency and cytotoxic effects of the adenovirus infection (Figure 10A). Western blot analysis of the cell lysates indicated that SKOV3 control cells without infection and with GFP adenoviral infection had higher levels of p110α protein compared to SKOV3 cells infected with p53 adenovirus. Therefore, after functional p53 was overexpressed in the cells, the p110α protein levels decreased, confirming regulation of p110α levels by p53. Increasing the concentration of p53 adenovirus added to the cells, increased the levels of p53, and in turn decreased the levels of p110α in the cells (Figure 10A). There was no apparent increase in cytotoxicity in the cells with higher adenovirus titer within the time period tested (48 hours). Furthermore, it appears that at volumes higher than 100μl of the virus, the p53 levels reached saturation, and did not significantly change. Therefore, for the remainder of the infections, 100μl of the p53 adenovirus diluted in 1ml of medium was used.

Table 3 lists the p53 staus of all the cancer lines tested as well as the type of mutation they harbour. The average copy number of the PIK3CA gene of the cancer lines that were known are also listed. MCF-7 breast cancer line, and A2780 and OVCAR4 ovarian cancer lines have wild-type p53 protein and pathways. Infection of p53 into these cells resulted in a decrease in p110α protein levels compared to uninfected and GFP infected control cells (Figure 10B). SKOV3, CaOV3, OVCAR3, OVCAR5, and OVCAR8 ovarian cancer cells have mutated p53 protein. In these cells, overexpression of wild-type p53 also resulted in a decrease in p110α levels compared to control uninfected and GFP infected cells (Figure 10B).

CaOV3 was the only cancer cell line tested that demonstrated phenotypic changes within the 48 hours after infection with p53 adenovirus. Some CaOV3 cells rounded up and detached from the culture dish. This phenotypic change was not observed in CaOV3 cells infected with the control GFP adenovirus. In addition, none of the other cancer lines demonstrated a morphological change after infection. All the cancer cells tested had close to 100% infection efficiency with the exception of OVCAR5 and OVCAR8 cells, which had approximately 50% infection efficiency as determined by the GFP adenovirus control.

In all cancer lines tested, regardless of their p53 status, p110α levels decreased after introduction of wild-type p53. The decrease in p110α levels in OVCAR3 cells, although evident, was less obvious compared to the other seven cancer lines tested (Figure 10B).

Table 3: p53 Status of Some Cancer Lines

Cancer Lines	p53 Status	Type of Mutation	Reference	Avergae PIK3CA Copy Number
A2780	WT	None	Brown et al., 1993	Unknown
CaOV3	Mutant	Nonesense	Yaginuma and Westphal, 1992	6.7
SKOV3	Mutant	Missense	Yaginuma and Westphal, 1992	3
OVCAR3	Mutant	Missense	Yaginuma and Westphal, 1992	6.1
OVCAR4	WT	None	O'Connor et al., 1997	Unknown
OVCAR5	Mutant	Other	O'Connor et al., 1997	Unknown
OVCAR8	Mutant	Other	O'Connor et al., 1997	Unknown
MCF-7	WT	None	Takahashi et al., 1993	2

FIGURE 10 (A and B)

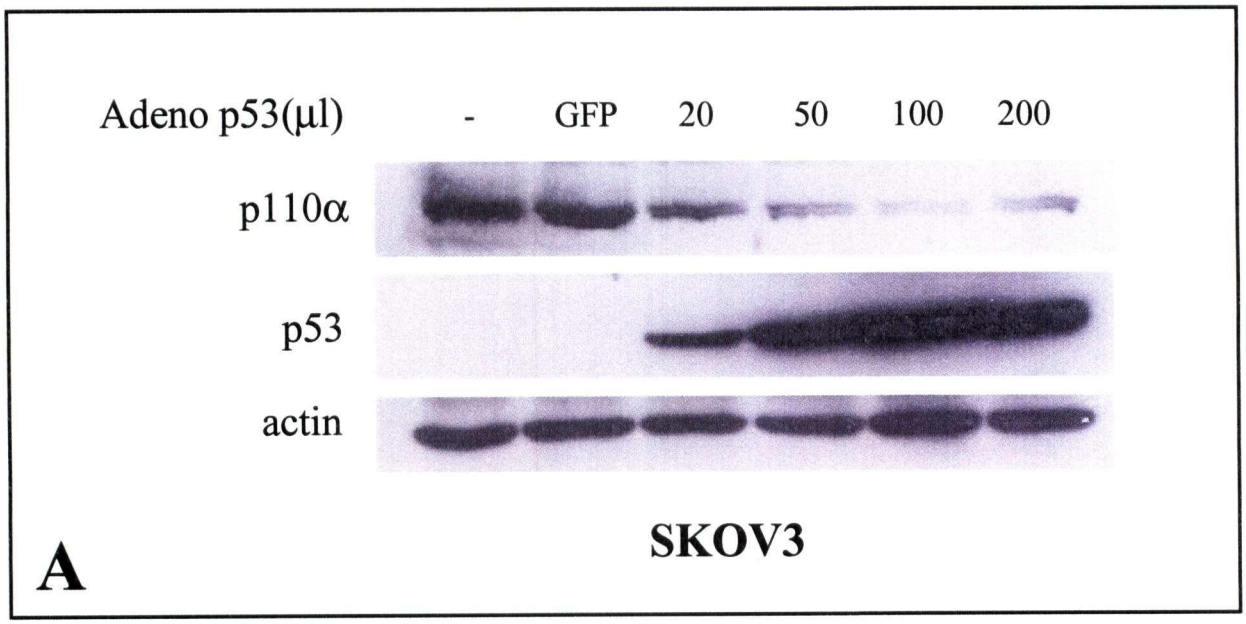

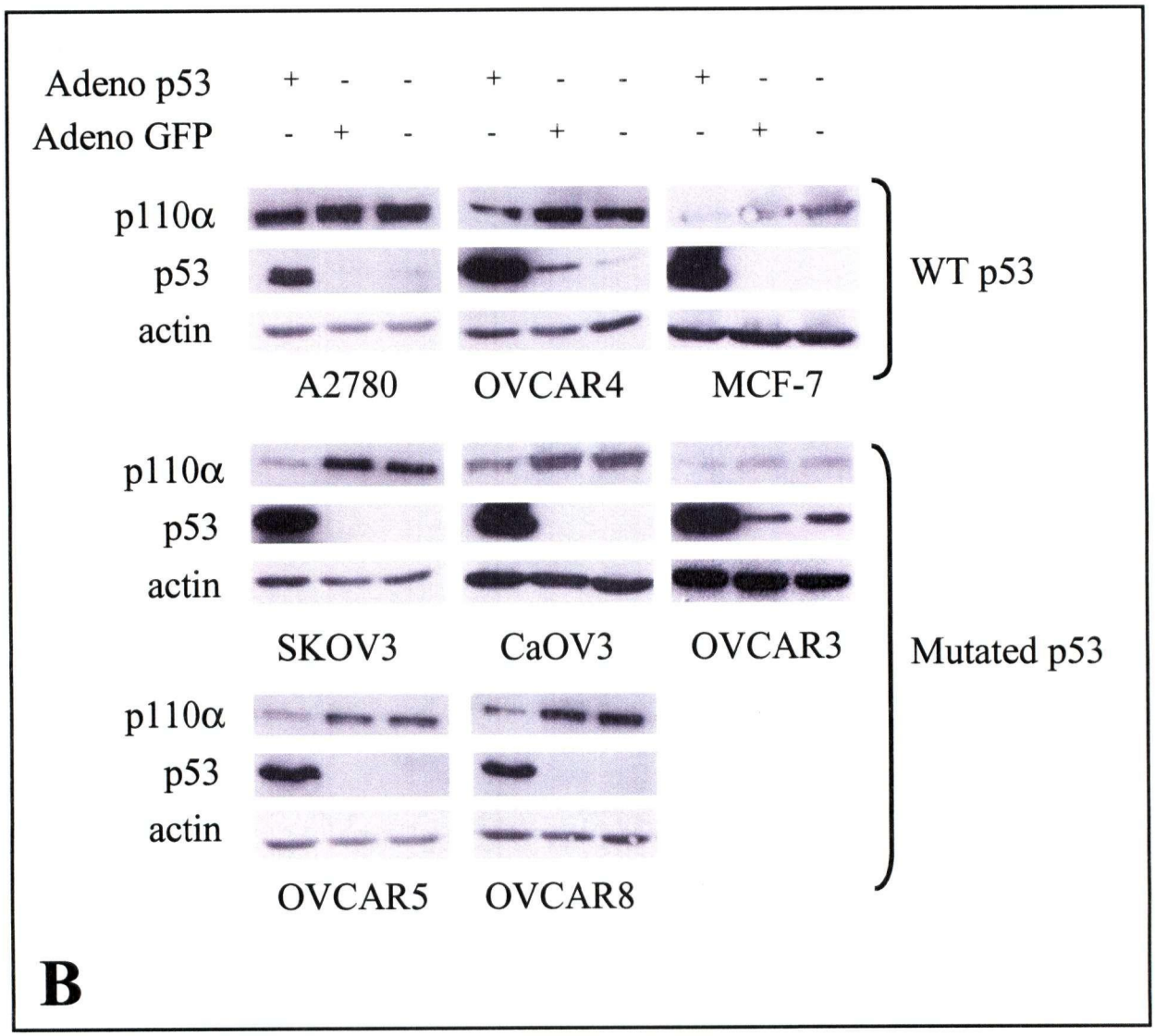

Figure 10: Effect of overexpression of wild-type p53 on p110α levels in cancer cells. (A) SKOV3 cells were infected with various amounts of p53 adenovirus, as well as control GFP adenovirus. SKOV3 cells with increasing titers of p53 adenovirus showed a decrease in p110α protein levels. **(B)** A wild-type p53 breast cancer (MCF-7), two wild-type p53 ovarian cancer, and five p53 mutant ovarian cancer cell lines were infected with wild-type p53 and GFP adenoviruses. In all of the cancer lines tested, the p110α levels decreased after the introduction of a functional p53.

3.7 Immunohistochemistry of inclusion cysts and deep invaginations did not show a conclusive correlation between p53 and p110α levels

Previous studies have demonstrated positive p53 staining in epithelium lining of inclusion cysts. To determine whether a correlation between p110α and p53 levels can be observed in tissue, immunohistochemistry on paraffin-embedded ovarian sections were performed. p110α levels were higher in the epithelium lining of some of the inclusion cysts, compared to the epithelium on the surface of the ovary (data not shown). However, p53 staining of serial sections of the same ovaries stained for p110α did not show p53 positivity.

We obtained additional paraffin-embedded sections from Dr. Schlosshauer (Mount Sinai School of Medicine, New York, NY) who previously detected p53 positivity, although weak and focal, in cells lining inclusion cysts and deep invaginations that were hyperplastic or dysplastic in ovaries removed prophylactically from women (Schlosshauer et al., 2003). Three of the five sections tested, belonged to women with previous breast cancer history, while the other two sections were BRCA positive. Dr. Schlosshauer provided us with parallel sections of the same ovaries in which he had detected p53 positive cells. Double-staining of these sections with anti-p53 and anti-p110α antibodies did not detect p53 positive cells, except for one case in which two p53 positive cells in an inclusion cyst were detected. These cells expressed high levels of p53, and the staining was cytoplasmic and not nuclear. In addition, these two cells expressed high p110α levels. However, other cells in the same inclusion cyst without p53 staining also had high p110α levels. Therefore, it would be difficult to show a correlation between p53 and p110α levels in these benign ovarian tissues with such limited number of p53 positive cells. Moreover, the already cut sections from Dr. Schlosshauer were over three years old and therefore the p53 antigen may have been degraded, which may account for our inability to detect p53. Therefore, more sections need to be studied in order to produce meaningful results.

3.8 Amplification of the 5' end of PIK3CA cDNA identified the presence of a new exon

The promoter region of the PIK3CA gene is not yet identified. In an attempt to look at direct interaction of p53 with the PIK3CA promoter, we required the knowledge about the location of the promoter. In order to identify the promoter, we first needed to identify the transcription start site. Abundance of CpG dinucleotides in the human genome is a dominant characteristic of promoter sequences (Wasserman and Sandelin, 2004). Approximately 60% of human promoters are located proximally to CpG islands (Gardiner-Garden and Frommer, 1987). Based on the UCSC genome browser, there was the presence of a CpG island 50,473 bps upstream of the translational start site (coordinates: chr3:180,348,768-180,399,240; May 2004 Human Assembly). Moreover, based on EST sequencing and a curated RefSeq cDNA sequence, there exists a putative first exon 50,228 bps upstream of the currently identified first exon (coordinates: chr3:180,349,013-180,399,240; May 2004 Human Assembly). The combination of transcript data and the CpG island suggested a possible location for the PIK3CA gene promoter. To confirm the presence of the upstream first exon and to determine the transcript 5' untranslated region (5'UTR), we used the Rapid Amplification of cDNA Ends technique (RACE).

Prior to RACE analysis the quality of gene specific primers (GSPs) were investigated using cDNA that was reverse transcribed from RNA obtained from OSEC2 cells (Figure 11A). The positions of GSP1, GSP2 and GSP3 are shown in Figure 3 of the methods section. GSP4 and GSP5 are forward primers that bind to exon1 and the RefSeq predicted exon respectively. All primer sets gave the appropriately sized bands. The amplification of the 5'end of cDNA was performed using the GSPs. The control reactions performed for RACE are demonstrated in Figure 11B. The first set of control reactions used cDNA synthesized from control RNA provided in the kit. The second set of control reactions used a combination of the control cDNA

and sample cDNA and assessed the presence of contamination in the test sample cDNA. Reverse control GSP2 and forward control GSP3 were used for amplification of the control reactions (Figure 11B). All of the control reactions produced gene products of the predicted size (500 bps). The control tailed cDNAs and no tail cDNAs (negative control) were PCR amplified with control GSP3 and the AAP that binds to the newly synthesized homopolymeric tail of cDNA. The presence of 711 bp bands in the tailed cDNA, and the mixture of tailed control cDNA and tailed sample cDNA, indicate a successful tailing reaction, and confirm the absence of contaminants in the test sample cDNA (Figure 11C). The tailed OSEC2 sample was PCR amplifed with GSP2 and AAP. There were no bands detected in the test samples after agarose gel analysis, indicating the presence of either low or no tail sample cDNA (Figure 11D). However, a subsequent nested amplification with GSP3 and AUAP on 1:100 dilution of the PCR product obtained in the first PCR resulted in a single band, approximately 500 bps in length, after agarose gel analysis. This band was gel purified and sequenced.

FIGURE 11 (A, B, andC)

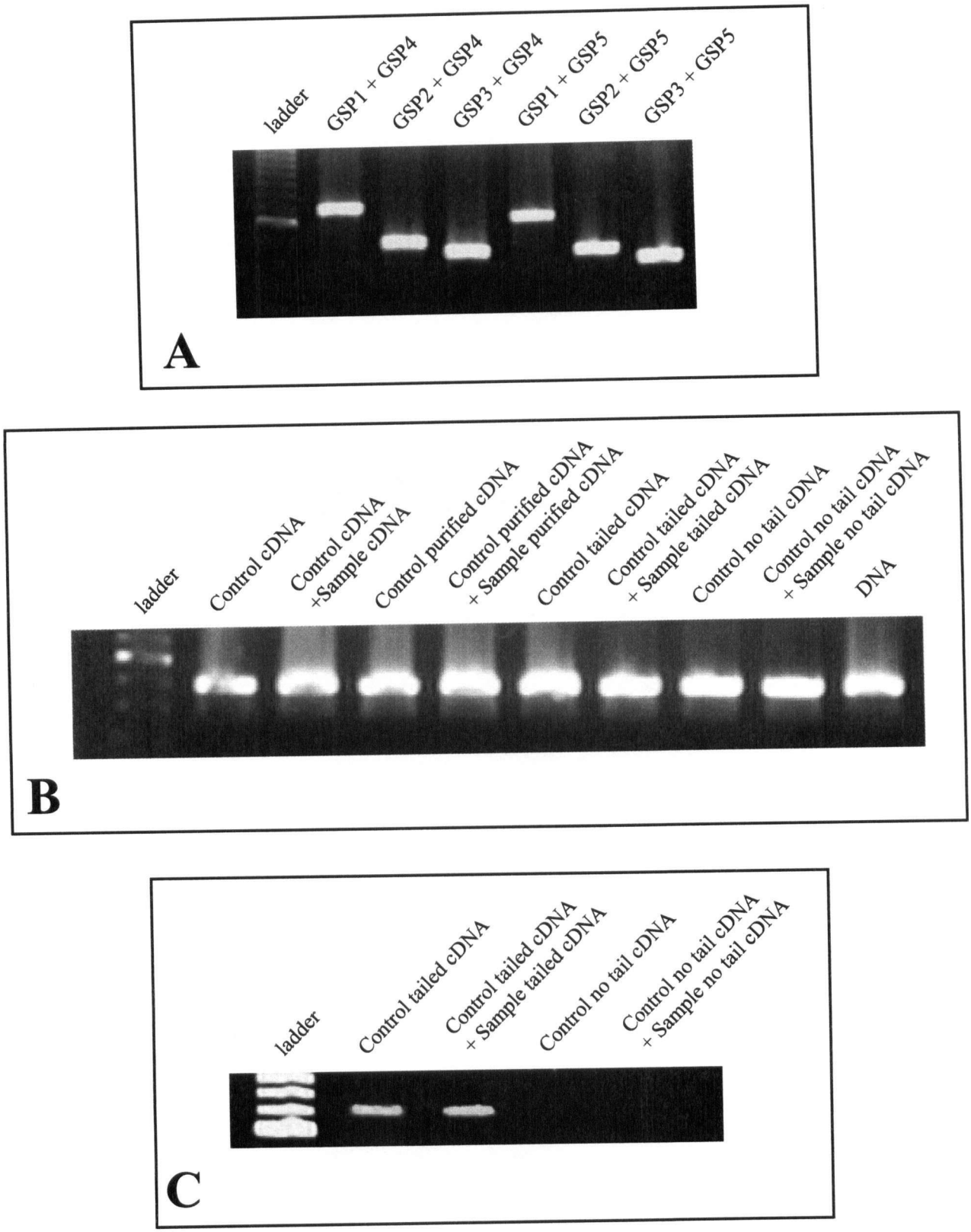

FIGURE 11 (D and E)

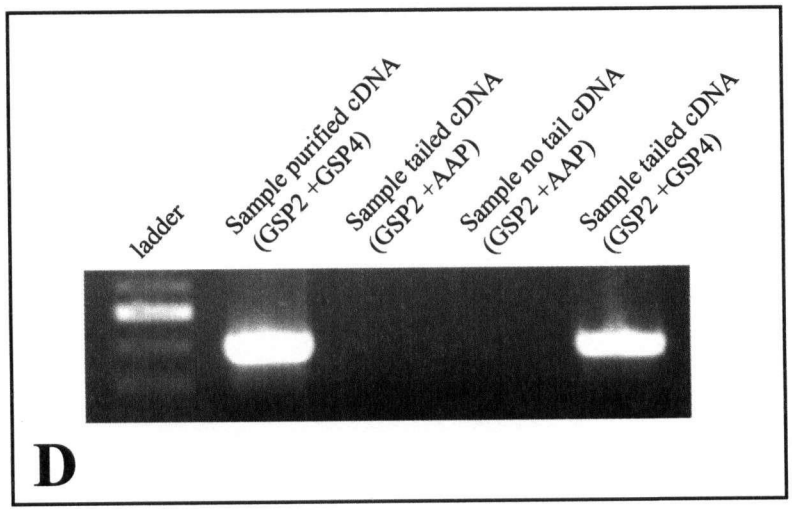

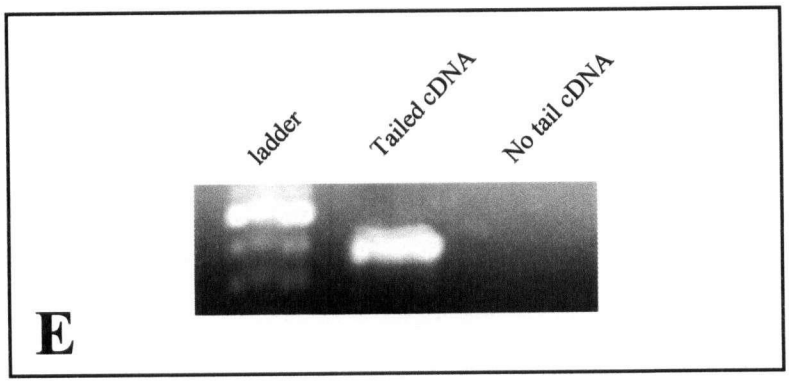

Figure 11: RACE analysis of the PIK3CA mRNA. (A) The efficacy of the primers for RACE analysis was tested using cDNA that was reverse transcribed from mRNA extracted from OSEC2 cells. **(B)** PCR reaction of a panel of control reactions with control GSP2 and GSP3 included as part of the kit were analyzed on an agarose gel. Presence of a 500 bp band in each lane indicates successful completion of each step of the RACE protocol. **(C)** A set of control reactions were used to test the efficiency of cDNA tailing. The tailed and no tail control cDNA samples were amplified using control GSP2 and AAP provided in the kit. Agarose gel analysis of the control tailed cDNA in presence or absence of the tailed sample cDNA demonstrated the presence of a 711 bp band as expected. The no tail control cDNA was a negative control for the PCR reaction. **(D)** The sample cDNA reverse transcribed from mRNA extracted from OSEC2 cells was PCR amplified with specific primers indicated in brackets. The agarose gel analysis of sample tailed cDNA amplified with GSP2 and AAP did not show a band. Amplification of sample purified cDNA and sample tailed cDNA with reverse GSP2 and forward GSP4 were positive controls (481 bp), while amplification of the sample no tail cDNA was a negative control. **(E)** A 1:100 dilution of the PCR product of sample tailed cDNA from **(D)** was reamplified by nested PCR and analyzed on an agarose gel. GSP3 and AUAP were used for the nested PCR amplification. A single band, approximately 500 bps, was detected, which was subsequently cut and purified for sequencing analysis. The diluted PCR product of no tail cDNA was amplified with GSP3 and AUAP as negative control.

The sequencing results of the RACE product were aligned against the PIK3CA sequence on the UCSC genome browser using the BLAT alignment software. This identified the presence of a new exon upstream of the current first exon. Figure 12A displays the screenshot of the UCSC Genome Browser showing a view of the PIK3CA gene with the currently known exon1, which we will now refer to as exon2(1) and the newly identified exon1, which we termed exon1a. Exon1a is 50,580 bps upstream of exon2(1) (coordinates: chr3:180,348,661-180,399,240; May 2004 Human Assembly) . The region containing exon1a is expanded to show the entire sequence of exon1a (Figure 12B). The sequencing of the RACE band demonstrated that exon1a splices directly to exon2(1). This is also evident by the presence of a 3' splice site at the end of exon1a and a 5'splice site at the start of exon2(1).

FIGURE 12

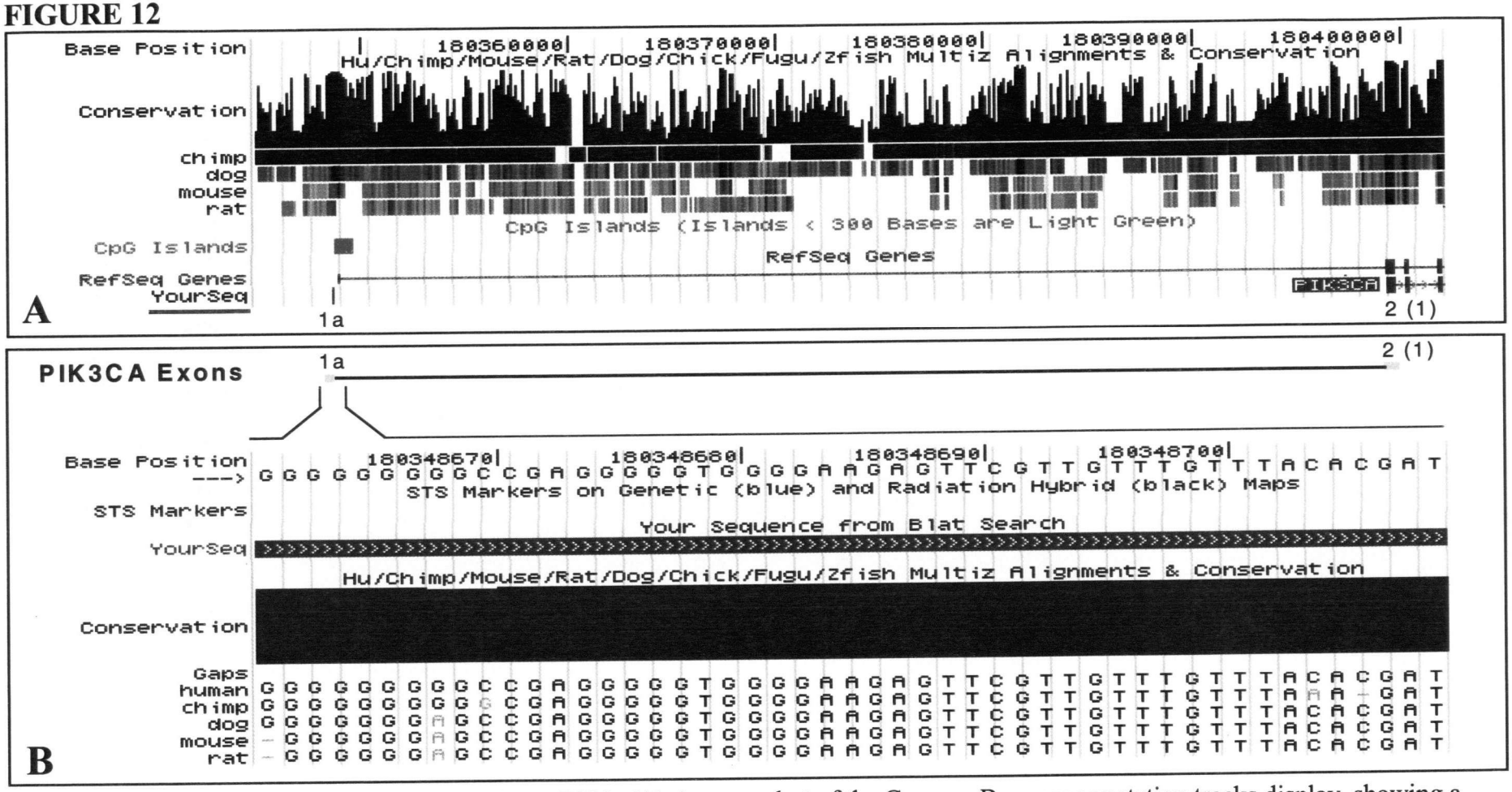

Figure 12: Sequence of Exon1a of the PIK3CA mRNA. (A) A screenshot of the Genome Browser annotation tracks display, showing a view of a part of chromosome 3 that encompasses the PIK3CA gene. The coordinates for the region shown are chr3:180,344,969-180,402,018. Labeled as Your Seq is the sequence obtained after aligning the sequence against the PIK3CA gene. Labeled on the diagram, as exon1a is the newly identified exon 50,580 bps upstream of the currently known exon1. We will refer to this new exon as exon1a, and the previously known exon1 as exon2(1). **(B)** Exon1a is magnified (coordinates: chr3:180,348,661-180,348,709) showing the nucleotide sequence of exon1a. This sequence is very highly conserved indicated at the bottom of **(B)**. The sequencing results also revealed that exon1a splices directly to exon2(1).

Interestingly, the sequence obtained from the RACE product was different from the sequence predicted to be an upstream exon based on RefSeq Genes. This new sequence (exon1a) is 353 bps upstream of the RefSeq Genes predicted exon (labeled as RefSeq Genes in Figure 12A). However, with the RACE analysis, we were not able to detect this exon by using the primers specific to the tail portion of the cDNA, perhaps due to the high GC content of this region. Furthermore, the presence of this GC rich upstream exon was confirmed by amplification of the tailed sample cDNA using an internal forward primer (GSP5) targeted to this predicted exon as well as a reverse primer (GSP3) to exon2(1). A 1:100 dilution of the initial PCR product of sample tailed cDNA (Figure 11D) was used to amplify this portion of exon1b. GSP3 and a primer to exon1a (GSP6) were used as positive control, and the presence of a second upstream exon to the currently known exon2(1) was confirmed (Figure 13). We will refer to this exon, which is in agreement with the RefSeq Gene exon prediction, as exon1b. This PCR product was subsequently gel purified and sequenced. Figure 14A displays the screenshot of the UCSC Genome Browser showing a view of the PIK3CA gene with the currently known exon2(1), exon1a and exon1b. Exons1a and 1b are 353 bps apart. Exon1b is more than 50,228 bps upstream of exon2(1). Figure 14B zooms into the region encompassing exon1b containing the entire predicted sequence of this exon. Our sequencing results only determined a part of this sequence since we used an internal forward primer (GSP5) to amplify this 5'UTR. The sequencing of the PCR product also demonstrated that exon1b splices directly into exon2(1). Analysis of the splice junctions of exons 1a, 1b and 2(1) determined the presence of splice sites on the 3' ends of exons 1a and 1b, and 5' end of exon2(1). Moreover, splice analysis of both exon1a and exon1b determined that these exons do not have splice junctions on their 5' ends, confirming that they are two alternate first exons, exons 1a and 1b, that splice separately into exon2(1). Therefore, our results indicate the presence of two alternate transcripts of the PIK3CA gene: mRNA1a containing exon1a and mRNA1b containing exon1b.

FIGURE 13

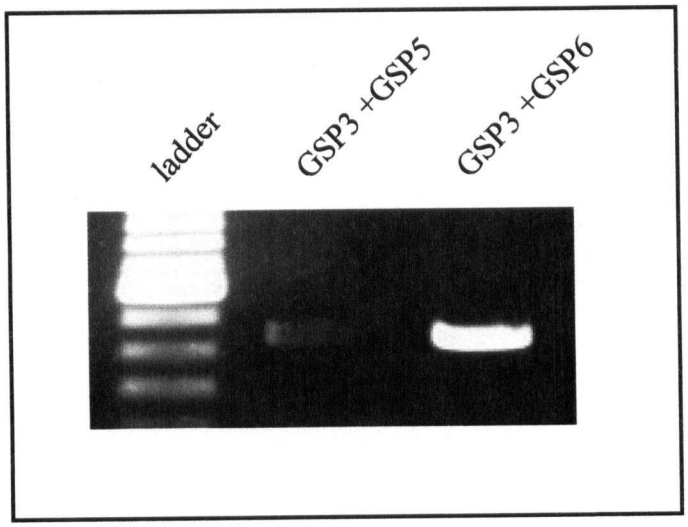

Figure 13: Further analysis of the PIK3CA mRNA. A 1:100 dilution of PCR product of sample tailed cDNA (Figure 10, Panel D), was amplified using primers indicated above the figure. GSP3 binds to exon2(1), while GSP6 and GSP5 bind to exons 1a and 1b respectively. GSP3 and GSP5 resulted in a 442 bp band that was subsequently gel purified for sequencing analysis. GSP3 and GSP6 were used as positive control (429 bp) to amplify the newly identified exon1a. GSP5 was designed within the predicted exon (based on RefSeq Genes, Figure 14). The presence of a band in the PCR reaction using GSP3 and GSP5 suggests that the RefSeq Genes predicted exon is also expressed in OSEC2.

FIGURE 14

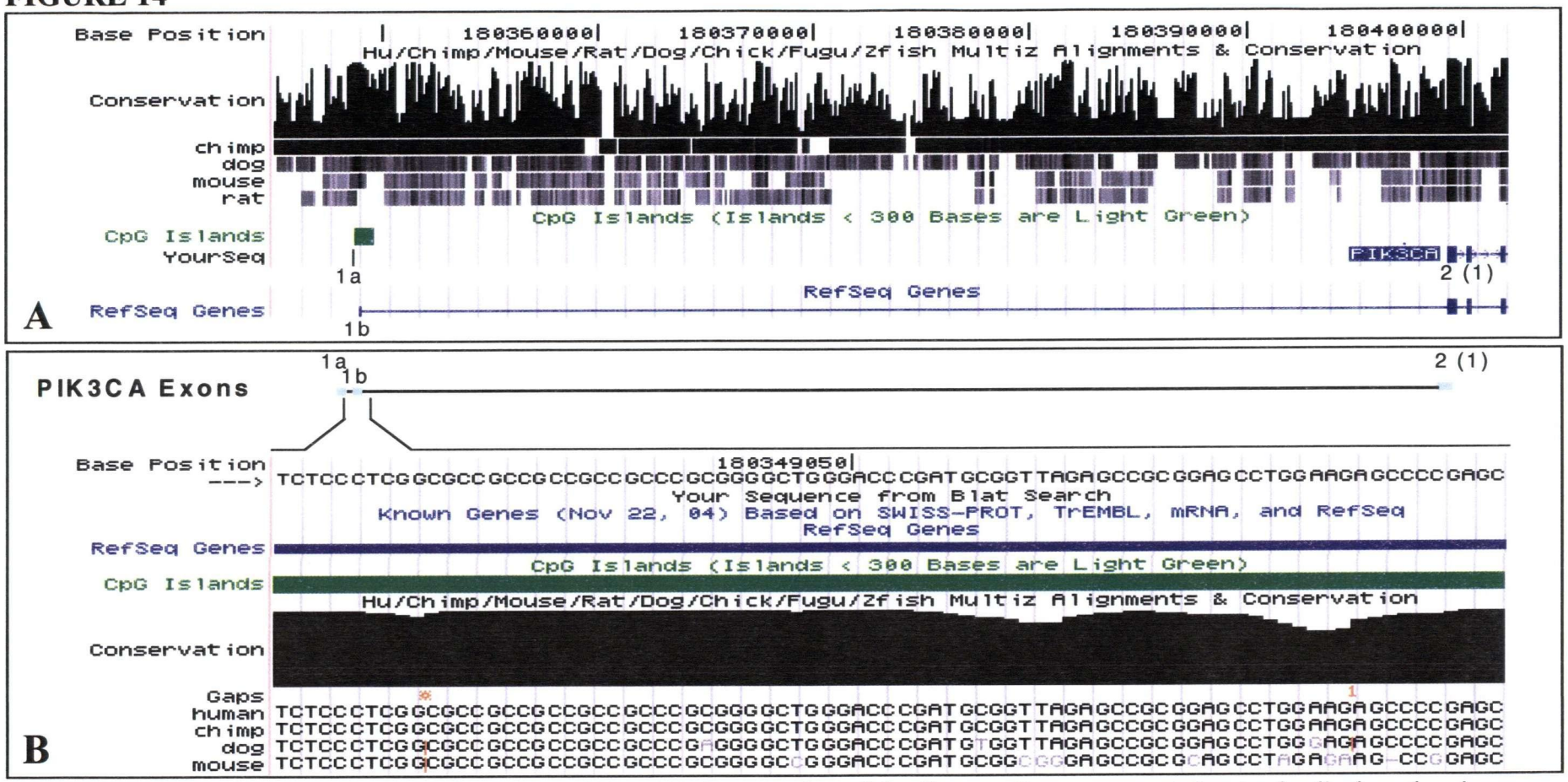

Figure 14: Sequence of Exon1b of the PIK3CA mRNA. (A) A screenshot of the Genome Browser annotation tracks display, showing a view of a part of chromosome 3 that encompasses the PIK3CA gene. The coordinates for the region shown are chr3:180,344,969-180,402,018. Labeled as RefSeq Genes is the sequence predicted to be an exon 50,228 bps upstream of the currently known exon1. The sequence obtained from sequencing of the PCR product (Figure 12) matched this sequence, although only partially since GSP5 was designed internal to this predicted exon. We will refer to this exon as exon1b, and the previously known exon1 as exon2(1). **(B)** A zoomed-in view (chr3:180,349,013-180,349,093) of exon1b showing the predicted nucleotide sequence. The sequencing analysis of 1:100 dilution of the RACE product amplified with GSP3 and GSP5 (Figure 12) revealed that exon1b splices directly to exon2(1). Exon1a and exon1b are 353 bps apart and splice alternatively to exon2(1).

3.9 p53 may bind directly to the PIK3CA promoter

RACE analysis identified two alternate 5' UTRs, exons 1a and 1b. Therefore, we predict the presence of two separate promoters for these two alternate transcripts. We refer to the region upstream of exon1a as promoter1a, and the region upstream of exon1b as promoter1b. We used the ConSite web based tool to look for putative p53 binding sites in these promoter regions and found putative p53 binding sites that scored between 60% and 66% of the maximum possible for the p53 binding profile. This score is consistent with potential binding. Table 3 lists the putative p53 binding sites and their percent similarity to the consensus binding site. Interestingly, these putative p53 binding sites are present on alternating strands of DNA, which is consistent with binding of p53 as a homotetramer on the positive and the negative strands of the DNA duplex (→←→←) (McLure and Lee, 1998). The putative p53 binding sites in the promoter regions are not highly conserved with the mouse sequence. However, we identified a region approximately 1500 bps downstream of promoter1b, which has a highly conserved p53 site with the mouse sequence. This region is within the long first intron of PIK3CA and may be a possible enhancer element region.

As described in the introduction, the p53 consensus binding site consists of two 10 nucleotide palindromes separated by 0 to 13 nucleotides (el-Deiry et al., 1992). However, the ConSite search of transcription factor binding sites is limited in identification of transcription factor binding sites that include spacer nucleotides. Therefore, we analyzed the PIK3CA promoter regions by searching for each half of the palindrome (i.e. quarter site) separately. This analysis determined several putative p53 binding sites, alternating between the positive and negative strands of the DNA duplex (→←→←), with spacer regions that range from 1 to 12 nucleotides in length. These p53 binding sites are within the same regions that the primers in Table 2 were designed to.

Table 4: Schematic diagram of putative p53 binding site on the PIK3CA gene

Sequence of Putative p53 Binding Sites (5' to 3')	TF Score (%)	Strand	Amplified with Primer Set
Promoter 1A			
CAAGACACTACCTTGAATCA	60.9	+	P1A1
CAGAAGACGTGGGGGATTTT	61.9	-	P1A1
AGGGCTGTGACAGTGCATTC	61.4	+	P1A2
GCCGACATGGTTTAAGTTGT	62.4	-	P1A2
TAAACCATGTCGGCAGAAGA	63.0	+	P1A2
CGAGATTAGTTCGGGGGTGA	62.5	-	P1A3
AAGCAGATGCGCAAAGAAGC	61.5	-	P1A4
Promoter 1B			
CCGGCCGGGCCCGAGCCCTG	60.4	-	P1B
TCGGGCCCGGCCGGGCAGCT	69.8	+	P1B
CCGGAGCTGCCCGGCCGGGC	69.2	-	P1B
CCGGGCAGCTCCGGAGCGGC	66.0	+	P1B
Enhancer			
GAGGGCAATATTGGTCATAT	60.2	+	Enh1
CATCACATGTTCTGGAAATT	67.4	+	Enh2
TAAAAATTTCCAGAACATGT	63.9	-	Enh2
CTGAAGAGGACTGTGTGTGT	60.9	+	Enh2

In order to look at direct binding of p53 to the PIK3CA gene, the chromatin immunoprecipitation (ChIP) technique was used. p53 bound segments of PIK3CA were immunoprecipitated and subsequently amplified by PCR. Primers (Table 2, methods) were designed around the putative p53 binding sites, so that the length of the PCR product would be between 150-250 bps. Figure 15A displays the screenshot of the UCSC Genome Browser showing a view of the PIK3CA gene with promoter1a, promoter1b, and putative enhancer regions. In Figure 15B, C and D, the putative p53 binding sites as well as the location of the primers designed to amplify the regions on promoters 1a, 1b and the enhancer regions respectively are shown.

FIGURE 15 (A)

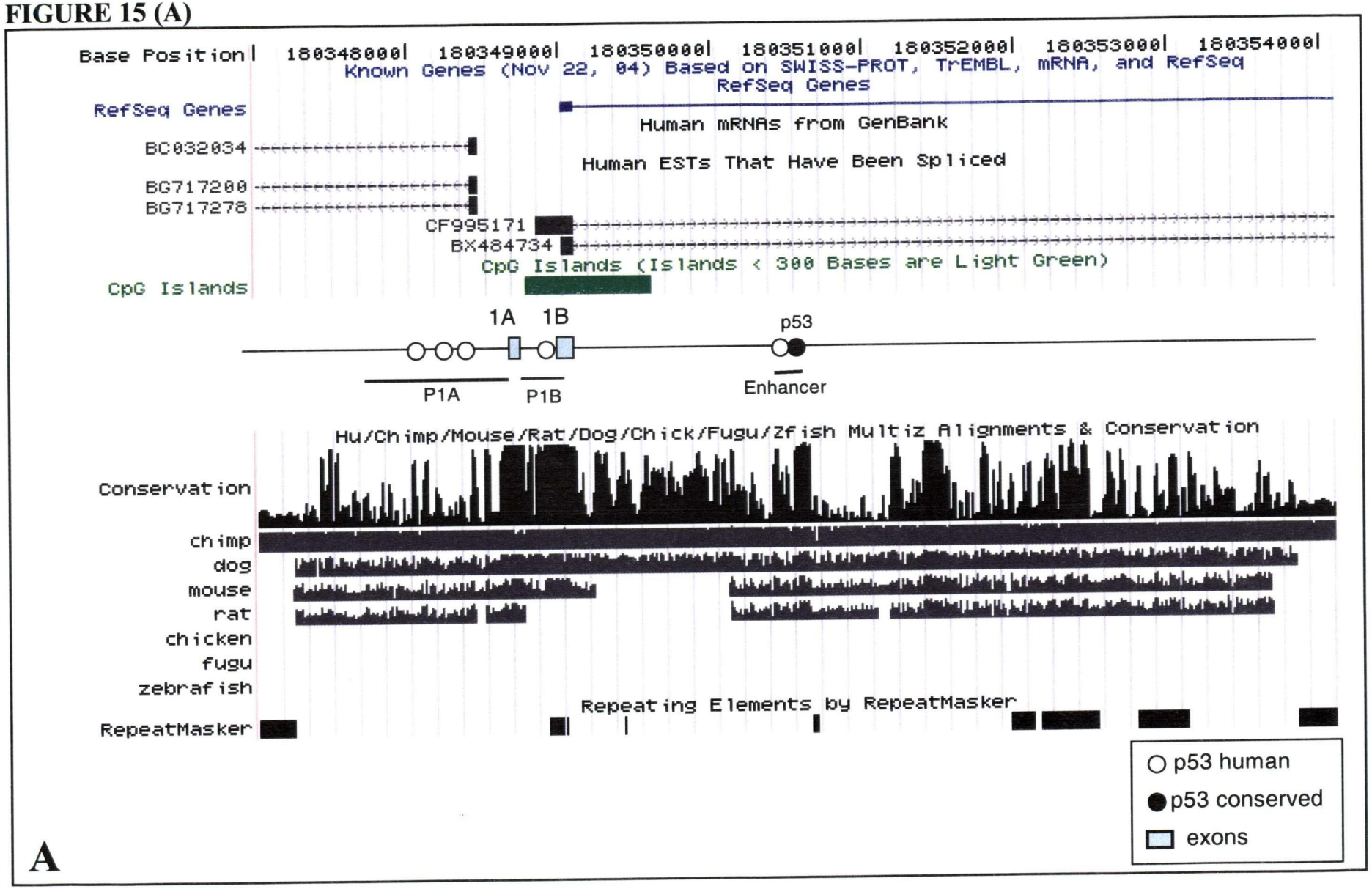
Base Position
180348000
180349000
180350000
180351000
180352000
180353000
180354000
Known Genes (Nov 22, 04) Based on SWISS-PROT, TrEMBL, mRNA, and RefSeq
RefSeq Genes
RefSeq Genes
Human mRNAs from GenBank
BC032034
Human ESTs That Have Been Spliced
BG717200
BG717278
CF995171
BX484734
CpG Islands (Islands < 300 Bases are Light Green)
CpG Islands
1A
1B
p53
P1A
P1B
Enhancer
Hu/Chimp/Mouse/Rat/Dog/Chick/Fugu/Zfish Multiz Alignments & Conservation
Conservation
chimp
dog
mouse
rat
chicken
fugu
zebrafish
Repeating Elements by RepeatMasker
RepeatMasker
p53 human
p53 conserved
exons
A

FIGURE 15 (B)

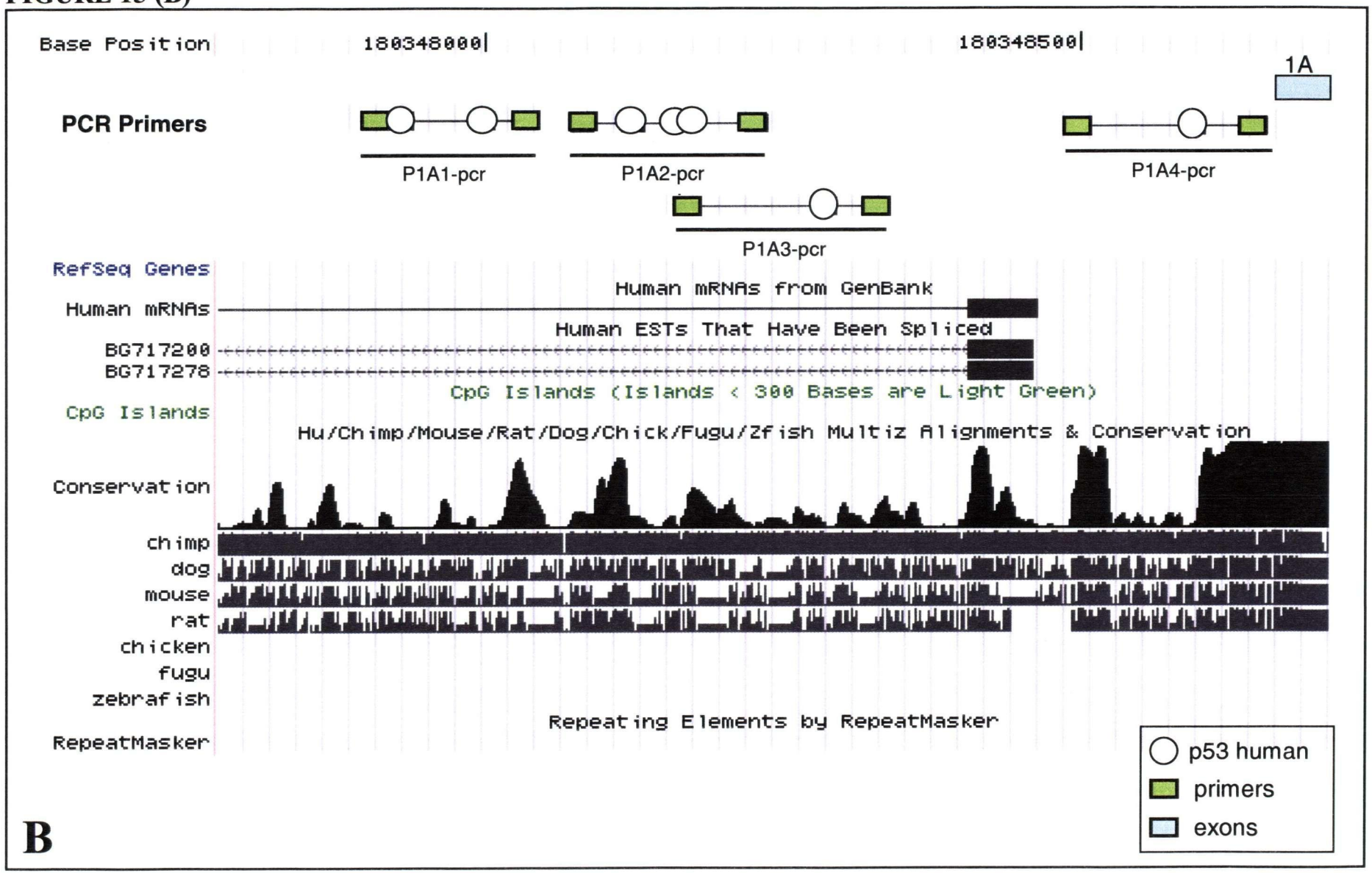
Base Position
180348000
180348500
1A
PCR Primers
P1A1-pcr
P1A2-pcr
P1A4-pcr
P1A3-pcr
RefSeq Genes
Human mRNAs from GenBank
Human mRNAs
Human ESTs That Have Been Spliced
BG717200
BG717278
CpG Islands (Islands < 300 Bases are Light Green)
CpG Islands
Hu/Chimp/Mouse/Rat/Dog/Chick/Fugu/Zfish Multiz Alignments & Conservation
Conservation
chimp
dog
mouse
rat
chicken
fugu
zebrafish
Repeating Elements by RepeatMasker
RepeatMasker
p53 human
primers
exons
B

FIGURE 15 (C)

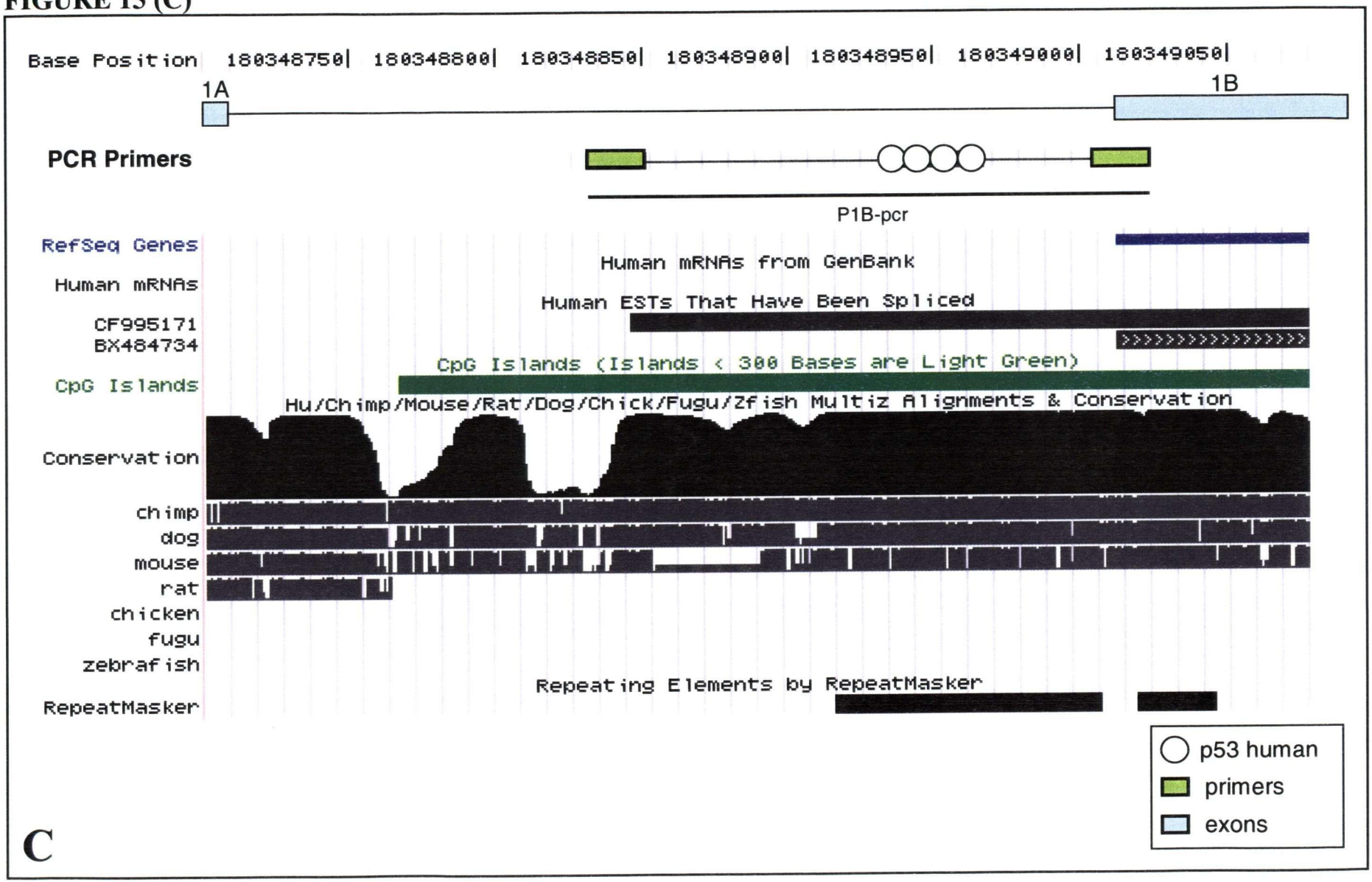
Base Position 180348750| 180348800| 180348850| 180348900| 180348950| 180349000| 180349050|
1A
1B
PCR Primers
P1B-pcr
RefSeq Genes
Human mRNAs from GenBank
Human mRNAs
Human ESTs That Have Been Spliced
CF995171
BX484734
CpG Islands (Islands < 300 Bases are Light Green)
CpG Islands
Hu/Chimp/Mouse/Rat/Dog/Chick/Fugu/Zfish Multiz Alignments & Conservation
Conservation
chimp
dog
mouse
rat
chicken
fugu
zebrafish
Repeating Elements by RepeatMasker
RepeatMasker
p53 human
primers
exons
C

FIGURE 15 (D)

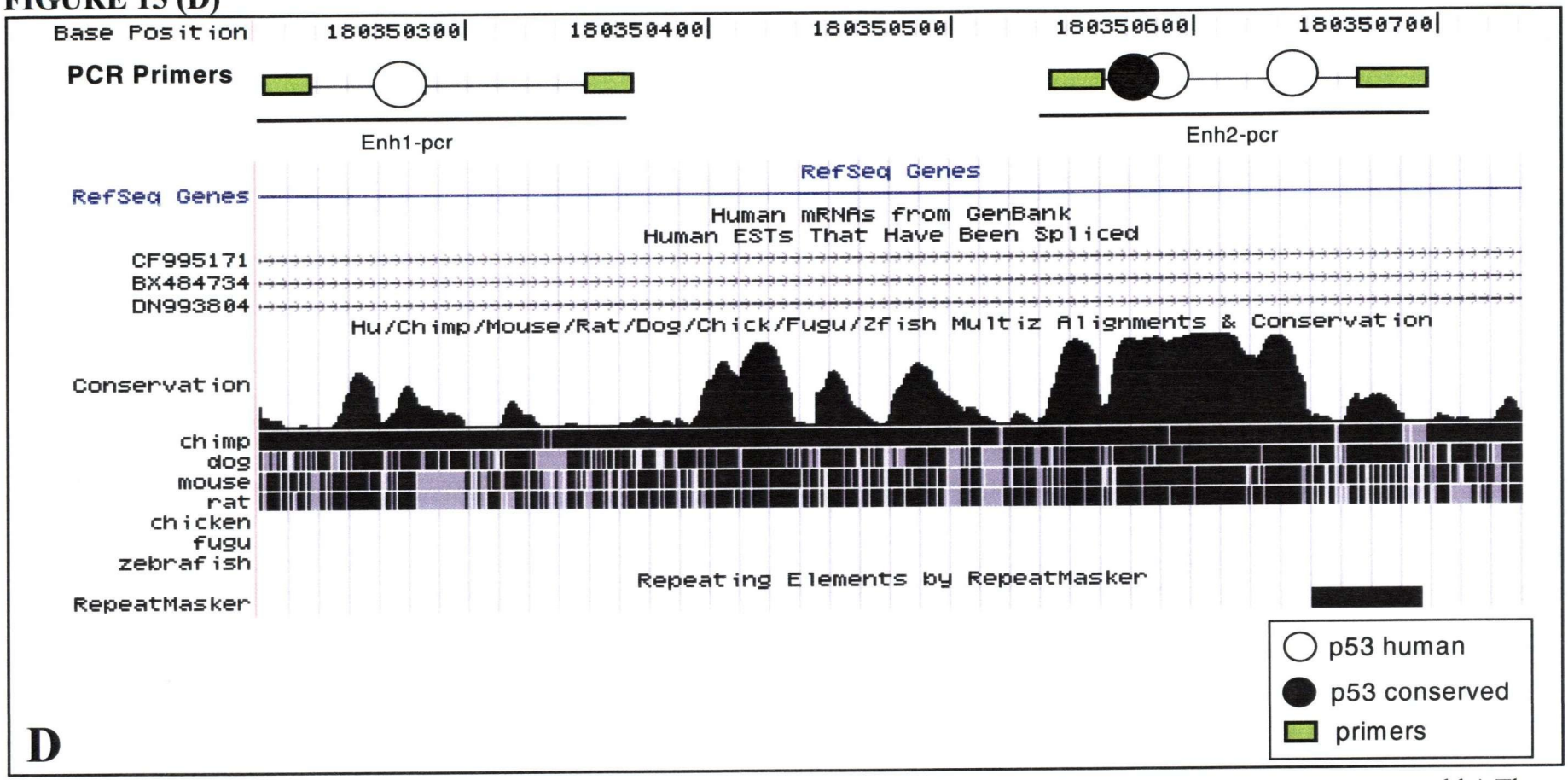

Figure 15: Analysis of promoter regions and p53 binding sites. (A) (chr3:180,347,000-180,354,093, May 2004 Human Assembly) The upstream regions of exons 1a and 1b, which we will refer to as promoters 1a and 1b respectively are displayed. Highly conserved regions within the long first intron with putative p53 binding sites are also displayed. Primers designed around putative p53 binding sites on the PIK3CA promoter1a, promoter1b, and putative enhancer regions are shown in **(B)**, **(C)** and **(D)** respectively. The coordinates for **(B)** are chr3:180,347,775-180,348,708. Promoter1a contains seven possible p53 binding sites, none of which is highly conserved with the mouse sequence (open circles). The coordinates for **(C)** are chr3:180,348,702-180,349,078. Promoter1b contains four possible p53 binding sites (open circles). This region is highly conserved but the p53 binding sites are not. The coordinates for **(D)** are chr3:180,350,215-180,350,733. This putative enhancer region has four putative p53 binding sites, one that shares 81% conservation with the mouse (black circle).

ChIP was used to detect direct binding of p53 protein to any of the putative p53 binding sites identified by the ConSite program. OSEC2 cells at 39°C were used for the ChIP assay to check binding of p53 to the PIK3CA promoter and putative enhancer regions. OSEC2 cells at 34°C were used as control to determine a change in the level of binding, since at 34°C Tag binds to p53 and inhibits its activity. We first optimized the sonication step of the assay to determine the appropriate number of pulses required to shear the chromatin effectively. Test samples of the OSEC2 cells at 39°C were placed under various conditions. The most effective shearing of DNA resulting in pieces between 200-1000 bps was achieved after eight 15 seconds pulses (figure 16A). OSEC2 at 34°C and 39°C were then prepared for ChIP analysis and sonicated on ice with eight 15 seconds pulses with 15 seconds wait after each pulse. The successful shearing of the DNA samples after sonication is demonstrated in Figure 16B. Prior to PCR amplification of the ChIP products, the quality of primers designed to amplify putative p53 regions was tested using genomic DNA. All the primer sets except for one designed to promoter1b resulted in an appropriately sized band (Figure 16C). The promoter1b region has a very high GC content, and a faint band was obtained after optimization of conditions with the FailSafe PCR kit (Figure 16C). An aliquot of DNA was removed before immunoprecipitation as input DNA for control to show that similar levels of DNA were present for immuoprecipitation in both OSEC2 cells at 34°C and 39°C. PCR reactions preformed using input DNA demonstrated that each primer set resulted in a band of similar intensity in OSEC2 cells at 34°C and 39°C (Figure 16D). However, no band was detected after PCR amplification of input DNA with the primer set to promoter1b and mixture J of the FailSafe Kit (Figure 16D). The bands obtained after PCR of the ChIP DNA are shown in Figure 16E. ChIP analysis of p53 binding with OSEC2 cells at 39°C showed the presence of bands with primers designed to all regions of promoter1a. There was no band detected using the primer set to promoter1b and mixture J of the FailSafe Kit. This may not necessarily be due to

lack of binding of p53 to this region, but perhaps reflects failure of amplification due to the high GC content of this region. However, a faint band was detected in the PCR reaction using genomic DNA (Figure 16C). There was also a band detected using primers to enhancer region2, which contains the conserved putative p53 binding site. However, there was no binding to the putative p53 binding site in enhancer region1. As a positive control for immunoprecipitaion with the p53 antibody, primers around a known p53 binding site on the p21 promoter were used. Amplification of the p53 immunoprecipitated sample with primers to a segment of the p21 promoter resulted in a band that was only present in the OSEC2 sample at 39°C and not at 34°C (Figure 16E). Interestingly, PCR amplification of ChIP products from OSEC2 cells at 34°C resulted in the presence of some but not all of the bands as the OSEC2 cells at 39°C. There were bands detected in regions of promoter1a2, promoter1a3, and enhancer region2. There were no bands detected in regions promoter1a1, promoter1a4, and positive control p21 promoter that were amplified with the immunoprecipitated DNA from OSEC2 cells at 39°C. In addition, as a control for background for the p53 antibody, immunoprecipitation with mouse IgG antibody was performed with the OSEC2 samples at 34°C and 39°C, which did not show any bands after PCR amplification and gel analysis. As positive control for the ChIP, an antibody to RNA Polymerase II was used to immunopreciptate the samples. Primers to a region of GAPDH were used for PCR amplification of RNA Polymerase II mmunoprecipitated samples. The appropriately sized band (166 bps) was detected, confirming that the ChIP protocol was successful.

FIGURE 16 (A and B)

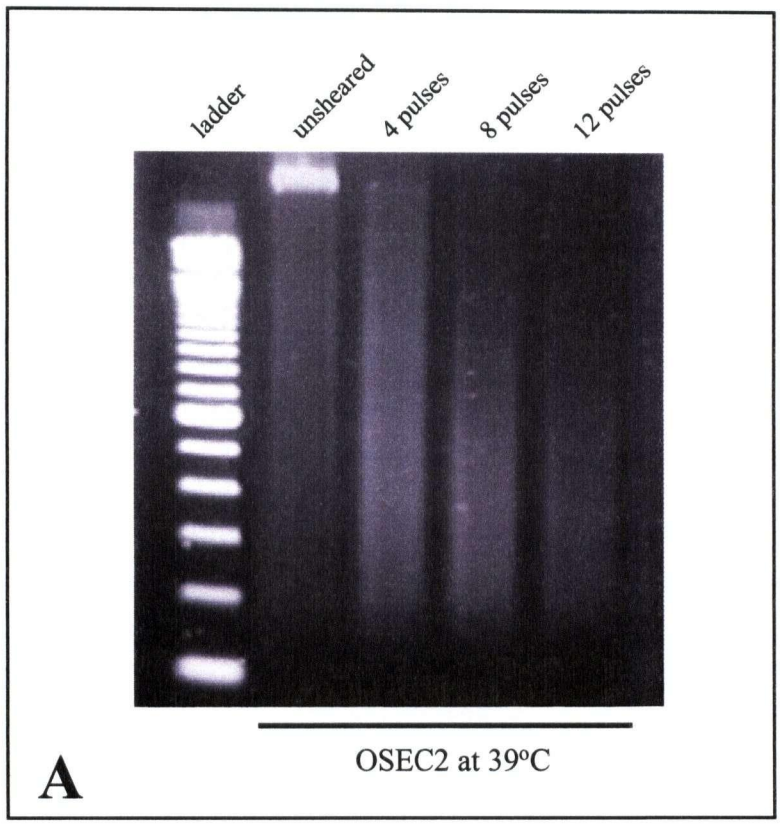

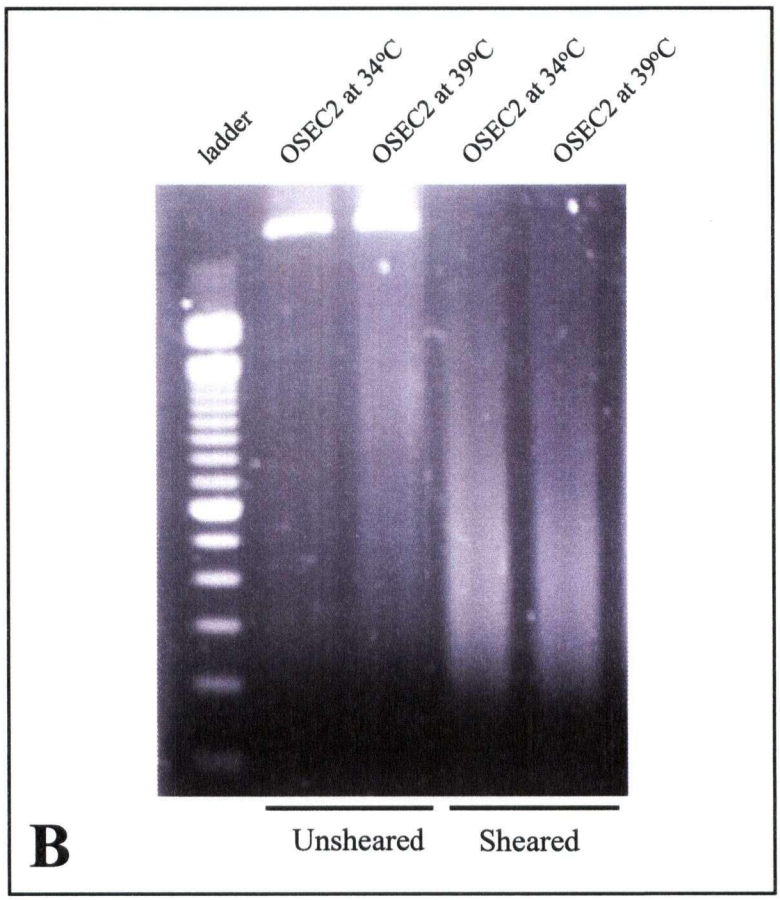

FIGURE 16 (C and D)

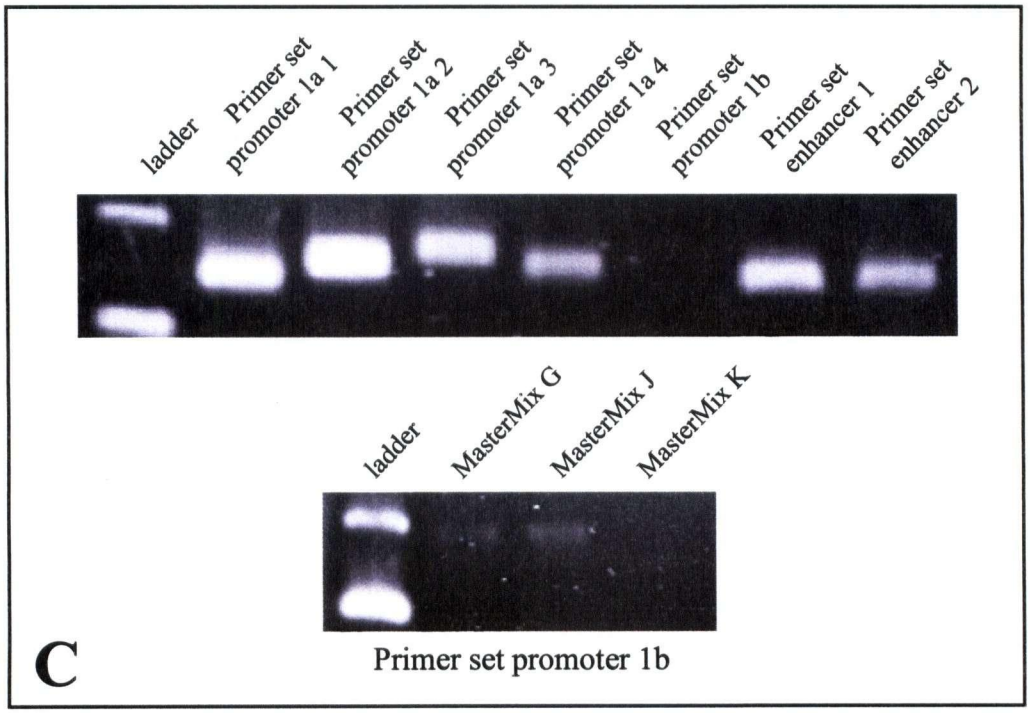

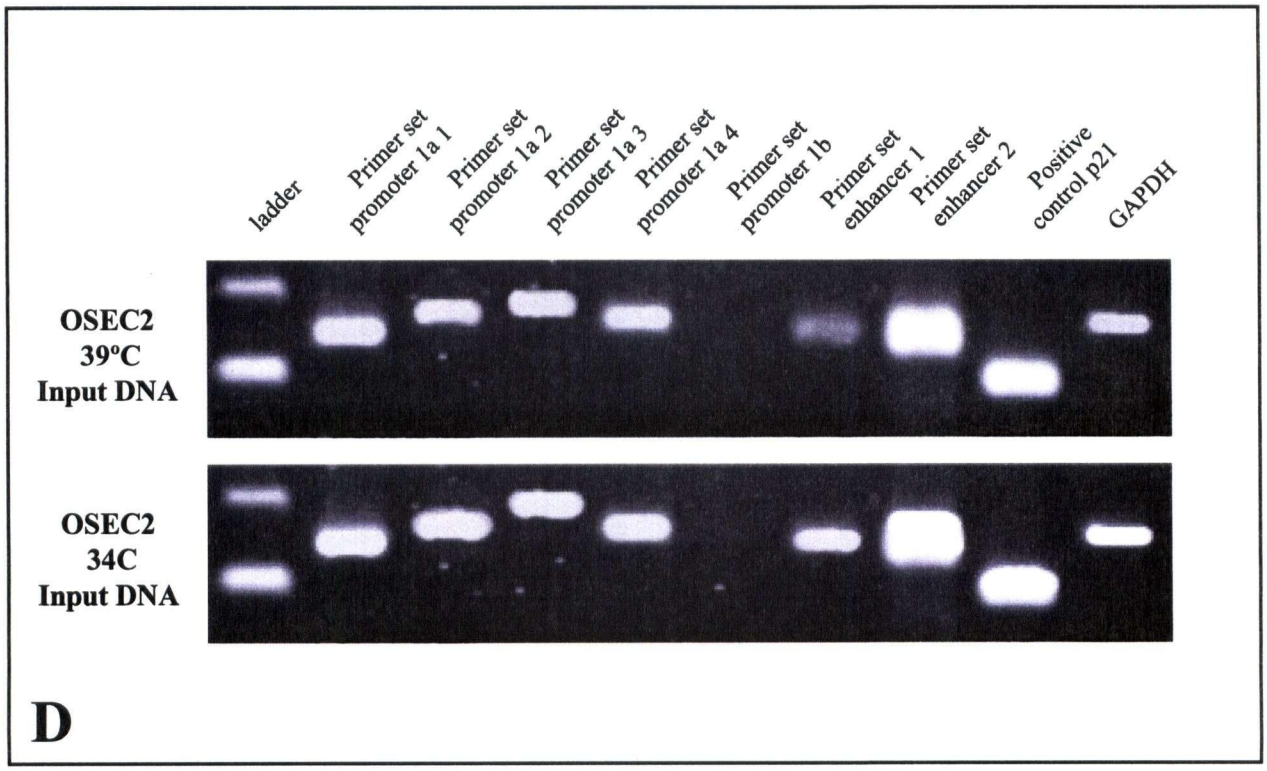

FIGURE 16 (E)

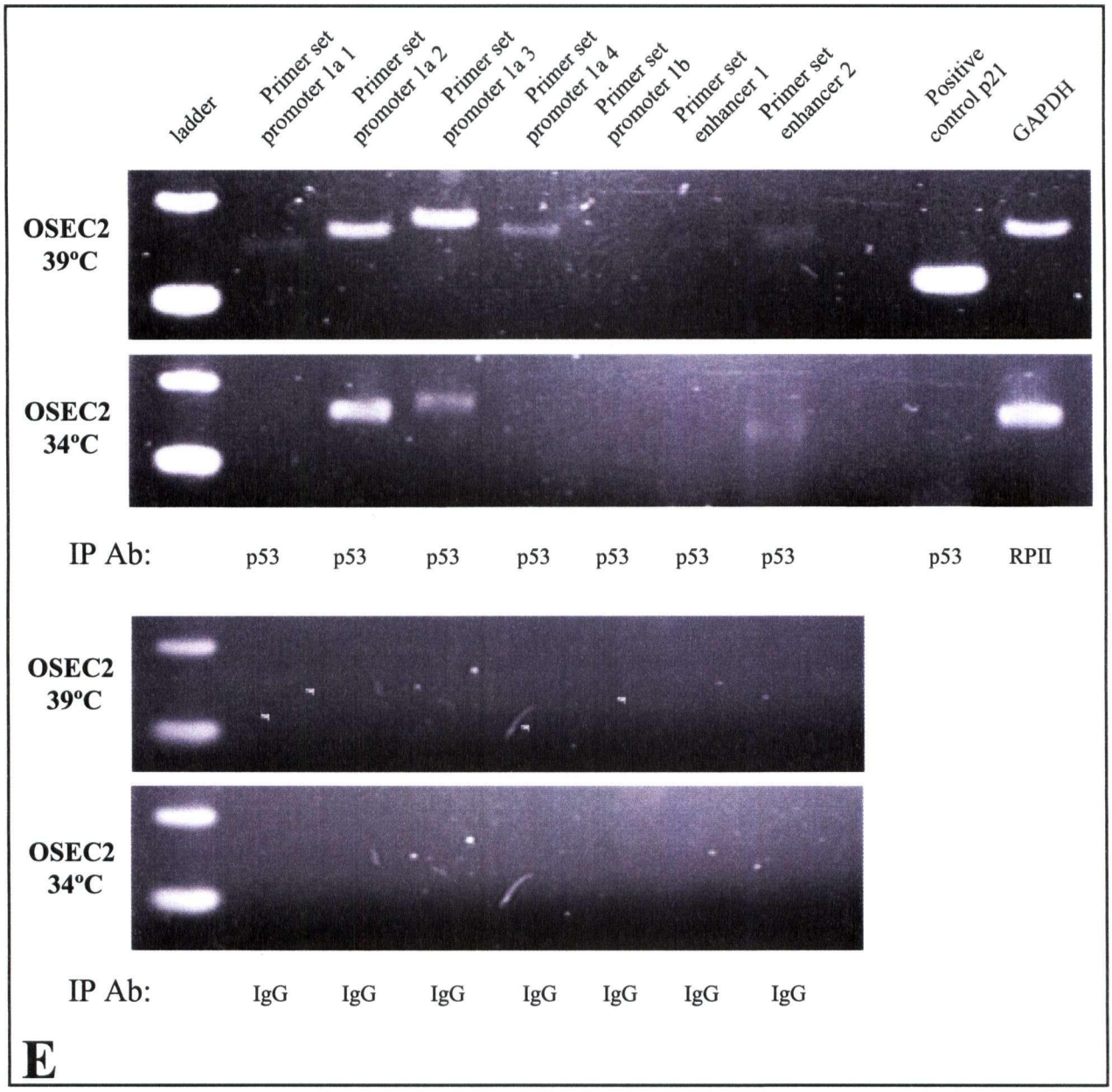
ladder
Primer set promoter 1a 1
Primer set promoter 1a 2
Primer set promoter 1a 3
Primer set promoter 1a 4
Primer set promoter 1b
Primer set enhancer 1
Primer set enhancer 2
Positive control p21
GAPDH
OSEC2 39°C
OSEC2 34°C
IP Ab:
p53 p53 p53 p53 p53 p53 p53 p53 RPII
OSEC2 39°C
OSEC2 34°C
IP Ab:
IgG IgG IgG IgG IgG IgG IgG
E

Figure 16: ChIP analysis for p53 binding sites on the PIK3CA gene. (A) The DNA of OSEC2 cells at 39°C were sonicated with various numbers of 15 second pulses. 8 cycles of sonication gave efficient level of shearing between 200 and 1000 bps. **(B)** The OSEC2 samples at 34°C and 39°C were sonicated for 8 pulses and a 10μl aliquot was removed for agarose gel analysis to confirm successful shearing. **(C)** The quality of primers were tested by PCR amplification using genomic DNA. Amplification with all of the primer sets except for primer set to promoter1b resulted in appropriately sized bands. Promoter1b has a very high GC content, so the FailSafe PCR kit mastermixes G, J, and K were used to improve PCR conditions. The bottom gel in **(C)** shows that with mastermix G and J a faint band of the appropriate size was detected. **(D)** The PCR reactions of the input DNA removed from samples before immunoprecipitation were analyzed on an agarose gel. This input DNA acts as control for levels of DNA present in each sample. No bands were detected with primer set 1b. **(E)** The PCR reactions after ChIP were analyzed on a gel. The primers used are indicated on top, and the antibody used for immunoprecipitation are indicated on the bottom of the figure. Primers to GAPDH provided in the ChIP kit were used as positive control with the DNA from OSEC2 cells immunoprecipitated with RNA-polymerase II (RPII). Primers to the p21 promoter were used as positive control for immuneprecipitation with the p53 antibody. OSEC2 cells at 34°C showed bands in PCR reactions amplified with primer set 1a2, 1a3, and enhancer2. OSEC2 cells at 39°C with functional p53 showed bands in PCR reactions with primer set 1a1, 1a2, 1a3, 1a4, and enhancer2. These bands indicate p53 binding to the regions of the PIK3CA gene. PCR amplification of the samples immunoprecipitated with mouse anti-IgG antibody did not result in amplified products, indicating that the bands observed with the anti-p53 antibody immunoprecipitation were specific. Primer set 1b was used with mastermix J in the PCR reaction of the ChIP samples.

CHAPTER 4:

DISCUSSION

4.1 Functional Interaction of p53 and PIK3CA

Ovarian cancer is commonly believed to arise from the epithelium (OSE) covering the ovary (Auersperg et al., 2001). In our studies, we used temperature sensitive immortalized OSE in culture to better understand the mechanism of ovarian carcinogenesis. By using this model, in which we could regulate the absence or presence of functional p53 in the cells through a shift in temperature, we were able to provide strong evidence that the PI3K pathway is regulated by p53.

Singh et al. (2002) demonstrated a link between p53 and PI3K in cancer. They suggested that negative effect of p53 induction on cell survival involves the transcriptional inhibition of PIK3CA. They demonstrated that induction of p53 by UVB in cell lines derived from upper aerodigestive tract (UADT) carcinomas with intact or absent PTEN protein expression, resulted in decreased PIK3CA protein and transcript levels. UADT includes tumors that arise from the head and neck, lung, and cervical esophagus. In addition, Singh et al. (2002) found that in EB1 colon cancer cells with wild-type p53 under control of a metallothionein promoter, there was a functional interaction between p53, PTEN and PIK3CA. They demonstrated that a progressive decrease in P-AKT levels resulted from p53 related PTEN induction and PIK3CA inhibition in these cancer cells (Singh et al., 2002).

Our findings support the findings by Singh et al. (2002) in that gain in p53 function results in decreased PIK3CA protein and transcript levels. Our studies, however, were performed with non-malignant IOSE cell lines. Therefore, we were able to show, for the first time, that there is functional interaction of p53 and PIK3CA in benign cells. Moreover, we demonstrated that overexpression of wild-type p53 in ovarian cancer cells with either normal or mutant p53 status, resulted in decreased levels of p110α protein, suggesting that the PIK3CA regulation by

p53 is also present in ovarian cancer cells. Therefore, our data suggest that loss of p53 function may be one of the mechanisms that contribute to increased p110α levels in cancer cells. Our studies showed decreased p110α levels after overexpression of wild-type p53, even in cells with PIK3CA gene amplification, suggesting a role for p53 in regulation of the amplified PIK3CA.

Studies by Singh et al. (2002) on UADT primary tumours and cancer lines demonstrated that none of the tumours with p53 mutations had PIK3CA amplification, thereby suggesting that mutation of p53 and amplification of PIK3CA are two mutually exclusive events in UADT and that either event is able to promote a malignant phenotype (Singh et al., 2002). This however, contradicts what is observed in ovarian cancers, as many of ovarian cancer cell lines that have p53 mutations also harbour PIK3CA gene amplifications. For example, CaOV3, SKOV3, and OVCAR3 ovarian cancer cell lines all have p53 mutations as well as increased PIK3CA copy number. Gene amplification does not always correlate with an increase in protein expression as protein levels are regulated at multiple levels including: transcription, post-transcription, and post-translation (Durbecq et al., 2004). Therefore, even in the presence of PIK3CA amplification, there is still a requirement for transcription regulation. Our studies demonstrate that p53 suppresses transcription of PIK3CA, and thus results in decreased PIK3CA transcript and p110α protein levels. Therefore, it is plausible that loss of p53 in ovarian cancers with amplified PIK3CA will result in loss of transcription suppression of PIK3CA and therefore increased PIK3CA transcript and p110α protein levels. This is consistent with findings of Shayesteh et al. (1999) that demonstrated that these cancer lines have increased p110α levels in addition to PIK3CA gene amplification (Shayesteh et al., 1999).

OVCAR420, OVCAR429, and OVCAR433 cells with wild-type p53 status, have been shown to have PIK3CA amplification as well as increased p110α protein levels (Shayesteh et al., 1999). In these cancer lines, it may be possible that there is up-regulation of a transcription factor

that is responsible for activation of PIK3CA transcription, which in turn leads to increased p110α levels even in the presence of p53. Because the PIK3CA promoter had not been previously described, there is no knowledge available on the transcriptional activation of the PIK3CA promoter. Our identification of the promoter opens the way for future studies, looking at regulation of transcription of PIK3CA by other transrepressors or transactivators.

OVCAR432 cells have mutated p53 as well as PIK3CA amplification; however, these cells do not show increased p110α levels. This may suggest that even in the absence of suppression by p53, the p110α levels cannot increase without the activity of transcriptional activators. This too will become clear through future studies looking at transcriptional regulation of the PIK3CA gene by other transcription factors. The p110α levels and p53 status of these cells suggest that p53 may be one mechanism by which p110α levels are regulated. More studies are required to determine which transcription factors are responsible for activation of the PIK3CA promoter and whether or not these transcription factors are overexpressed in EOC.

Suzuki et al. (2000) suggested that gain of 3q26-qter may be an early event in ovarian cancer development since this gain occurs frequently in low grade and low stage tumours (Suzuki et al., 2000). However, gene amplifications generally occur late in tumourigenesis (Lengauer et al., 1998). The mechanisms of gene amplification generation are largely unknown. Although amplifications can occur in cancer cells with wild-type p53, a potential player in the process of gene amplification is p53 (Livingstone et al., 1992), since amplifications have been shown to occur more easily when p53 is inactivated in mammalian cells (El-Hizawi et al., 2002; Livingstone et al., 1992; Yin et al., 1992). One theory is that if gene amplification occurs in cells with an intact p53 pathway, DNA damage signals will set off p53 mediated apoptosis, while the cells that lack p53 function will survive and accumulate additional problems (Lengauer et al.,

1998). Mutations of p53 in ovarian cancer are believed to be an early step occurring in inclusion cysts and deep invaginations (Schlosshauer et al., 2003). Therefore, ovarian cancer may in part initiate due to loss of p53 regulation, which leads to increases in p110α levels. In addition to loss of negative regulation of PIK3CA by p53, the loss of p53 may also contribute to the generation of the common PIK3CA gene amplification observed in ovarian cancers and thereby the increase in p110α levels.

Our results demonstrated that p110α protein levels decrease upon gain in p53 function. This decrease in p110α levels may suggest decreased protein expression or increased protein degradation. However, in addition to protein levels we looked at PIK3CA transcript levels in OSEC2 cells with and without functional p53. Quantitative real time RT-PCR analysis showed concomitant decrease in PIK3CA transcript levels. Therefore, we suggest that it is likely that the p110α levels decrease, at least in part, due to lower levels of available transcript for protein expression. The decrease in PIK3CA transcript levels could suggest lower levels of activity of the promoter, and thus lower levels of transcription, or it could suggest increased degradation of the transcript. However, we provided evidence that the decrease in PIK3CA transcript levels is associated with lower levels of transcription, since the ChIP analysis, looking at binding of p53 to the PIK3CA promoter, indicated direct binding of p53 to the PIK3CA promoter. The direct binding of p53 to PIK3CA needs to be studied in more detail by use of reporter constructs and mutations, in order to be considered as functional binding sites. The ChIP study and implications will be discussed in more detail below.

In addition to p110α protein and PIK3CA transcript levels, our studies showed that PI3K activity significantly decreases upon gain in p53 function. Previous studies by Stambolic et al. (2001) have demonstrated that PTEN levels are positively regulated by p53 through direct

interaction of p53 with the PTEN promoter (Stambolic et al., 2001). Consistent with findings of Stambolic et al. (2001), we also demonstrated that PTEN levels increase upon gain in p53 function in ovarian cells. Thereby we provide evidence that both PTEN and p110α levels are regulated by p53 in our model system, and that most likely, the decrease in PI3K activity after the gain in p53 function is due to a combination of these factors.

Our proliferation studies showed that the number of proliferative cells dramatically decreased even one day after the shift in temperature. It has been shown that LY294002 can significantly inhibit proliferation of cells (Hu et al., 2000). Ki-67 is present in all active parts of the cell cycle, with levels rising during the S phase, highest in the G2 and M phase of the cell cycle, and then rapidly degrade. The half-life of Ki-67 is approximately one hour (Li et al., 1995). In our studies, OSEC2 cells treated with LY294002 stained positive for Ki-67 antigen, although the staining was less frequent and less intense compared to the untreated cells. We speculate that fixation after only one hour of treatment does not allow enough time for degradation of Ki-67, since the half-life of Ki-67 is approximately 1 hour. Therefore, it is possible that Ki-67 remained in the nuclei of the LY294002 treated cells, due to its slow turnover time.

Moreover, OSEC2 cells at 39°C with functional p53 underwent more apoptosis, compared to OSEC2 cells at 34°C. Interestingly, OSEC2 cells after one day at 39°C had a significantly higher proportion of apoptotic cells than the OSEC2 cells after 3 and 5 days at 39°C. Davies et al. (2003) established the OSEC2 cells and studied characteristics of these cells under the permissive and non-permissive conditions. Davies et al. (2003) concluded that after the shift in temperature, the cells initially undergo apoptosis, while the remaining cells show induction of a senescent phenotype (Davies et al., 2003). This may provide an explanation for the observed decline in apoptosis in OSESC2 cells after 3 and 5 days, compared to only 1 day at

39°C. On day 1, the majority of cells may undergo apoptosis, while after a few days at 39°C more cells undergo senescence. It is not known what controls the cells' decision to undergo senescence or apoptosis. Davies et al. suggest that other factors, such as mutations in other components of the cell cycle control, degree of damage, the age, or the number of replications that the cells have undergone may contribute to the cell's decision (Davies et al., 2003).

Proliferation of mammalian cells is tightly regulated by multiple factors, primarily adhesion to the extracellular matrix (ECM), cell-cell adhesion, and soluble factors such as growth factors, cytokines, hormones, and inhibitors (Schwartz and Assoian, 2001). These factors activate different downstream signalling pathways. It has been shown that the PI3K pathway is required for proliferation of cells; however, other signaling pathways such as MAPKs are also involved in this regulation (Goncharova et al., 2002; Zhang and Liu, 2002). Numerous studies have implicated the PI3K/AKT pathway as the one involved in conveying survival signals. Sabbatini et al. (1999) showed for the first time the direct link between PI3K/AKT signalling and p53-mediated apoptosis. They demonstrated that constitutively active PI3K and PKB/AKT could significantly delay the onset of p53-mediated apoptosis (Sabbatini and McCormick, 1999). In addition, several studies have demonstrated increased proliferation and resistance to apoptosis in cells after overexpression of constitutively active p110α (Hu et al., 2002; Singh et al., 2002; Woods Ignatoski et al., 2003; Zhao et al., 2003). In OSEC2 cells, upon gain in p53 function, the cells were less proliferative and underwent more apoptosis. While these changes may in part be due to the decrease in levels of p110α and PI3K activity, any of the p53 downstream mediators may be involved. To determine whether the increase in apoptosis and the decrease in proliferation observed in the OSEC2 cells after the shift in temperature to 39°C were mediated, at least partly, through the down-regulation of the PI3K pathway by p53, a stable OSEC2 cell line expressing the constitutively active form of p110α (OSEC2 Myr-p110α*-Myc) was

established (data not shown). Currently, studies are in progress to determine whether the OSEC2 Myr-p110α*-Myc cells can maintain proliferation and inhibit apoptosis after the shift in temperature to 39°C where p53 becomes functional. Preliminary results showed that after 5 days at 39°C, OSEC2 cells stop proliferating whereas OSEC2 Myr-p110α*-Myc cells continue to proliferate. These cells will be maintained at 39°C to determine whether constitutively active p110α in these cells can completely rescue the cells from cell cycle arrest and apoptosis. Moreover, it will be interesting to compare P-AKT levels of the OSEC2 Myr-p110α*-Myc and OSEC2 cells after the switch in temperature. At 39°C the PTEN levels increase because of p53 binding to the PTEN promoter, so the increase in PTEN levels may not allow for P-AKT levels to increase even in the presence of constitutively active p110α. This may be one reason that Sabbatini et al. (1999) observed a delay in the onset of apoptosis, but not resistance to apoptosis, after overexpression of constitutively active p110α.

Several studies have suggested a role for p53 in negative regulation of cellular survival through binding to the PTEN promoter (Franke et al., 1997b; Henry et al., 2001; Sabbatini and McCormick, 1999; Stambolic et al., 2001). Our studies suggest a role for p53 in negative regulation of survival through direct binding to the PIK3CA promoter. We identified the PIK3CA promoter and studied in addition to functional interaction, the physical interaction of p53 and PIK3CA, using an ovarian model. We identified several putative p53 binding sites on the PIK3CA promoter and provided evidence that there may be direct binding of p53 to the PIK3CA promoter. The direct interaction of p53 and PIK3CA are discussed below.

4.2 Direct Interaction of p53 and PIK3CA

The promoter region of PIK3CA had not been characterized to date. In an attempt to determine whether the regulation of PIK3CA by p53 is direct or via other signalling mediators, we had to first identify the PIK3CA promoter region. We identified two upstream exons (1a and 1b) in the 5' untranslated region (UTR). We determined that these two alternate first exons alternatively splice into exon2(1) where translation starts. We assigned the regions upstream to these exons as promoters, and therefore identified two alternate promoter regions, promoter1a and promoter1b. The two alternate 5' UTRs of the PIK3CA gene that were identified in our studies may be responsible for translational regulation of PIK3CA, however, further studies are required to determine the importance of alternate transcription start sites for PIK3CA function.

The presence of transcripts that differ only in their 5' UTR has been described for many genes (Arrick et al., 1994; Brown et al., 1999; Hempel et al., 2004; Savitsky et al., 1997; Sobczak and Krzyzosiak, 2002). This occurrence has mostly been interpreted as an evolutionary gain for refined transcriptional and translational control (Duga et al., 1999). These studies provide evidence that due to the length and sequence of the mRNA upstream of AUG, secondary structures can occur, which will block ribosome scanning and result in various promoter activity and translational efficiency (Meric and Hunt, 2002). The translation efficiency of eukaryotic mRNAs may vary considerably depending on the properties of their 5' UTRs. Statistically, 5' UTRs of low expression mRNAs are longer and their GC content is higher (Kochetov et al., 1998). BRCA1 is a specific example of a gene with alternate mRNA transcripts. Similarly to PIK3CA, BRCA1 has two alternate first exons (1a and 1b), and two alternate promoters upstream that produce these alternate transcripts (Xu et al., 1997). For BRCA1, the longer mRNA transcript that also has a higher GC content forms a stable secondary structure, which inhibits efficient translation resulting in lower levels of the protein (Sobczak and Krzyzosiak, 2002). Future studies are required to determine the levels and ratios of the alternate PIK3CA

transcripts and the difference in their ability to translate protein. PIK3CA mRNA transcript containing exon1b (mRNA1b) is longer and has a higher GC content compared to the transcript containing exon1a (mRNA1a). If PIK3CA is similar to the other genes that contain more than one 5' UTR, then it is possible that the PIK3CA mRNA1b can also form secondary structures and result in less efficient translation compared to mRNA1a. In our studies, we provided evidence for p53 binding to promoter1a, but not promoter1b. This gives rise to an additional hypothesis that will require further investigation. We hypothesize that in normal cells, p53 binds to regions on promoter1a and suppresses transcription starting from this promoter. mRNA1b, with possible lower translation efficiency can be used by normal cells to maintain basal levels of p110α (Figure 17A). In the absence of functional p53 protein, the suppression of promoter1a is removed, and transcription can begin from promoter1a, giving rise to higher levels of mRNA1a with possible higher translational efficiency (Figure 17B). This may provide one explanation for the increased p110α levels in ovarian cancers.

FIGURE 17 (A and B)

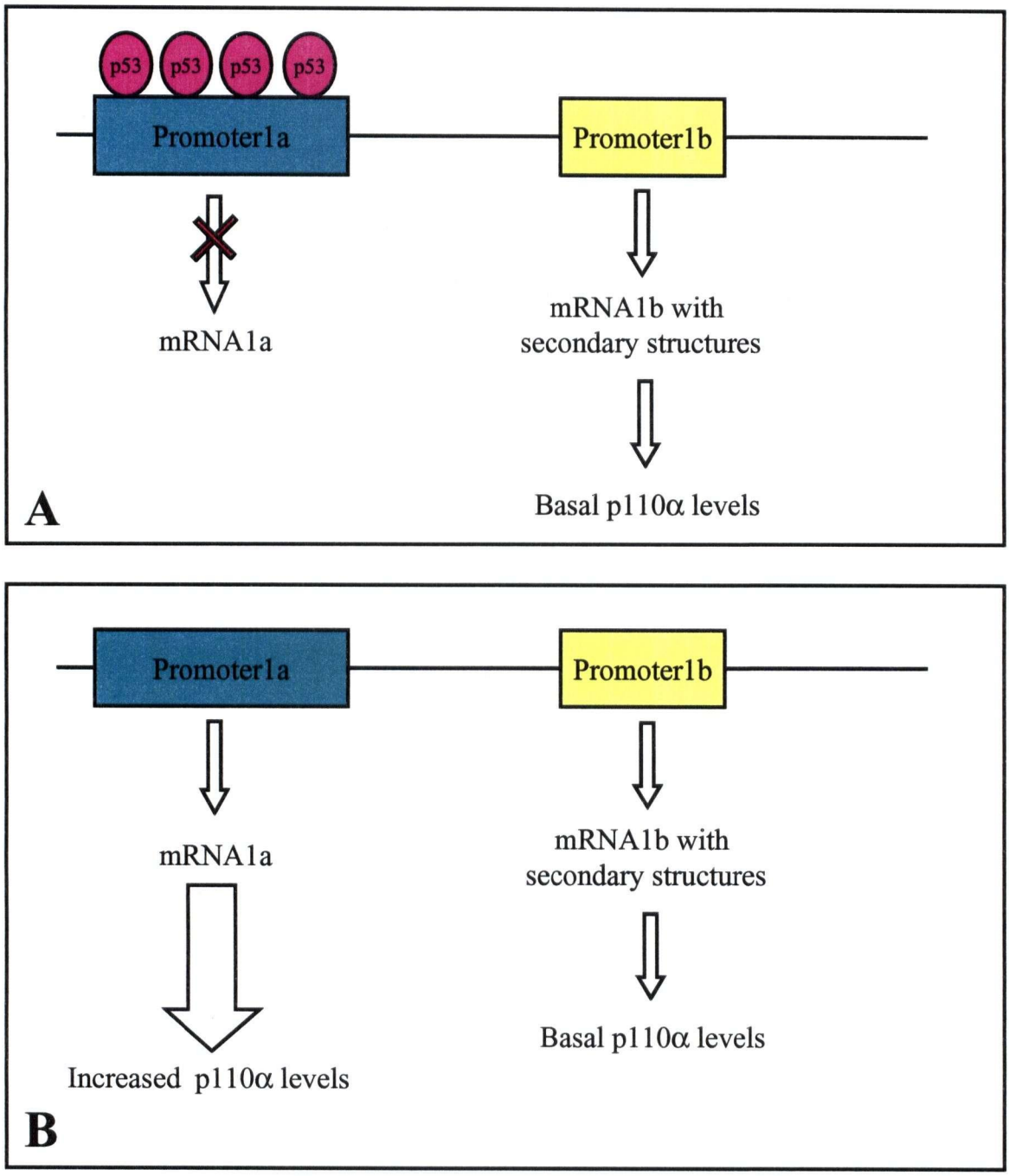

Figure 17: One proposed mechanism that leads to increased p110α levels in ovarian cancer. **(A)** A proposed mechanism by which normal cells maintain basal levels of p110α is demonstrated. p53 binds to promoter1a, thereby suppressing transcription of mRNA1a. Meanwhile promoter1b transcribes mRNA1b, which may form secondary structures and result in low levels of translation leading to basal p110α levels. **(B)** A proposed mechanism by which cancer cells increase levels of p110α is demonstrated. Loss of p53 results in loss of transcriptional repression on promoter1a, which may result in transcription of mRNA1a that has high translation efficiency and will result in increased levels of the p110α protein.

The RACE analysis also determined the presence of a long first intron of approximately 50,000 bps between the first (exon 1a/1b) and the second (exon 2(1)) PIK3CA exons. Long first introns of some other genes have been shown to contain important regulatory cis elements (Bergers et al., 1995; Molinero et al., 2004; van Dijck et al., 1993; Wu and Barger, 2004). Therefore, in addition to the sequences 5' to the start of transcription of the PIK3CA gene, our analysis was extended to this first intron. Analysis of this long first intron revealed a region that contained a p53 binding site that shares 81% conservation when aligned with the mouse sequence. Moreover, the ChIP analysis determined p53 binding to this region of the long first intron that we suggested to be an enhancer element. Further studies with the luciferase reporter constructs will determine whether this region participates in responsiveness of PIK3CA to p53.

ChIP analysis provided evidence that p53 binds directly to the PIK3CA promoter in order to suppress its transcription. Because PCR amplification of samples immunoprecipitated with the anti IgG antibody did not show any bands at either 34°C or 39°C, the presence of bands in the ChIP analysis of OSEC2 cells at 34°C and 39°C is likely not due to non-specific background during immunoprecipitation with the anti-p53 antibody. The p53 binding present in OSEC2 cells at 34°C, may be due to the presence of some p53 proteins that have escaped from binding to SV40 Tag. Jiang et al. (Jiang et al., 1993) demonstrated that coexpression of Tag significantly reduced, but did not completely block, p53-GAL4-mediated transcription from a GAL-4-dependent CAT reporter and also a p53-mediated transcription from a consensus p53 binding site in vivo. Moreover, Sladek et al. (Sladek et al., 2000) demonstrated by western blot and immunofluorescence that the levels of p53 in cells vary with different levels of Tag expression. Therefore, depending on the levels of Tag in the OSEC2 cells, it is possible that there are some levels of functional p53 that is free to bind DNA. The fact that there are fewer bands present in ChIP analysis of the OSEC2 cells at 34°C compared to OSEC2 cells at 39°C suggests that at the

higher temperature there is more functional p53 available to bind p53 binding sites on DNA. Moreover, p53 acts through binding as a homotetramer, therefore low levels of p53 may not result in functional p53 protein if not all of the four sites are occupied.

The ChIP results, although not conclusive, suggest that there is direct binding of p53 to the PIK3CA promoter. Although several candidate regions on promoter1a were determined to have p53 binding, whether there is a functional effect of binding at this region needs to be confirmed. Reporter assays need to be performed through cloning of the PIK3CA promoter and enhancer regions into luciferase constructs. Checking the activity of luciferase will indicate whether the binding of p53 to PIK3CA affects the activity of the promoter. These experiments are currently in progress. We are constructing five luciferase constructs containing: 1) promoter1a in a pGL3 basic vector, 2) promoter1b in a pGL3 basic vector, 3) enhancer region in a pGL3 promoter vector, 4) combination of promoter1a and enhancer region in pGL3 basic vector, and 5) combination of promoter1b and enhancer region in pGL3 basic vector. Transfection of these constructs into OSEC2 cells at 34°C and 39°C will determine whether the luciferase activity is inhibited through p53 function. Moreover, these studies will determine whether the p53 binding to the PIK3CA promoter, observed through the ChIP studies, results in suppression of the PIK3CA promoter activity.

There are several putative p53 binding sites in the regions that showed direct p53 binding to PIK3CA with the ChIP assay. Future studies are required to determine which specific binding sites p53 is directly binding to. Through point mutations or larger deletions of the putative p53 binding sites within the luciferase constructs, the specific p53 binding sites responsible for transcriptional repression of PIK3CA can be determined.

The mechanism by which transcriptional repression of promoters by p53 occurs is relatively unknown. Many promoters are repressed by p53 through physical interaction of p53 with a promoter bound transcriptional activator (Iotsova and Stehelin, 1996; Kanaya et al., 2000; Kubicka et al., 1999; Ohlsson et al., 1998; Subbaramaiah et al., 1999; Sun et al., 1999; Yun et al., 1999). Other promoters have been found to be repressed through direct binding of p53 (Budhram-Mahadeo et al., 1999; Hoffman et al., 2002; Johnson et al., 2001; Lee et al., 1999; Ori et al., 1998). El-Deiry identified the consensus p53-binding site that was defined as two palindromes separated by 0 to 13 nucleotides (el-Deiry et al., 1992). It has previously been shown that some of the promoters that are repressed through direct p53 binding have consensus binding sites with longer spacers, while canonical binding sequence of p53 on activating promoters generally have no spacers (Budhram-Mahadeo et al., 1999; Deng et al., 1995; Hoffman et al., 2002). Interestingly, on promoter1a the regions that were amplified after ChIP using promoter sets 1a1 and 1a4, contained putative p53 binding sites with spacers between 1 to 12 nucleotides. Regions 1a1 and 1a4 were exclusively amplified in the OSEC2 cells at 39°C, but not OSEC2 cells at 34°C. In addition, in regions of promoter1a that were amplified with primer sets 1a2 and 1a3, there are putative p53 binding sites present that have no spacer nucleotides. Regions 1a2 and 1a3 were amplified in OSEC2 cells at both 34°C and 39°C. Similar to other p53 repressed genes, the binding sites on the PIK3CA promoter regions 1a1 and 1a4, which contain spacer nucleotides, may play a role in regulating repression of PIK3CA by p53. Binding of p53 to regions 1a1 and 1a4 that have p53 binding sites with spacer nucleotides, may change the orientation of the binding sites, so that the dimers are no longer on the same face of the DNA helix as is required for transactivation. This, as suggested by Hoffman et al. (2002) may lead to passive binding of p53, which will inhibit transcriptional activation through interfering with binding of other transactivators (Hoffman et al., 2002). The mechanisms of repression in some promoters that display direct binding by p53 have been shown to be through binding to an

overlapping site of a transcriptional activator, resulting in a net decrease in transcription. For example, p53 binding to the Bcl-2 promoter results in displacement of the Brn-3a transcriptional activator (Budhram-Mahadeo et al., 1999). Moreover, Hoffman et al. (2002), in a study of the Survivin promoter, showed that p53 and E2F proteins occupy the promoter region at the same time creating a transcriptional repressor (Hoffman et al., 2002).

Although our findings suggest that direct binding of p53 to PIK3CA represses transcription, we have no evidence of mechanisms by which p53 regulates this repression. The mechanisms of transcriptional activation of the PIK3CA promoter are still unknown. Because there is no information on potential transactivators of PIK3CA transcription, it is difficult to determine if p53 is interfering with the activity of a potential transactivator. As a basis for our speculation that p53 may be interfering with a transcriptional activator's function by binding to the promoter, we analyzed putative E2F binding sites on the PIK3CA promoter with the ConSite web based tool. This analysis revealed several putative E2F transcription factor binding sites on the PIK3CA promoter that overlap or are adjacent to the putative p53 binding sites. This raises the possibility that p53 and E2F bind directly to the PIK3CA promoter and associate to form a transcriptional repressor. This mechanism of interfering with transcriptional activators will become clear as knowledge about transcriptional activation of PIK3CA becomes available. Our identification of the PIK3CA transcription start sites and promoter regions leads the way for future studies looking at transcriptional regulation of this important oncogene, PIK3CA.

4.3 Concluding Remarks

In conclusion, in temperature sensitive conditionally immortalized OSE cells, gain in p53 function resulted in a significant down-regulation of PIK3CA transcript levels, p110α protein levels, and PI3K activity. These results are in agreement with the results obtained by Singh et al.

(Singh et al., 2002). Singh et al. (2002) used cancer cells to show the functional interaction of p53 and PIK3CA. However, our results show for the first time that a functional and physical interaction exists between p53 and PIK3CA in non-malignant cells. We also identified two alternate promoters for the PIK3CA gene, and showed direct interaction of p53 with the PIK3CA promoter.

Our studies suggest a unique mechanism in the regulation of PI3K levels and activity in ovarian cancer. Figure 17A is a cartoon depicting direct binding of p53 homotetramer to the PIK3CA promoter that may result in repression of the promoter and decreased PIK3CA transcript levels. Our evidence suggests that the loss of p53 and thus reduced negative regulation of PIK3CA may contribute to increased PI3K levels and activity. Figure 17B demonstrates a simple diagram of how the p53 and PI3K pathways may regulate one another. Previous findings by Stambolic et al. (2001), demonstrated that p53 binds to the PTEN promoter and activates PTEN transcription (Stambolic et al., 2001). Our studies demonstrated that p53 binds to the PIK3CA promoter and suppresses PIK3CA transcription. In addition to p53 regulation of the PI3K pathway either through positive regulation of PTEN levels or negative regulation of p110α levels, the PI3K pathway in turn regulates p53 levels. Activated AKT phosphorylates MDM-2, which targets MDM-2 to the nucleus where it binds to and degrades p53 (Mayo and Donner, 2001). Therefore, this is a feedback loop by which loss of p53 leads to increases in P-AKT levels which in turn lead to increases in degradation of p53, and loss of even more p53 function. Combination of these factors may contribute to increases in p110α levels and PI3K activity in ovarian cancer cells.

FIGURE 17 (A and B)

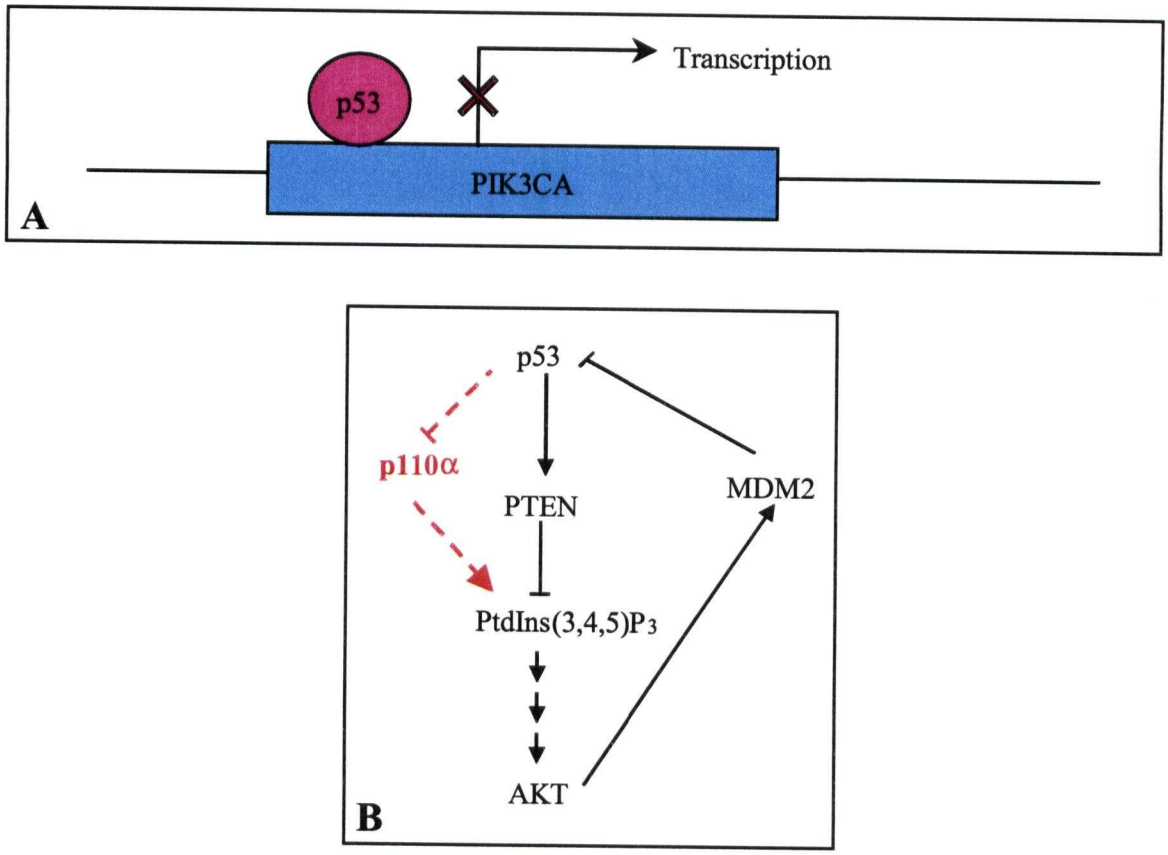

Figure 17: Interaction of p53 and PI3K pathways. (A) p53 binds directly to the PIK3CA promoter, thereby repressing its transcription. **(B)** p53 and PI3K pathways regulate one another. p53 positively regulates PTEN levels which reverse PI3K action by dephosphorylating PtdIns(3,4,5)P_3. Our contribution to this figure is outlined in red (dashed lines and arrows), demonstrating that p53 directly regulates PIK3CA transcription resulting in decreased p110α and PtdIns(3,4,5)P_3 levels. PtdIns(3,4,5)P_3 recruit AKT to the membrane where AKT becomes phosphorylated and activated. In turn, activated AKT phosphorylates MDM-2, which binds to and degrades p53.

Understanding the processes that lead to initiation and progression of ovarian cancer will aid in the development of effective therapies and earlier detection methods, which are key to improving the outcome of patients with ovarian cancer. The relationship between p53 and PIK3CA described in this work offers novel and valuable insights into the process of tumorigenesis and could thus aid in the design and development of treatments for ovarian cancer.

Through our characterization of the PIK3CA promoter, regulation of the PIK3CA gene by other transcription factors can be studied. The increasing knowledge on transcriptional regulation of PIK3CA, will lead to discovery of new targets and ways to inhibit PI3K transcription and/or regulate its levels. Furthermore, understanding how PIK3CA is regulated will give us more opportunities to manipulate the PI3K pathway in cancer therapy.

Currently, a combination of chemotherapy, usually a platinum-based drug, coupled with paclitaxel is the preferred treatment regimen for ovarian cancer. However, the development of chemoresistance is a problem that reduces the success of the treatments (Fraser et al., 2003a). Cancer cells respond to chemotherapeutic agents in part due to their apoptotic capacity. Moreover, drug-induced apoptosis is not only directed by the upregulation of pro-apoptotic factors or tumor suppressors, but also by modulation of cell survival factors (Fraser et al., 2003a). Therefore, deregulation of these signals can lead to chemoresistance. Understanding the relationship between p53 and PIK3CA may allow us to explain and exploit mechanisms by which ovarian cancers respond to chemotherapy.

Several studies have demonstrated evidence of a role for the PI3K/AKT pathway in the resistance to chemotherapeutic agents. It has been demonstrated that cells expressing a constitutively active AKT2 are resistant to cisplatin (Fraser et al., 2003b; Yuan et al., 2003), and cells expressing constitutively active p110α are resistant to paclitaxel (Hu et al., 2002). In mice, treatment with LY294002 was shown to reverse the resistance to paclitaxel (Hu et al., 2002). It has been suggested that inhibition of the PI3K/AKT pathway could potentially act as a potent

adjuvant to traditional chemotherapies (Fraser et al., 2003a). Our studies direct the way for future studies investigating the regulation of PIK3CA by transcription factors other than p53. Understanding the mechanisms of regulation of this important oncogene can lead to the identification of potential therapeutic targets for cancer.

Appendix 1:

Role of PI3K Signalling in Ovarian Carcinogenesis

HYPOTHESIS AND AIMS:

The aim of our study was to define more clearly the role of PI3K in early stages of ovarian carcinogenesis. We tested the hypothesis that amplification of the p110α catalytic subunit of PI3K contributes to malignant transformation of OSE. Our aim was to introduce constitutively active p110α into non-transformed IOSE cells and look for phenotypic changes that are generally acquired during malignancy.

MATERIALS AND METHODS:

Constructs:

Dr. GB Mills (MD Anderson Cancer Center, Houston, TX) provided us with two expression vectors containing the sequence that codes for p110α. One construct is the wild-type (WT) p110α derived from the bovine gene cloned into a pcDNA3 vector. This bovine derived protein has 99% homology to the human p110α. The WT-p110α protein expression vector is engineered with a C-terminal nucleotide sequence that encodes the haemagglutinin (influenza virus (HA)) epitope tag (HA-p110α). For activation, the HA-p110α requires heterodimerization with p85, present in abundance in cells, and recruitment to the plasma membrane. Stimulating these cells with growth factors will target the HA-p110α to the membrane where the substrates are located.

The second p110α construct was derived from the murine gene. This murine p110α has 98% homology to the human protein. This gene was fused in frame with a Myc epitope tag. Moreover, the p110α N-terminus was modified by the pp60 c-Src myristoylation sequence (Deichaite et al., 1988; Kaplan et al., 1990). This modification targets the p110α to the membrane where its activity is required. Thus this construct is constitutively active, however for maximal activation of this exogenous p110α, the iSH2 region of p85 is covalently linked to its binding site at the N-terminus of p110α using a flexible hinge region (Klippel et al., 1996). This construct is referred to as Myr-p110α*-Myc. This Myr-p110α*-Myc insert is cloned into a pBJ-1 vector that does not contain a selection marker for obtaining stable cell lines. Therefore, this construct needs to be cotransfected with pcDNA3 that contains the neomycin resistance gene. The transfection was performed in a 3:1 ratio of Myr-p110α-Myc: pcDNA3, and the cells were selected with 200μg/ml of G418.

Cell Lines:

IOSE 80pc cells were previously transfected with SV40 early genes (Maines-Bandiera et al., 1992). They have gone through crisis and thus have gained the ability to replicate endlessly. IOSE 80telo lines are also truly immortalized through an additional transfection with hTERT, the catalytic subunit of human telomerase. IOSE 80pc and IOSE 80telo cells were previously transfected with Myr-p110α*-Myc and HA-p110α constructs. The successful transfection of the HA-p110α construct was confirmed by PCR. The successful transfection of the Myr-p110α*-Myc construct was confirmed by western blot and immunofluorescence analysis using anti-Myc-tag monoclonal (9B11) antibody (Cell Signaling Technologies Catalog #2276).

For all experiments, IOSE 80pc and telo cells transfected with the pcDNA3 vector were used as controls. The transfected cell lines were designated as IOSE 80pc Myr-p110α*-Myc (1),

IOSE 80pc HA-p110α (1) and IOSE 80pc vector control (1), IOSE 80telo Myr-p110α*-Myc, IOSE 80telo HA-p110α and IOSE 80telo vector control. Transfection of IOSE 80pc cells with the constructs was repeated using Fugene6 (Roche) as recommended by the manufacturer. These cells are referred to as IOSE 80pc Myr-p110α*-Myc (2), IOSE 80pc HA-p110α (2) and IOSE 80pc vector control (2). After selection with 200μg/ml of G418, all these cells were maintained in 199:105 medium supplemented with 5% serum and 100μg/ml G418 in a 37°C incubator with 5% CO2/air atmosphere. All the experiments performed were repeated at least three times.

Proliferation and Serum Independence:

For proliferation studies, the cells were grown in 96 strip-well plates (Fisher). Cells were seeded at 2000 cells per well in six replicates. When the cells were ready for the assay, the wells were washed with warm serum-free medium, filled with cold methanol and maintained at -20°C until all time points were ready for the assay. The wells were rinsed with PBS and Hoechst dye 33258 was added at 5μg/ml for 2 minutes. The wells were washed with PBS three times for 5 minutes each and the absorbance read using the Fluorescence Plate Reader FL600 (Bio-Tek).

Anchorage Independence:

Colony formation in soft agar was assayed by suspending 2.0×10^4 cells in 1 ml of medium 199:105 supplemented with 5%FBS. The suspension was mixed with 1ml of 1% agarose (Life Technologies) and 1ml of 2x medium (2x 199:105 medium + 20% FBS). This suspension was added on top of 5 ml of solidified 0.5% agarose in the above medium. Triplicate cultures for each cell type were maintained for 14 days at 37°C in a 5% CO_2 atmosphere with fresh medium added after 1 week. Colonies were counted after 2 weeks.

RESULTS and DISCUSSION:

1. IOSE 80pc (1) Cells Transfected with p110α

IOSE 80pc Myr-p110α*-Myc (1) cells had an interesting morphology (Figure App1). As the cultures became close to confluence, they retracted and had thin filamentous extensions, which suggested the possibility that the PI3K is activating some downstream targets involved in cytoskeleton rearrangement or adhesiveness. This unique morphology was not observed in IOSE 80pc vector control (1) cells.

FIGURE App1

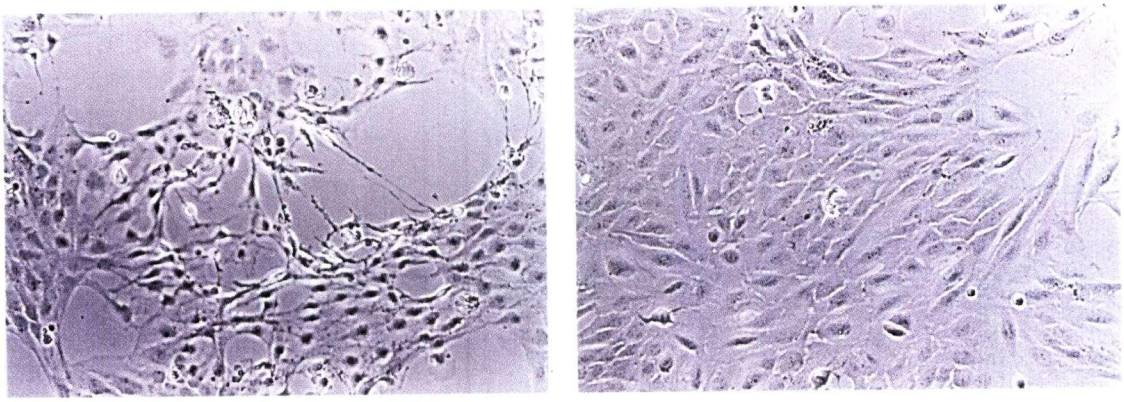

IOSE 80pc Myr-p110α*-Myc (1) IOSE 80pc vector control (1)

Figure App1: Effect of p110α overexpression on morphology. As IOSE 80pc Myr-p110α*-Myc (1) cells became confluent, they retracted and had thin filamentous extensions. IOSE 80pc vector control (1) cells did not display this morphological characeteristic.

We wanted to determine the characteristics gained in these cells after tranfection with p110α. Fluorometric DNA measurements determined that both IOSE 80pc Myr-p110α*-Myc (1), and IOSE 80pc HA-p110α (1) cells had increased growth rates and reached higher saturation densities compared to the vector control cells (Figure App2). IOSE 80pc Myr-p110α*-Myc (1) cells proliferated until they got very crowded and lifted off as sheets of cells (Figure App2A). In contrast, the IOSE 80pc vector control (1) and the IOSE 80pc HA-p110α (1) cells stopped proliferating when they reached a certain density. The IOSE 80pc HA-p110α (1) cells require growth factor stimulation for membrane localization. IOSE 80pc HA-p110α (1) cells were significantly more proliferative than IOSE 80pc vector control (1) cells (Figure App2B). This significant increase in proliferation is likely due to the presence of 5% FBS in our culture medium acting to stimulate at least some of the exogenous HA-p110α.

FIGURE App2

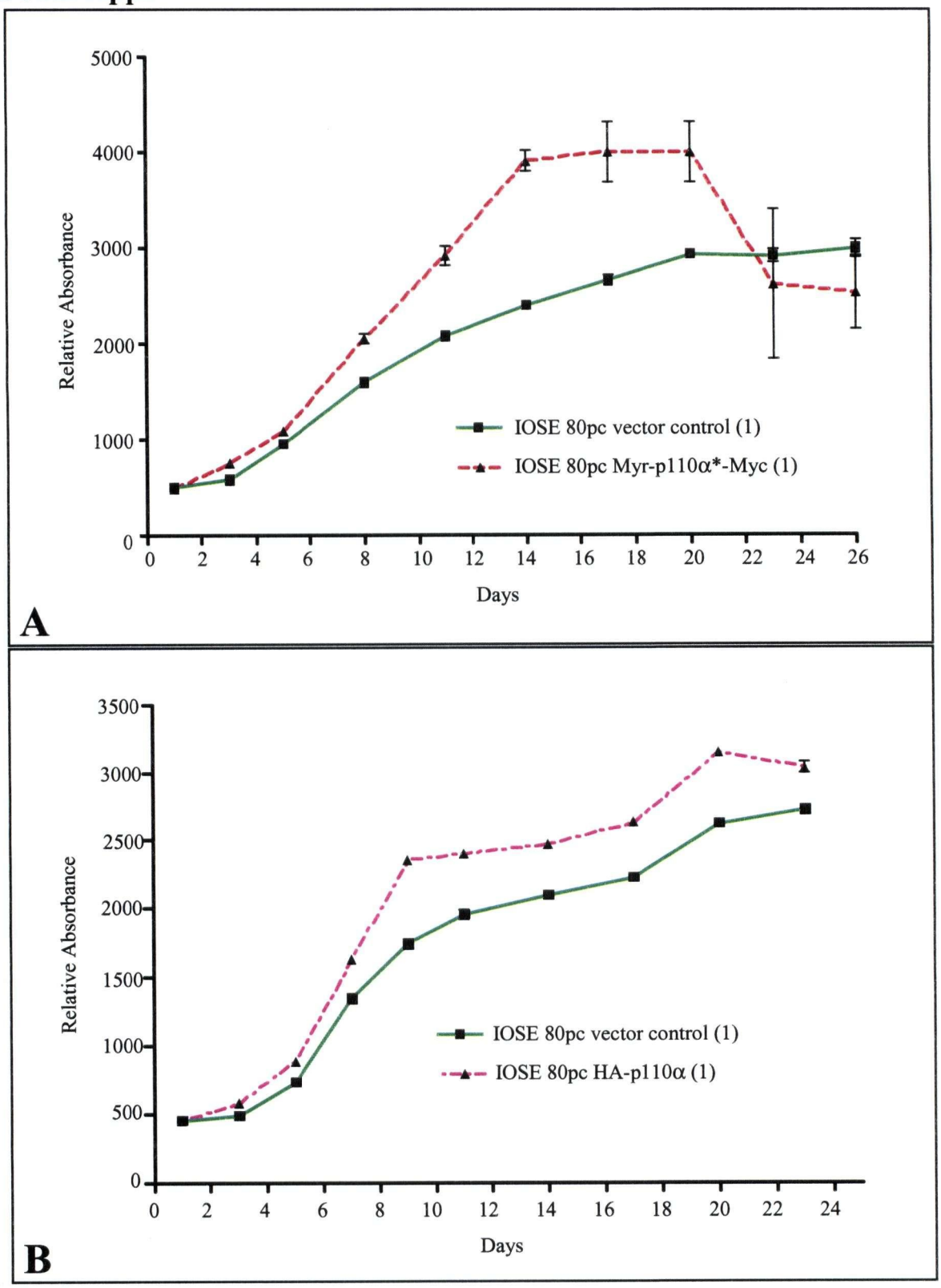

Figure App2: Effect of p110α overexpression on proliferation rate. (A) IOSE 80pc Myr-p110α*-Myc (1) cells proliferated faster and reached higher saturation densities compared to IOSE 80pc vector control (1) cells. **(B)** IOSE 80pc HA-p110α (1) cells grew significantly faster than IOSE 80pc vector control (1) cells, although not to the same extent as IOSE 80pc Myr-p110α*-Myc (1) cells.

Another phenotypic change that was characterized was the ability of the cells to grow independent of anchorage. IOSE 80pc Myr-p110α*-Myc (1) cells had the ability to grow in soft agar (i.e. they are anchorage independent), while IOSE 80pc vector control (1) cells did not (Figure App3). LY294002 significantly reduced the ability of these cells to form colonies in soft agar. There was a dose dependent reduction in the number of colonies, while the relative number of colonies in each size range did not change significantly. This suggests that the constitutive activation of the PI3K pathway is giving these cells the ability to form colonies in soft agar. The fact that the sizes of the colonies did not decrease after treatment with the PI3K inhibitor suggests that PI3K is directly involved in colony formation and not just proliferation that would affect the size of the colonies. Moreover, the IOSE 80pc HA-p110α (1) and the vector control (1) cells did not form any colonies. Since HA-p110α requires stimulation for membrane localization and activation, the lack of growth of colonies in soft agar in these cells in not surprising. Even though IOSE 80pc HA-p110α (1) cells overexpress the p110α protein, they still require simulation in order for the p110α to be recruited to the membrane where it can function to phosphorylate its substrates.

FIGURE App3

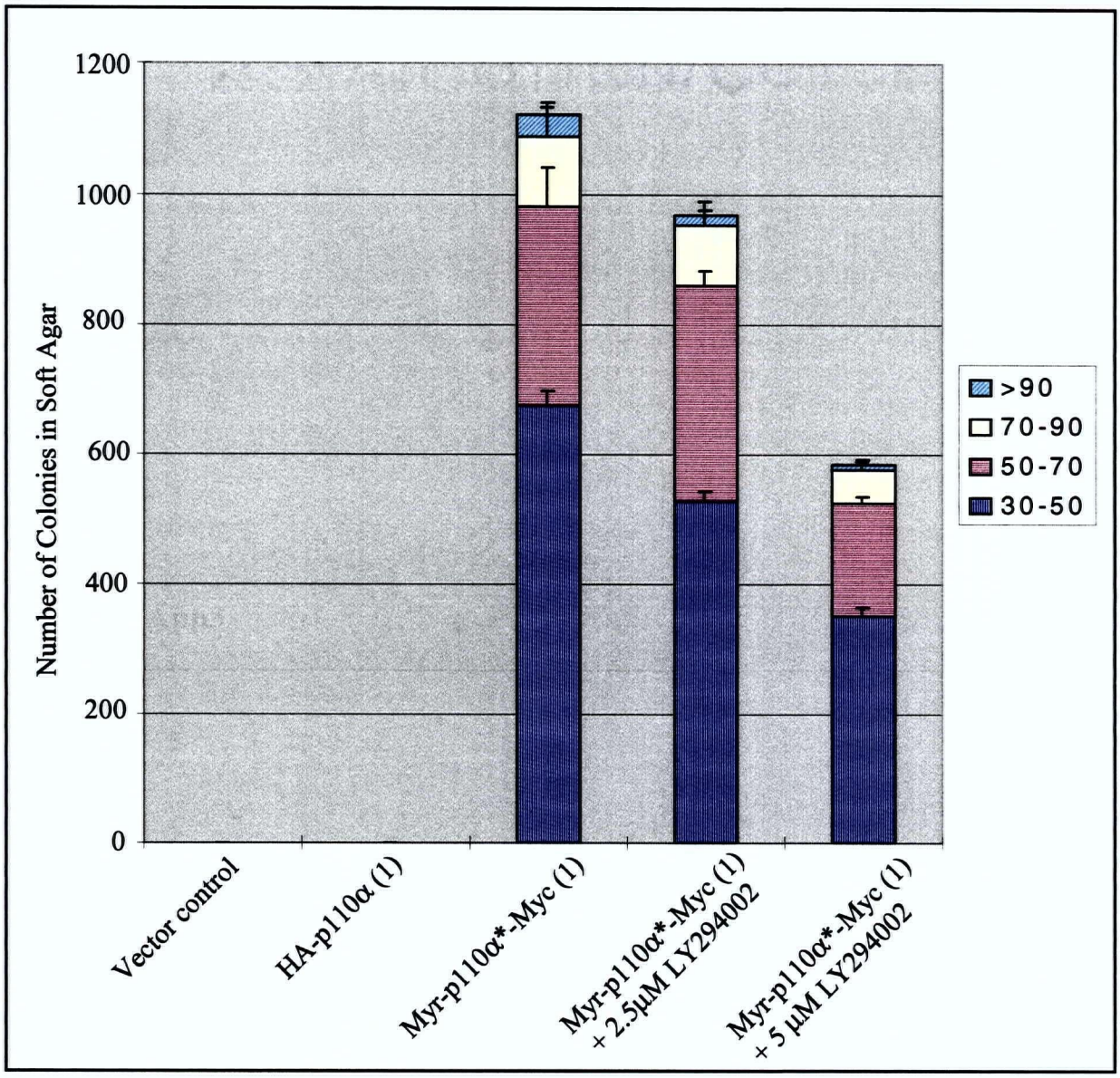

Figure App3: Effect of p110α overexpression on anchorage independent growth. The ability of IOSE 80pc Myr-p110α*-Myc (1), IOSE 80pc HA-p110α (1) and IOSE 80pc vector control (1) cells to form colonies in soft agar were tested. Only IOSE 80pc Myr-p110α*-Myc cells were able to form colonies in soft agar. The number of colonies significantly declined after treatment with LY294002, in a dose dependent manner. The size distribution of the colonies were not affected. The different colours in the bars represent the range of the diameters that the colonies reached, in microns

IOSE 80pc Myr-p110α*-Myc (1) cells were also treated with varying concentrations of LY294002 daily for 3 days. After 3 days, the cells without any treatment had significantly increased in number, while a dose dependent decrease in the number of cells resulted from PI3K inhibition (Figure App4).

FIGURE App4

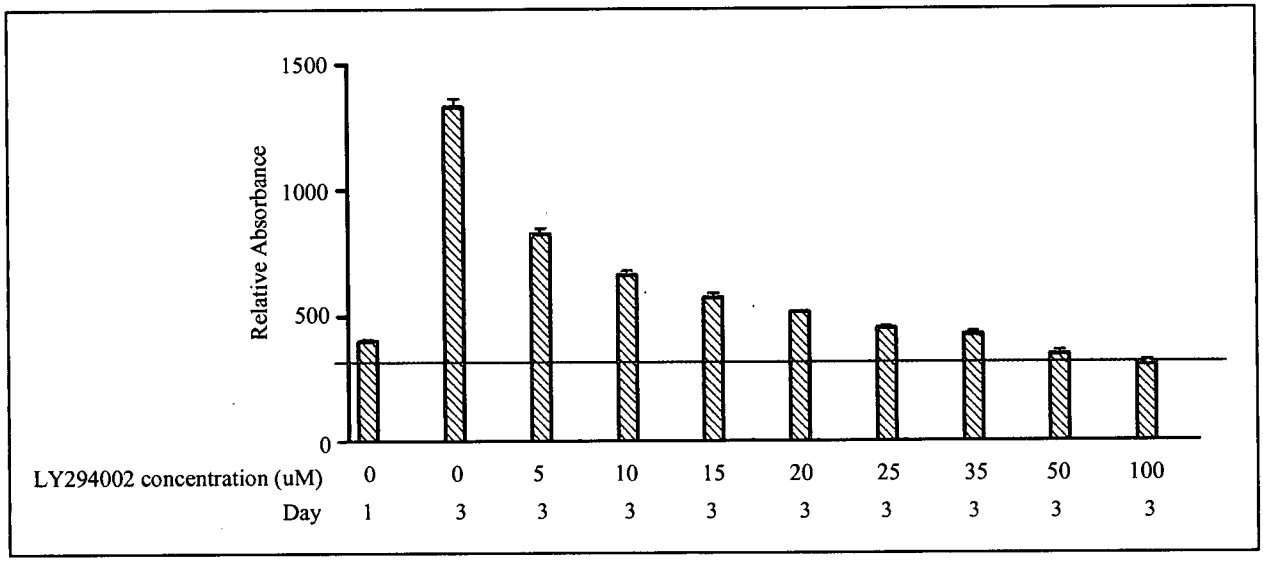

Figure App4: Effect of PI3K inhibition on proliferation. The cells were cultured in 96 well strip plates with 6 replicates. A strip of replicates were fixed in methanol on day 1. Another strip of replicates were left untreated, and the remainder were treated with different concentrations of LY294002 everyday for 3 days. On day 3, the cells were fixed with methanol at -20°C. The cells were stained with Hoechst 33258, and subsequently the relative absorbance was measured on a fluoremetric reader. There was a dose dependent decrease in the number of IOSE 80pc Myr-p110α*-Myc (1) cells after LY294002 treatment.

2. IOSE 80telo Cells Transfected with p110α

Proliferation and anchorage independent growth were tested on IOSE 80telo Myr-p110α*-Myc and IOSE 80telo HA-p110α cells. These cells did not have the ability to form colonies in soft agar, and their proliferation was not significantly different from IOSE 80telo vector control cells. These experiments were done in replicates and repeated at least three times.

3. IOSE 80pc (2) Cells Transfected with p110α

To confirm that the phenotypic changes observed with IOSE 80pc Myr-p110α*-Myc (1) cells were due to the transfection with the constitutively active form of p110α, transfection of IOSE 80pc cells was repeated. We referred to these new transfected cells as IOSE 80pc Myr-p110α*-Myc (2), IOSE 80pc HA-p110α (2), and IOSE 80pc vector control (2). After selection of stable cell lines with G418 (200μg/ml), the expression of the transgene was confirmed by RT-PCR. RNA was extracted from the transfected cells, digested with deoxyribonuclease I (Invitrogen), reverse transcribed and subsequently used for PCR. A forward primer that spans part of the sequence of the tag and part of the p110α sequence was used to amplify only the exogenous sequence. The agarose gel analysis showed the presence of appropriately sized bands indicating successful transfection of IOSE 80pc cells with both HA-p110α and Myr-p110α*-Myc constructs (Figure App5). For positive control in these PCR reactions, relatively early and later passages of IOSE 80pc Myr-p110α*-Myc (1) and IOSE 80pc HA-p110α (1) cells were used. To our surprise, PCR analysis of earlier and late passage IOSE 80pc Myr-p110α*-Myc (1) cells showed no band (Figure App5A), even though these cells previously tested positive for expression of the transgene by PCR and western blot analysis with anti Myc-tag antibody. Therefore, we speculate that these cells lost the p110α transgene after subsequent passaging.

FIGURE App5

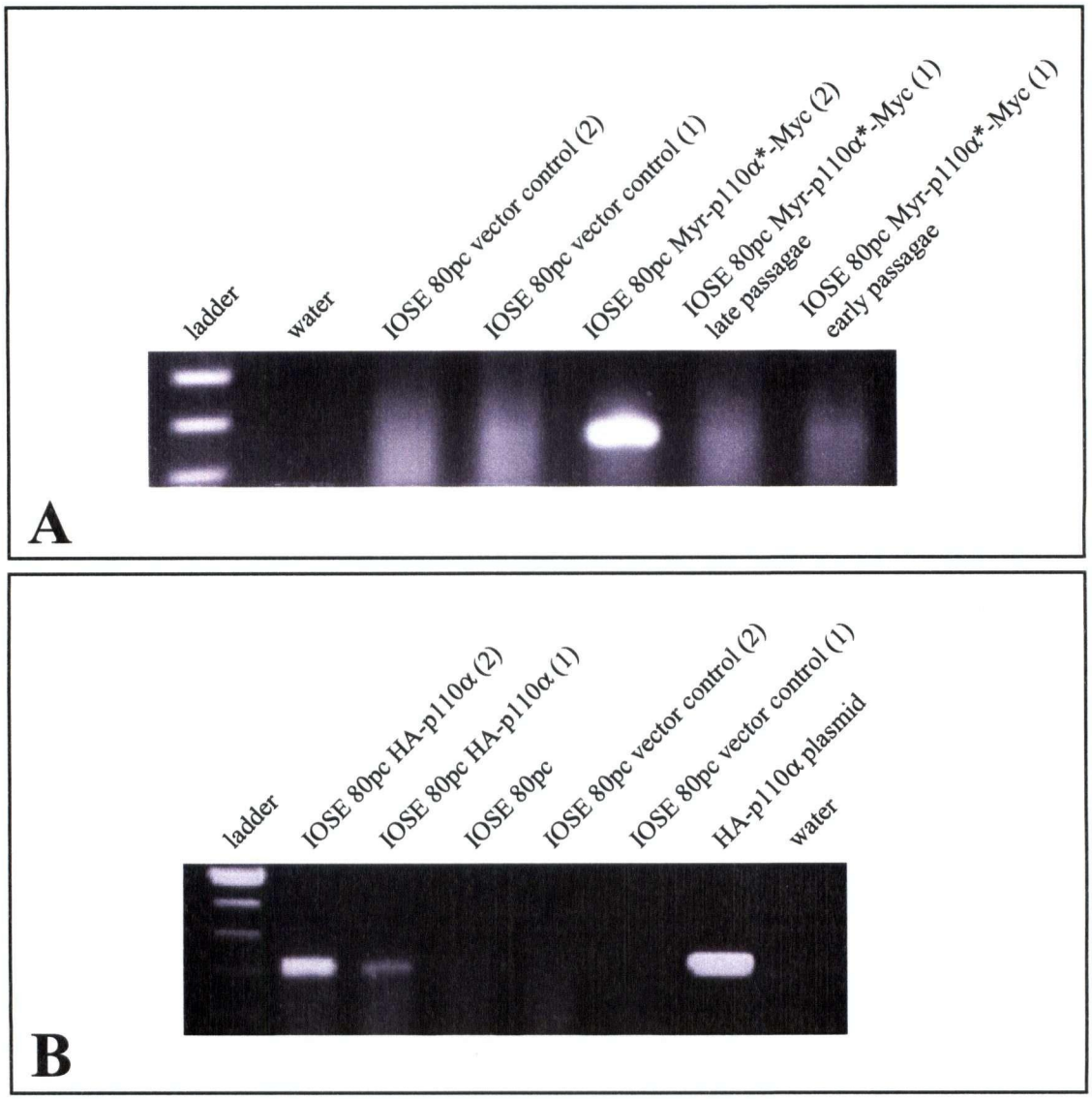

Figure App5: RT-PCR showing expression of the transgene. RNA was extracted from IOSE 80pc Myr-p110α*-Myc, IOSE 80pc HA-p110α, IOSE 80pc vector control cells. **(A)** IOSE 80pc Myr-p110α*-Myc (2) cells expressed the transgene. Interestingly, both earlier and late passages of IOSE 80pc Myr-p110α*-Myc (1) cells did not express the transgene. **(B)** IOSE 80pc HA-p110α (2) and IOSE 80pc HA-p110α (1) cells both expressed the trasngene.

Western blot analysis was performed on all IOSE 80pc transfected cell lystaes with the anti-Myc and anti-HA antibodies to detect expression of the transgene. However, expression of the transgene could not be detected in any of the transfected cell lines. Moreover, an anti-p110α antibody was used to look at possible increases in the PI3K protein levels in the transfected cell lines. The Myr-p110α*-Myc protein is significantly larger than the endogenous p110α and thus should appear as a heavier band on the western blot. Using anti-p110α antibody, the western blots of the transfected IOSE 80pc cell lysates were all negative for the additional p110α band, and did not show an increase in the level of protein compared to the vector control cells (Figure App6). An anti P-AKT antibody was also used to determine if the transfected cells have higher PI3K activity. Interestingly, without EGF stimulation the IOSE 80pc Myr-p110α*-Myc (1) cells had the highest P-AKT levels. However, upon EGF stimulation IOSE 80pc Myr-p110α*-Myc (2) cells had the highest levels of P-AKT (Figure App6).

FIGURE App6

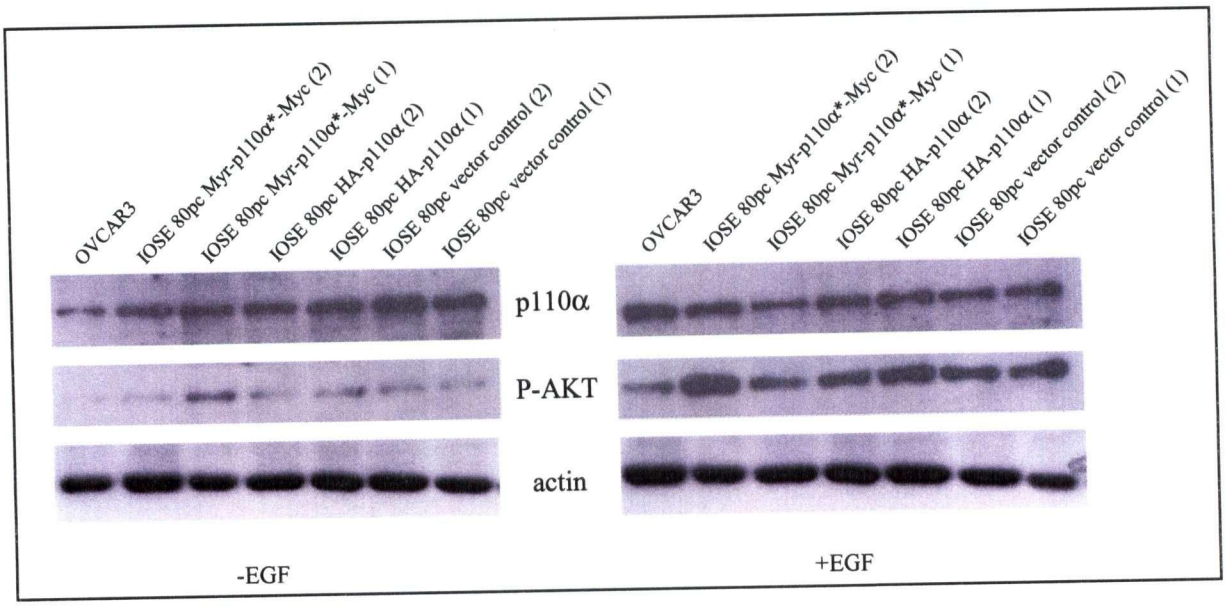

FigureApp6: Western blot analysis determined lack of protein expression of the p110α constructs. Western blot analysis with anti p110α antibody did not detect an additional band or an increase in p110α levels between p110α transfected and vector control cells. The cells in the right blot were treated with EGF for 30 minutes prior to cell lysis, while the cells in the left blot were left untreated. Phosphorylated AKT levels were looked at using an anti P-AKT antibody. In the cells without stimulation (left blot), IOSE 80pc Myr-p110α*-Myc (1) cells had the highest levels of P-AKT, while in the cells stimulated with EGF (right blot), IOSE 80pc Myr-p110α*-Myc (2) cells had the highest P-AKT levels. Anti-actin antibody was used to determine equal loading of the protein samples. OVCAR3 cells were used as positive control.

Immunofluorescence was used to determine if the transfected IOSE 80pc cells expressed the transgene. Immunofluorescence of IOSE 80pc HA-p110α (2) cells with anti-HA antibody was negative, confirming that these cells did not express the exogenous protein, even though they expressed the transcript based on the RT-PCR results (Figure App5B). Immunofluorescence studies of the IOSE 80pc Myr-p110α*-Myc (2) cells with anti-Myc tag antibody showed strong positive staining of the nuclei relative to the IOSE 80pc vector control (2) cells with minimal background staining (Figure App7). It must, however, be noted that the Myr-p110α*-Myc construct has the c-Src myristoylation sequence that should target the protein to the plasma membrane. Interestingly, this nuclear staining was also previously observed with the IOSE 80pc Myr-p110α*-Myc (1) cells.

FIGURE App7

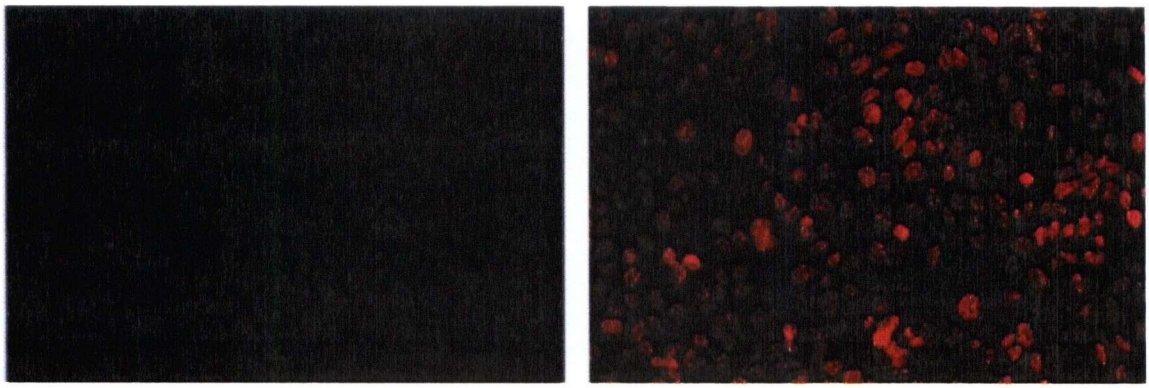

IOSE 80pc vector control (2) IOSE 80pc Myr-p110α*-Myc (2)

Figure App7: Immunofluoresence analysis determined nuclear localization of the Myc tag. Immunofluoresnce analysis of IOSE 80pc Myr-p110α*-Myc cells with anti-Myc tag antibody determined strong nuclear staining in IOSE 80pc Myr-p110α*-Myc (2) cells while weak staining in IOSE 80pc vector control (2) cells.

IOSE 80pc Myr-p110α*-Myc (2) cells did not show the same pulled back morphology as was observed with IOSE 80pc Myr-p110α*-Myc (1) cells (Figure App1). Proliferation and ability to grow in soft agar was tested in transfected IOSE 80pc (2) cells. Proliferation studies of IOSE 80pc Myr-p110α*-Myc (2) cells showed that, compared to IOSE 80pc vector control (2) cells, IOSE 80pc Myr-p110α*-Myc (2) cells actually proliferate more slowly (Figure App8). This was contrary to what was observed with IOSE 80pc Myr-p110α*-Myc (1) cells (Figure App2A), in which the cells proliferated more rapidly and reached higher saturation densities. IOSE 80pc HA-p110α (2) cells proliferated similarly to IOSE 80pc vector control (2) cells. Upon EGF stimulation, both IOSE 80pc HA-p110α (2) and IOSE 80pc vector control cells (2) reached higher saturation densities relative to no EGF stimulation, yet there was no difference between the growth rates of the two cell lines (Figure App8).

FIGURE App8

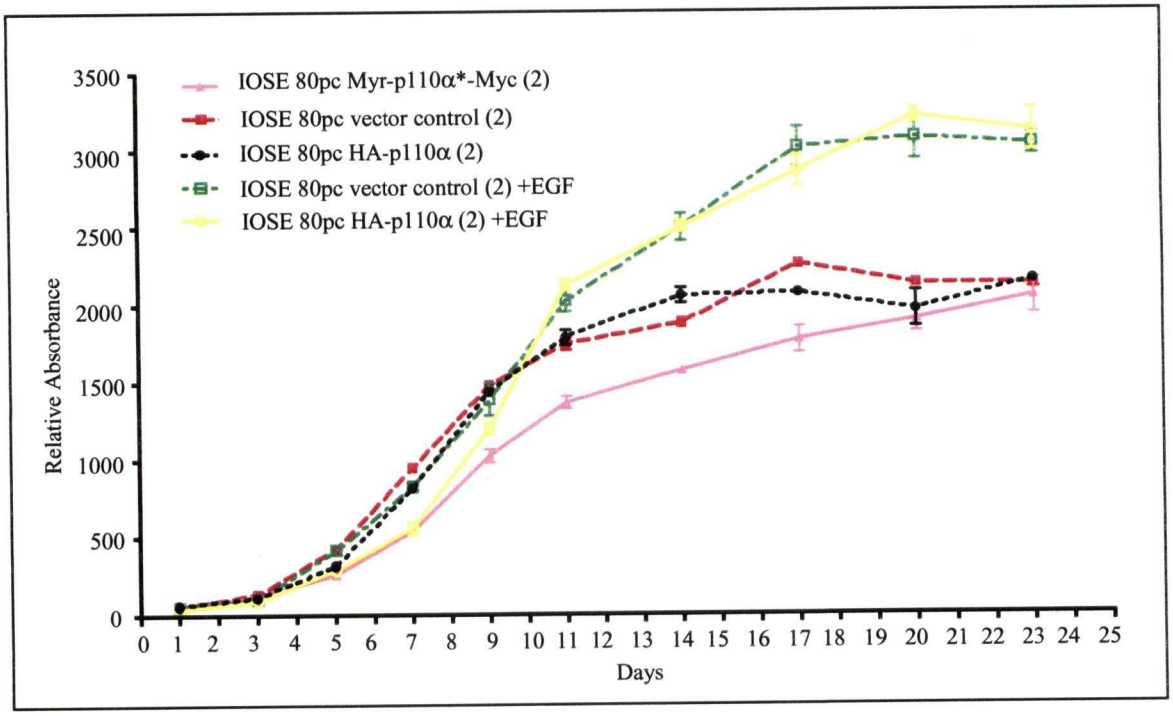

Figure App8: IOSE 80pc Myr-p110α*-Myc (2) cells do not have a higher proliferation rate. IOSE 80pc Myr-p110α*-Myc (2) cells proliferated more slowly compared to IOSE 80pc vector control (2) cells. There was no significant difference in proliferation between IOSE 80pc HA-p110α (2) and IOSE 80pc vector control (2) cells with or without EGF stimulation. After EGF stimulation both had increased proliferation and reached higher saturation densities.

The ability to grow in soft agar was tested with IOSE 80pc Myr-p110α*-Myc (2), IOSE 80pc HA-p110α (2), and IOSE 80pc vector control (2) in the presence or absence of EGF stimulation (Figure App9). With EGF stimulation these cells were able to form colonies in soft agar. However, the same was true for IOSE 80pc vector control (2) cells. Interestingly, IOSE 80pc Myr-p110α*-Myc (2) cells did not form colonies in the absence of EGF. After EGF stimulation, compared to IOSE 80pc HA-p110α (2) and IOSE 80pc vector control (2) cells, the IOSE 80pc Myr-p110α*-Myc (2) cells made about five fold less colonies in soft agar. The ability of IOSE 80pc Myr-p110α*-Myc (2) cells to form colonies in soft agar was different from IOSE 80pc Myr-p110α*-Myc (1) cells, which did display anchorage independent growth (Figure App3).

FIGURE App9

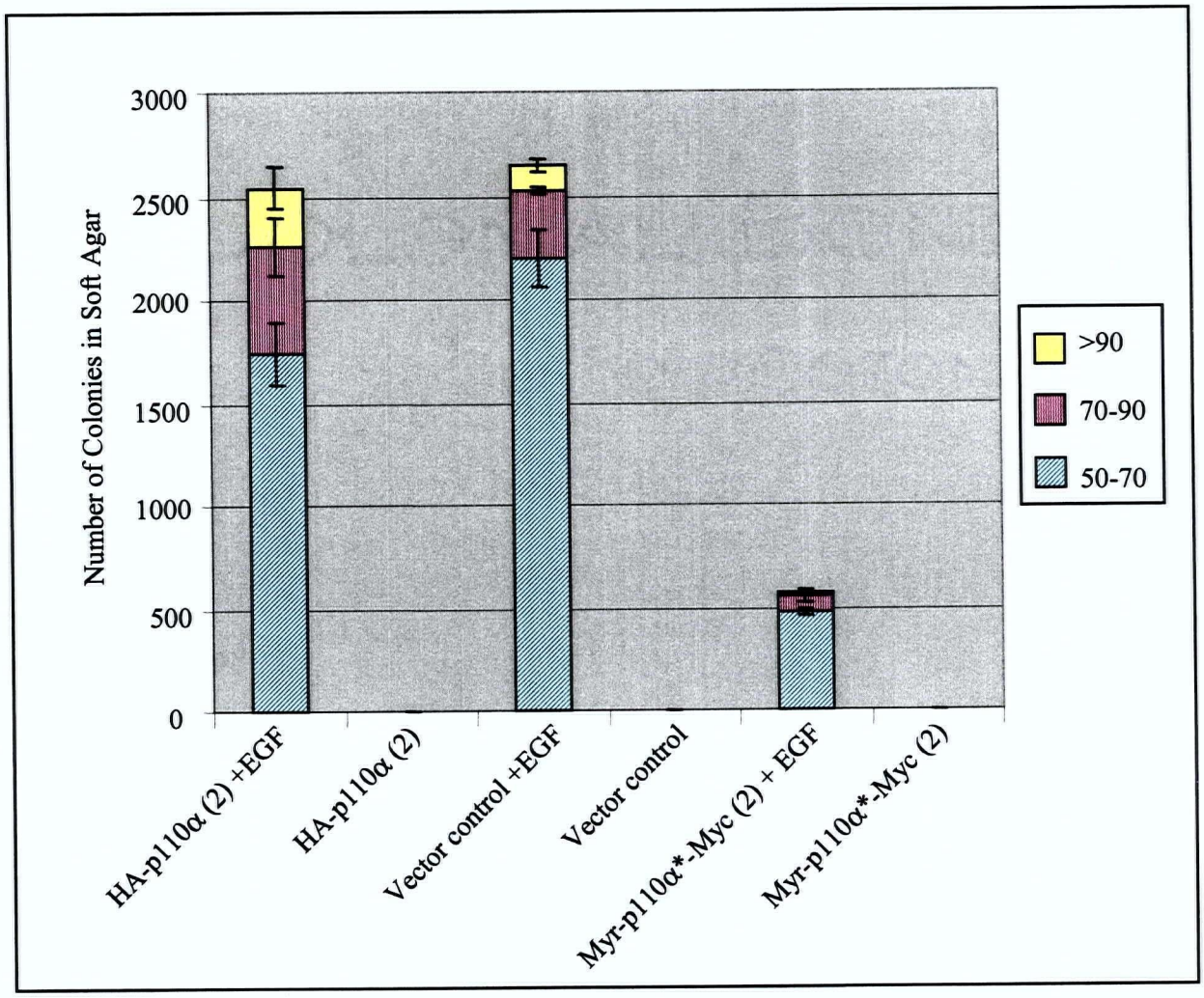

Figure App9: IOSE 80pc Myr-p110α*-Myc (2) cells are not anchorage independent. IOSE 80pc Myr-p110α*-Myc (2) cells were not able to form colonies in soft agar. IOSE 80pc HA-p110α (2) and IOSE 80pc vector control (2) cells formed colonies in soft agar after stimulation with EGF, but not without stimulation. The colonies of the IOSE 80pc HA-p110α cells were significantly larger in size compared to the vector control cells. Even with EGF stimulation, IOSE 80pc Myr-p110α*-Myc cells did not form many colonies in soft agar. The different colours in the bars represent the range of the diameters that the colonies reached, in microns.

Treatment of transfected IOSE 80pc cells with LY294002 produced a dose-dependent decrease in cell number as indicated by fluorometric DNA measurements (Figure App10). The IOSE 80pc Myr-p110α*-Myc (1) cells were the most proliferative and reached the highest cell numbers during the course of the experiment. Both of the vector control cells had similar growth patterns, while IOSE 80pc Myr-p110α*-Myc (2) cells had the lowest number of cells. Although this experiment demonstrates that the two IOSE 80pc Myr-p110α*-Myc cells, (1) and (2), have different growth potentials, it also shows that the responsiveness to the PI3K inhibitor in all four cell lines is similar, independent of the transfections.

FIGURE App10

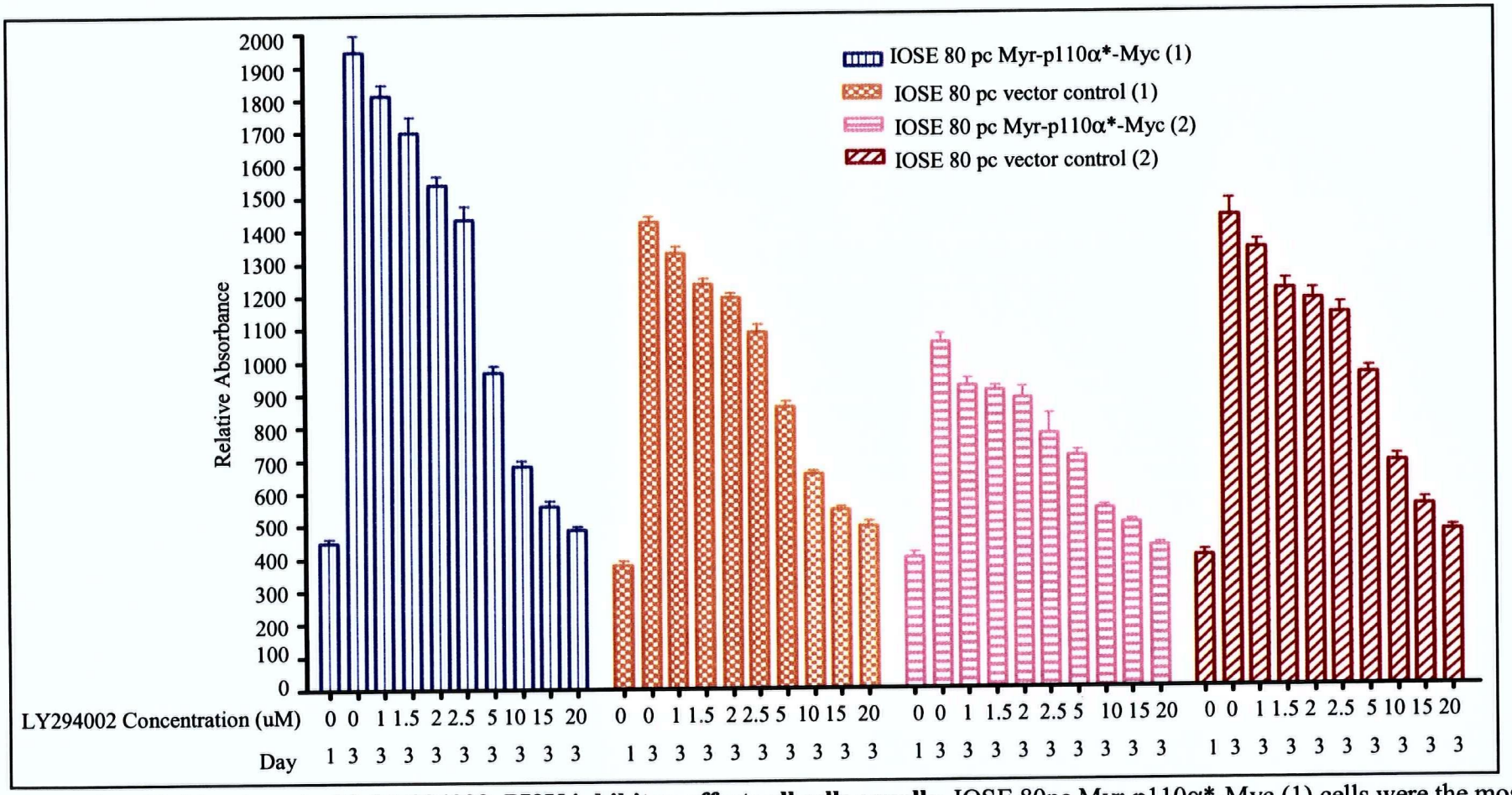

Figure App10: Treatment with LY294002, PI3K inhibitor, effects all cells equally. IOSE 80pc Myr-p110α*-Myc (1) cells were the most proliferative and reached highest number of cells in culture within 5 days. IOSE 80pc Myr-p110α*-Myc (2) cells proliferated more slowly compared to IOSE 80pc vector control (2) cells. There was no significant difference in proliferation between IOSE 80pc HA-p110α (2) and IOSE 80pc vector control (2) cells. The effect of LY294002 on the cells follows the same pattern in all cells tested, showing a decrease in cell number with the increase in LY294002 concentration.

CONCLUSIONS:

Although IOSE 80pc Myr-p110α*-Myc (1) cells showed significant phenotypic changes relative to the IOSE 80pc vector control (1) cells, these results were not reproducible. We were not able to show successful expression of the exogenous p110α in the transfected IOSE 80pc cells. Moreover, repeated transfections did not result in the same phenotypes as observed with IOSE 80pc Myr-p110α*-Myc (1) cells. We speculate that the characteristics observed with the IOSE 80pc Myr-p110α*-Myc (1) cells may be unrelated to the p110α transfection. IOSE 80pc cells are genomically unstable and go through genetic modifications after continuous passaging in culture. Therefore, it is possible that IOSE 80pc Myr-p110α*-Myc (1) cells gained those phenotypic characteristics through genetic modification of the cells, which were independent of the transfections.

Appendix 2.

Development of a New Post-Crisis Cell Line

A new post-crisis cell line, IOSE 120pc, was developed. Normal human somatic cells, including OSE cells, undergo a limited number of cell divisions in vitro before entering senescence, which is defined as an irreversible growth-arrest state (Cristofalo et al., 1998). However, viral oncogenes such as SV40 Large T antigen can result in an extension of growth potential of the cells, which finally reach "crisis," or progressive cell death (Shay et al., 1991). IOSE cells routinely undergo crisis after 30-40 population doublings, if they are maintained in standard culture medium (199:105 medium supplemented with 5% FBS). A small number of cells can overcome crisis and acquire an indefinite lifespan. This change is accompanied by stabilization of telomere length, either though gain in hTERT or alternate mechanism of telomere maintenance (Jha et al., 1998). To determine whether EGF/Hydocortisone treatment would allow IOSE to overcome crisis, we maintained IOSE 120 cells in standard medium supplemented with 10μg of EGF with Hydrocortisone for 200 population doublings. EGF was then removed from the growth medium and the cells were continuously passaged for another 200 population doublings, without showing signs of senescence or slowed proliferation. The IOSE 120pc cells are special as other IOSE lines tested (IOSE 80 and IOSE 144) previously in our lab underwent crisis even in the presence of EGF. Telomerase assay performed on these IOSE120pc cells indicated the presence of telomerase.

The advantage of post-crisis cell lines is that they have an infinite life span; therefore, they can more easily be used in studies that require stable transfections. IOSE cells with finite life span are difficult to stably transfect since after transfection and selection they have already gone through many population doublings and are close to senescence. These IOSE 120pc cells

can be used for future experiments that require large numbers of cells with limitless replicative potential.

REFERENCES

Alessi, D. R., Andjelkovic, M., Caudwell, B., Cron, P., Morrice, N., Cohen, P., and Hemmings, B. A. (1996). Mechanism of activation of protein kinase B by insulin and IGF-1. Embo J *15*, 6541-6551.

Alessi, D. R., James, S. R., Downes, C. P., Holmes, A. B., Gaffney, P. R., Reese, C. B., and Cohen, P. (1997). Characterization of a 3-phosphoinositide-dependent protein kinase which phosphorylates and activates protein kinase Balpha. Curr Biol *7*, 261-269.

Arrick, B. A., Grendell, R. L., and Griffin, L. A. (1994). Enhanced translational efficiency of a novel transforming growth factor beta 3 mRNA in human breast cancer cells. Mol Cell Biol *14*, 619-628.

Auersperg, N., Siemens, C. H., and Myrdal, S. E. (1984). Human ovarian surface epithelium in primary culture. In Vitro *20*, 743-755.

Auersperg, N., Wong, A. S., Choi, K. C., Kang, S. K., and Leung, P. C. (2001). Ovarian surface epithelium: biology, endocrinology, and pathology. Endocr Rev *22*, 255-288.

Beeton, C. A., Chance, E. M., Foukas, L. C., and Shepherd, P. R. (2000). Comparison of the kinetic properties of the lipid- and protein-kinase activities of the p110alpha and p110beta catalytic subunits of class-Ia phosphoinositide 3-kinases. Biochem J *350 Pt 2*, 353-359.

Bellacosa, A., de Feo, D., Godwin, A. K., Bell, D. W., Cheng, J. Q., Altomare, D. A., Wan, M., Dubeau, L., Scambia, G., Masciullo, V., and et al. (1995). Molecular alterations of the AKT2 oncogene in ovarian and breast carcinomas. Int J Cancer *64*, 280-285.

Bergers, G., Graninger, P., Braselmann, S., Wrighton, C., and Busslinger, M. (1995). Transcriptional activation of the fra-1 gene by AP-1 is mediated by regulatory sequences in the first intron. Mol Cell Biol *15*, 3748-3758.

Brown, C. Y., Mize, G. J., Pineda, M., George, D. L., and Morris, D. R. (1999). Role of two upstream open reading frames in the translational control of oncogene mdm2. Oncogene *18*, 5631-5637.

Brown, R., Clugston, C., Burns, P., Edlin, A., Vasey, P., Vojtesek, B., and Kaye, S. B. (1993). Increased accumulation of p53 protein in cisplatin-resistant ovarian cell lines. Int J Cancer *55*, 678-684.

Budhram-Mahadeo, V., Morris, P. J., Smith, M. D., Midgley, C. A., Boxer, L. M., and Latchman, D. S. (1999). p53 suppresses the activation of the Bcl-2 promoter by the Brn-3a POU family transcription factor. J Biol Chem *274*, 15237-15244.

Campbell, I. G., Russell, S. E., Choong, D. Y., Montgomery, K. G., Ciavarella, M. L., Hooi, C. S., Cristiano, B. E., Pearson, R. B., and Phillips, W. A. (2004). Mutation of the PIK3CA gene in ovarian and breast cancer. Cancer Res *64*, 7678-7681.

Canadian Cancer Society/National Cancer Institute of Canada: Canadian Cancer Statistics 2005, Toronto, Canada, (2005).

Cantley, L. C. (2002). The phosphoinositide 3-kinase pathway. Science *296*, 1655-1657.

Carpenter, C. L., Auger, K. R., Duckworth, B. C., Hou, W. M., Schaffhausen, B., and Cantley, L. C. (1993). A tightly associated serine/threonine protein kinase regulates phosphoinositide 3-kinase activity. Mol Cell Biol *13*, 1657-1665.

Chehab, N. H., Malikzay, A., Stavridi, E. S., and Halazonetis, T. D. (1999). Phosphorylation of Ser-20 mediates stabilization of human p53 in response to DNA damage. Proc Natl Acad Sci U S A *96*, 13777-13782.

Chen, H. C., and Guan, J. L. (1994). Stimulation of phosphatidylinositol 3'-kinase association with foca adhesion kinase by platelet-derived growth factor. J Biol Chem *269*, 31229-31233.

Chou, J. Y., Avila, J., and Martin, R. G. (1974). Viral DNA synthesis in cells infected by temperature-sensitive mutants of simian virus 40. J Virol *14*, 116-124.

Coffer, P. J., Geijsen, N., M'Rabet, L., Schweizer, R. C., Maikoe, T., Raaijmakers, J. A., Lammers, J. W., and Koenderman, L. (1998). Comparison of the roles of mitogen-activated protein kinase kinase and phosphatidylinositol 3-kinase signal transduction in neutrophil effector function. Biochem J *329 (Pt 1)*, 121-130.

Cowell, J. K. (1990). The nuclear oncoproteins: RB and p53. Semin Cancer Biol *1*, 437-446.

Cristofalo, V. J., Allen, R. G., Pignolo, R. J., Martin, B. G., and Beck, J. C. (1998). Relationship between donor age and the replicative lifespan of human cells in culture: a reevaluation. Proc Natl Acad Sci U S A *95*, 10614-10619.

Cuny, M., Kramar, A., Courjal, F., Johannsdottir, V., Iacopetta, B., Fontaine, H., Grenier, J., Culine, S., and Theillet, C. (2000). Relating genotype and phenotype in breast cancer: an analysis of the prognostic significance of amplification at eight different genes or loci and of p53 mutations. Cancer Res *60*, 1077-1083.

Davies, B. R., Steele, I. A., Edmondson, R. J., Zwolinski, S. A., Saretzki, G., von Zglinicki, T., and O'Hare, M. J. (2003). Immortalisation of human ovarian surface epithelium with telomerase and temperature-sensitive SV40 large T antigen. Exp Cell Res *288*, 390-402.

Deichaite, I., Casson, L. P., Ling, H. P., and Resh, M. D. (1988). In vitro synthesis of pp60v-src: myristylation in a cell-free system. Mol Cell Biol *8*, 4295-4301.

Delcommenne, M., Tan, C., Gray, V., Rue, L., Woodgett, J., and Dedhar, S. (1998). Phosphoinositide-3-OH kinase-dependent regulation of glycogen synthase kinase 3 and protein kinase B/AKT by the integrin-linked kinase. Proc Natl Acad Sci U S A *95*, 11211-11216.

Deligdisch, L., Einstein, A. J., Guera, D., and Gil, J. (1995). Ovarian dysplasia in epithelial inclusion cysts. A morphometric approach using neural networks. Cancer *76*, 1027-1034.

Deng, C., Zhang, P., Harper, J. W., Elledge, S. J., and Leder, P. (1995). Mice lacking p21CIP1/WAF1 undergo normal development, but are defective in G1 checkpoint control. Cell *82*, 675-684.

Dhand, R., Hiles, I., Panayotou, G., Roche, S., Fry, M. J., Gout, I., Totty, N. F., Truong, O., Vicendo, P., Yonezawa, K., and et al. (1994). PI 3-kinase is a dual specificity enzyme: autoregulation by an intrinsic protein-serine kinase activity. Embo J *13*, 522-533.

Dong, L. Q., and Liu, F. (2005). PDK2: the missing piece in the receptor tyrosine kinase signaling pathway puzzle. Am J Physiol Endocrinol Metab *289*, E187-196.

Duga, S., Asselta, R., Del Giacco, L., Malcovati, M., Ronchi, S., Tenchini, M. L., and Simonic, T. (1999). A new exon in the 5' untranslated region of the connexin32 gene. Eur J Biochem *259*, 188-196.

Dunton, C. J. (1997). New options for the treatment of advanced ovarian cancer. Semin Oncol *24*, S5-2-S5-11.

Durbecq, V., Desmed, C., Paesmans, M., Cardoso, F., Di Leo, A., Mano, M., Rouas, G., Leroy, J. Y., Sotiriou, C., Piccart, M., and Larsimont, D. (2004). Correlation between topoisomerase-IIalpha gene amplification and protein expression in HER-2 amplified breast cancer. Int J Oncol *25*, 1473-1479.

el-Deiry, W. S., Kern, S. E., Pietenpol, J. A., Kinzler, K. W., and Vogelstein, B. (1992). Definition of a consensus binding site for p53. Nat Genet *1*, 45-49.

El-Hizawi, S., Lagowski, J. P., Kulesz-Martin, M., and Albor, A. (2002). Induction of gene amplification as a gain-of-function phenotype of mutant p53 proteins. Cancer Res *62*, 3264-3270.

Farmer, G., Colgan, J., Nakatani, Y., Manley, J. L., and Prives, C. (1996). Functional interaction between p53, the TATA-binding protein (TBP), andTBP-associated factors in vivo. Mol Cell Biol *16*, 4295-4304.

Foster, F. M., Traer, C. J., Abraham, S. M., and Fry, M. J. (2003). The phosphoinositide (PI) 3-kinase family. J Cell Sci *116*, 3037-3040.

Foukas, L. C., Beeton, C. A., Jensen, J., Phillips, W. A., and Shepherd, P. R. (2004). Regulation of phosphoinositide 3-kinase by its intrinsic serine kinase activity in vivo. Mol Cell Biol *24*, 966-975.

Foukas, L. C., and Shepherd, P. R. (2004). eIF4E binding protein 1 and H-Ras are novel substrates for the protein kinase activity of class-I phosphoinositide 3-kinase. Biochem Biophys Res Commun *319*, 541-549.

Franke, T. F., Kaplan, D. R., and Cantley, L. C. (1997a). PI3K: downstream AKTion blocks apoptosis. Cell *88*, 435-437.

Franke, T. F., Kaplan, D. R., Cantley, L. C., and Toker, A. (1997b). Direct regulation of the Akt proto-oncogene product by phosphatidylinositol-3,4-bisphosphate. Science *275*, 665-668.

Fraser, M., Leung, B., Jahani-Asl, A., Yan, X., Thompson, W. E., and Tsang, B. K. (2003a). Chemoresistance in human ovarian cancer: the role of apoptotic regulators. Reprod Biol Endocrinol *1*, 66.

Fraser, M., Leung, B. M., Yan, X., Dan, H. C., Cheng, J. Q., and Tsang, B. K. (2003b). p53 is a determinant of X-linked inhibitor of apoptosis protein/Akt-mediated chemoresistance in human ovarian cancer cells. Cancer Res *63*, 7081-7088.

Friedman, P. N., Chen, X., Bargonetti, J., and Prives, C. (1993). The p53 protein is an unusually shaped tetramer that binds directly to DNA. Proc Natl Acad Sci U S A *90*, 3319-3323.

Fruman, D. A., Meyers, R. E., and Cantley, L. C. (1998). Phosphoinositide kinases. Annu Rev Biochem *67*, 481-507.

Gardiner-Garden, M., and Frommer, M. (1987). CpG islands in vertebrate genomes. J Mol Biol *196*, 261-282.

Goncharova, E. A., Ammit, A. J., Irani, C., Carroll, R. G., Eszterhas, A. J., Panettieri, R. A., and Krymskaya, V. P. (2002). PI3K is required for proliferation and migration of human pulmonary vascular smooth muscle cells. Am J Physiol Lung Cell Mol Physiol *283*, L354-363.

Gordon, A. N., Hancock, K. C., Matthews, C. M., Messing, M., Stringer, C. A., Doherty, M. G., and Teneriello, M. (2002). Phase I study of alternating doublets of topotecan/carboplatin and paclitaxel/carboplatin in patients with newly diagnosed, advanced ovarian cancer. Gynecol Oncol *85*, 129-135.

Gu, W., and Roeder, R. G. (1997). Activation of p53 sequence-specific DNA binding by acetylation of the p53 C-terminal domain. Cell *90*, 595-606.

Gu, W., Shi, X. L., and Roeder, R. G. (1997). Synergistic activation of transcription by CBP and p53. Nature *387*, 819-823.

Halazonetis, T. D., and Kandil, A. N. (1993). Conformational shifts propagate from the oligomerization domain of p53 to its tetrameric DNA binding domain and restore DNA binding to select p53 mutants. Embo J *12*, 5057-5064.

Harries, M., and Gore, M. (2002a). Part I: chemotherapy for epithelial ovarian cancer-treatment at first diagnosis. Lancet Oncol *3*, 529-536.

Harries, M., and Gore, M. (2002b). Part II: chemotherapy for epithelial ovarian cancer-treatment of recurrent disease. Lancet Oncol *3*, 537-545.

Hempel, N., Wang, H., LeCluyse, E. L., McManus, M. E., and Negishi, M. (2004). The human sulfotransferase SULT1A1 gene is regulated in a synergistic manner by Sp1 and GA binding protein. Mol Pharmacol *66*, 1690-1701.

Henry, M. K., Lynch, J. T., Eapen, A. K., and Quelle, F. W. (2001). DNA damage-induced cell-cycle arrest of hematopoietic cells is overridden by activation of the PI-3 kinase/Akt signaling pathway. Blood *98*, 834-841.

Hill, M. M., Feng, J., and Hemmings, B. A. (2002). Identification of a plasma membrane Raft-associated PKB Ser473 kinase activity that is distinct from ILK and PDK1. Curr Biol *12*, 1251-1255.

Hoffman, W. H., Biade, S., Zilfou, J. T., Chen, J., and Murphy, M. (2002). Transcriptional repression of the anti-apoptotic survivin gene by wild type p53. J Biol Chem *277*, 3247-3257.

Hu, L., Hofmann, J., Lu, Y., Mills, G. B., and Jaffe, R. B. (2002). Inhibition of phosphatidylinositol 3'-kinase increases efficacy of paclitaxel in in vitro and in vivo ovarian cancer models. Cancer Res *62*, 1087-1092.

Hu, L., Zaloudek, C., Mills, G. B., Gray, J., and Jaffe, R. B. (2000). In vivo and in vitro ovarian carcinoma growth inhibition by a phosphatidylinositol 3-kinase inhibitor (LY294002). Clin Cancer Res *6*, 880-886.

Hutson, R., Ramsdale, J., and Wells, M. (1995). p53 protein expression in putative precursor lesions of epithelial ovarian cancer. Histopathology *27*, 367-371.

Iotsova, V., and Stehelin, D. (1996). Down-regulation of fibronectin gene expression by the p53 tumor suppressor protein. Cell Growth Differ *7*, 629-634.

Iwabuchi, H., Sakamoto, M., Sakunaga, H., Ma, Y. Y., Carcangiu, M. L., Pinkel, D., Yang-Feng, T. L., and Gray, J. W. (1995). Genetic analysis of benign, low-grade, and high-grade ovarian tumors. Cancer Res *55*, 6172-6180.

Jha, K. K., Banga, S., Palejwala, V., and Ozer, H. L. (1998). SV40-Mediated immortalization. Exp Cell Res *245*, 1-7.

Jiang, D., Srinivasan, A., Lozano, G., and Robbins, P. D. (1993). SV40 T antigen abrogates p53-mediated transcriptional activity. Oncogene *8*, 2805-2812.

Johnson, R. A., Ince, T. A., and Scotto, K. W. (2001). Transcriptional repression by p53 through direct binding to a novel DNA element. J Biol Chem *276*, 27716-27720.

Kanaya, T., Kyo, S., Hamada, K., Takakura, M., Kitagawa, Y., Harada, H., and Inoue, M. (2000). Adenoviral expression of p53 represses telomerase activity through down-regulation of human telomerase reverse transcriptase transcription. Clin Cancer Res *6*, 1239-1247.

Kaplan, J. M., Varmus, H. E., and Bishop, J. M. (1990). The src protein contains multiple domains for specific attachment to membranes. Mol Cell Biol *10*, 1000-1009.

Karolchik, D., Baertsch, R., Diekhans, M., Furey, T. S., Hinrichs, A., Lu, Y. T., Roskin, K. M., Schwartz, M., Sugnet, C. W., Thomas, D. J., *et al.* (2003). The UCSC Genome Browser Database. Nucleic Acids Res *31*, 51-54.

Katso, R., Okkenhaug, K., Ahmadi, K., White, S., Timms, J., and Waterfield, M. D. (2001). Cellular function of phosphoinositide 3-kinases: implications for development, homeostasis, and cancer. Annu Rev Cell Dev Biol *17*, 615-675.

Katso, R. M., Manek, S., O'Byrne, K., Playford, M. P., Le Meuth, V., and Ganesan, T. S. (1997). Molecular approaches to diagnosis and management of ovarian cancer. Cancer Metastasis Rev *16*, 81-107.

Kawakami, Y., Nishimoto, H., Kitaura, J., Maeda-Yamamoto, M., Kato, R. M., Littman, D. R., Leitges, M., Rawlings, D. J., and Kawakami, T. (2004). Protein kinase C betaII regulates Akt phosphorylation on Ser-473 in a cell type- and stimulus-specific fashion. J Biol Chem *279*, 47720-47725.

Kihana, T., Tsuda, H., Teshima, S., Okada, S., Matsuura, S., and Hirohashi, S. (1992). High incidence of p53 gene mutation in human ovarian cancer and its association with nuclear accumulation of p53 protein and tumor DNA aneuploidy. Jpn J Cancer Res *83*, 978-984.

Klippel, A., Escobedo, J. A., Hirano, M., and Williams, L. T. (1994). The interaction of small domains between the subunits of phosphatidylinositol 3-kinase determines enzyme activity. Mol Cell Biol *14*, 2675-2685.

Klippel, A., Kavanaugh, W. M., Pot, D., and Williams, L. T. (1997). A specific product of phosphatidylinositol 3-kinase directly activates the protein kinase Akt through its pleckstrin homology domain. Mol Cell Biol *17*, 338-344.

Klippel, A., Reinhard, C., Kavanaugh, W. M., Apell, G., Escobedo, M. A., and Williams, L. T. (1996). Membrane localization of phosphatidylinositol 3-kinase is sufficient to activate multiple signal-transducing kinase pathways. Mol Cell Biol *16*, 4117-4127.

Kochetov, A. V., Ischenko, I. V., Vorobiev, D. G., Kel, A. E., Babenko, V. N., Kisselev, L. L., and Kolchanov, N. A. (1998). Eukaryotic mRNAs encoding abundant and scarce proteins are statistically dissimilar in many structural features. FEBS Lett *440*, 351-355.

Kubbutat, M. H., Jones, S. N., and Vousden, K. H. (1997). Regulation of p53 stability by Mdm2. Nature *387*, 299-303.

Kubicka, S., Kuhnel, F., Zender, L., Rudolph, K. L., Plumpe, J., Manns, M., and Trautwein, C. (1999). p53 represses CAAT enhancer-binding protein (C/EBP)-dependent transcription of the albumin gene. A molecular mechanism involved in viral liver infection with implications for hepatocarcinogenesis. J Biol Chem *274*, 32137-32144.

Kupryjanczyk, J., Thor, A. D., Beauchamp, R., Merritt, V., Edgerton, S. M., Bell, D. A., and Yandell, D. W. (1993). p53 gene mutations and protein accumulation in human ovarian cancer. Proc Natl Acad Sci U S A *90*, 4961-4965.

Lam, K., Carpenter, C. L., Ruderman, N. B., Friel, J. C., and Kelly, K. L. (1994). The phosphatidylinositol 3-kinase serine kinase phosphorylates IRS-1. Stimulation by insulin and inhibition by Wortmannin. J Biol Chem *269*, 20648-20652.

Lane, D. P., and Crawford, L. V. (1979). T antigen is bound to a host protein in SV40-transformed cells. Nature *278*, 261-263.

Lee, K. C., Crowe, A. J., and Barton, M. C. (1999). p53-mediated repression of alpha-fetoprotein gene expression by specific DNA binding. Mol Cell Biol *19*, 1279-1288.

Lemmon, M. A., Ferguson, K. M., and Schlessinger, J. (1996). PH domains: diverse sequences with a common fold recruit signaling molecules to the cell surface. Cell *85*, 621-624.

Lengauer, C., Kinzler, K. W., and Vogelstein, B. (1998). Genetic instabilities in human cancers. Nature *396*, 643-649.

Levine, D. A., Bogomolniy, F., Yee, C. J., Lash, A., Barakat, R. R., Borgen, P. I., and Boyd, J. (2005). Frequent mutation of the PIK3CA gene in ovarian and breast cancers. Clin Cancer Res *11*, 2875-2878.

Liang, S. H., and Clarke, M. F. (1999a). A bipartite nuclear localization signal is required for p53 nuclear import regulated by a carboxyl-terminal domain. J Biol Chem *274*, 32699-32703.

Liang, S. H., and Clarke, M. F. (1999b). The nuclear import of p53 is determined by the presence of a basic domain and its relative position to the nuclear localization signal. Oncogene *18*, 2163-2166.

Linzer, D. I., and Levine, A. J. (1979). Characterization of a 54K dalton cellular SV40 tumor antigen present in SV40-transformed cells and uninfected embryonal carcinoma cells. Cell *17*, 43-52.

Linzer, D. I., Maltzman, W., and Levine, A. J. (1979). The SV40 A gene product is required for the production of a 54,000 MW cellular tumor antigen. Virology *98*, 308-318.

Liu, A. X., Testa, J. R., Hamilton, T. C., Jove, R., Nicosia, S. V., and Cheng, J. Q. (1998). AKT2, a member of the protein kinase B family, is activated by growth factors, v-Ha-ras, and v-src through phosphatidylinositol 3-kinase in human ovarian epithelial cancer cells. Cancer Res *58*, 2973-2977.

Livingstone, L. R., White, A., Sprouse, J., Livanos, E., Jacks, T., and Tlsty, T. D. (1992). Altered cell cycle arrest and gene amplification potential accompany loss of wild-type p53. Cell *70*, 923-935.

Luo, J., Manning, B. D., and Cantley, L. C. (2003). Targeting the PI3K-Akt pathway in human cancer: rationale and promise. Cancer Cell *4*, 257-262.

Maehama, T., and Dixon, J. E. (1998). The tumor suppressor, PTEN/MMAC1, dephosphorylates the lipid second messenger, phosphatidylinositol 3,4,5-trisphosphate. J Biol Chem *273*, 13375-13378.

Maines-Bandiera, S. L., Kruk, P. A., and Auersperg, N. (1992). Simian virus 40-transformed human ovarian surface epithelial cells escape normal growth controls but retain morphogenetic responses to extracellular matrix. Am J Obstet Gynecol *167*, 729-735.

Marks, J. R., Davidoff, A. M., Kerns, B. J., Humphrey, P. A., Pence, J. C., Dodge, R. K., Clarke-Pearson, D. L., Iglehart, J. D., Bast, R. C., Jr., and Berchuck, A. (1991). Overexpression and mutation of p53 in epithelial ovarian cancer. Cancer Res *51*, 2979-2984.

May, P., and May, E. (1999). Twenty years of p53 research: structural and functional aspects of the p53 protein. Oncogene *18*, 7621-7636.

Mayo, L. D., and Donner, D. B. (2001). A phosphatidylinositol 3-kinase/Akt pathway promotes translocation of Mdm2 from the cytoplasm to the nucleus. Proc Natl Acad Sci U S A *98*, 11598-11603.

McLure, K. G., and Lee, P. W. (1998). How p53 binds DNA as a tetramer. Embo J *17*, 3342-3350.

Meric, F., and Hunt, K. K. (2002). Translation initiation in cancer: a novel target for therapy. Mol Cancer Ther *1*, 971-979.

Molinero, L. L., Fuertes, M. B., Girart, M. V., Fainboim, L., Rabinovich, G. A., Costas, M. A., and Zwirner, N. W. (2004). NF-kappa B regulates expression of the MHC class I-related chain A gene in activated T lymphocytes. J Immunol *173*, 5583-5590.

Moll, U. M., Riou, G., and Levine, A. J. (1992). Two distinct mechanisms alter p53 in breast cancer: mutation and nuclear exclusion. Proc Natl Acad Sci U S A *89*, 7262-7266.

Nakamura, M., Katabuchi, H., Ohba, T., Fukumatsu, Y., and Okamura, H. (1994). Isolation, growth and characteristics of human ovarian surface epithelium. Virchows Arch *424*, 59-67.

Obata, K., Morland, S. J., Watson, R. H., Hitchcock, A., Chenevix-Trench, G., Thomas, E. J., and Campbell, I. G. (1998). Frequent PTEN/MMAC mutations in endometrioid but not serous or mucinous epithelial ovarian tumors. Cancer Res *58*, 2095-2097.

O'Brate, A., and Giannakakou, P. (2003). The importance of p53 location: nuclear or cytoplasmic zip code? Drug Resist Updat *6*, 313-322.

O'Connor, P. M., Jackman, J., Bae, I., Myers, T. G., Fan, S., Mutoh, M., Scudiero, D. A., Monks, A., Sausville, E. A., Weinstein, J. N., *et al.* (1997). Characterization of the p53 tumor suppressor pathway in cell lines of the National Cancer Institute anticancer drug screen and correlations with the growth-inhibitory potency of 123 anticancer agents. Cancer Res *57*, 4285-4300.

O'Hare, M. J., Bond, J., Clarke, C., Takeuchi, Y., Atherton, A. J., Berry, C., Moody, J., Silver, A. R., Davies, D. C., Alsop, A. E., *et al.* (2001). Conditional immortalization of freshly isolated human mammary fibroblasts and endothelial cells. Proc Natl Acad Sci U S A *98*, 646-651.

Ohlsson, C., Kley, N., Werner, H., and LeRoith, D. (1998). p53 regulates insulin-like growth factor-I (IGF-I) receptor expression and IGF-I-induced tyrosine phosphorylation in an osteosarcoma cell line: interaction between p53 and Sp1. Endocrinology *139*, 1101-1107.

Ori, A., Zauberman, A., Doitsh, G., Paran, N., Oren, M., and Shaul, Y. (1998). p53 binds and represses the HBV enhancer: an adjacent enhancer element can reverse the transcription effect of p53. Embo J *17*, 544-553.

Parker, P. J., and Murray-Rust, J. (2004). PKC at a glance. J Cell Sci *117*, 131-132.

Parmar, M. K., Ledermann, J. A., Colombo, N., du Bois, A., Delaloye, J. F., Kristensen, G. B., Wheeler, S., Swart, A. M., Qian, W., Torri, V., *et al.* (2003). Paclitaxel plus platinum-based chemotherapy versus conventional platinum-based chemotherapy in women with relapsed ovarian cancer: the ICON4/AGO-OVAR-2.2 trial. Lancet *361*, 2099-2106.

Pipas, J. M., and Levine, A. J. (2001). Role of T antigen interactions with p53 in tumorigenesis. Semin Cancer Biol *11*, 23-30.

Powell, B., Soong, R., Iacopetta, B., Seshadri, R., and Smith, D. R. (2000). Prognostic significance of mutations to different structural and functional regions of the p53 gene in breast cancer. Clin Cancer Res *6*, 443-451.

Rane, M. J., Coxon, P. Y., Powell, D. W., Webster, R., Klein, J. B., Pierce, W., Ping, P., and McLeish, K. R. (2001). p38 Kinase-dependent MAPKAPK-2 activation functions as 3-phosphoinositide-dependent kinase-2 for Akt in human neutrophils. J Biol Chem *276*, 3517-3523.

Reihsaus, E., Kohler, M., Kraiss, S., Oren, M., and Montenarh, M. (1990). Regulation of the level of the oncoprotein p53 in non-transformed and transformed cells. Oncogene *5*, 137-145.

Rodriguez, M. S., Desterro, J. M., Lain, S., Midgley, C. A., Lane, D. P., and Hay, R. T. (1999). SUMO-1 modification activates the transcriptional response of p53. Embo J *18*, 6455-6461.

Rodriguez-Viciana, P., Marte, B. M., Warne, P. H., and Downward, J. (1996a). Phosphatidylinositol 3' kinase: one of the effectors of Ras. Philos Trans R Soc Lond B Biol Sci *351*, 225-231; discussion 231-222.

Rodriguez-Viciana, P., Warne, P. H., Vanhaesebroeck, B., Waterfield, M. D., and Downward, J. (1996b). Activation of phosphoinositide 3-kinase by interaction with Ras and by point mutation. Embo J *15*, 2442-2451.

Rondinone, C. M., Carvalho, E., Rahn, T., Manganiello, V. C., Degerman, E., and Smith, U. P. (2000). Phosphorylation of PDE3B by phosphatidylinositol 3-kinase associated with the insulin receptor. J Biol Chem *275*, 10093-10098.

Roth, J., Dobbelstein, M., Freedman, D. A., Shenk, T., and Levine, A. J. (1998). Nucleo-cytoplasmic shuttling of the hdm2 oncoprotein regulates the levels of the p53 protein via a pathway used by the human immunodeficiency virus rev protein. Embo J *17*, 554-564.

Sabbatini, P., and McCormick, F. (1999). Phosphoinositide 3-OH kinase (PI3K) and PKB/Akt delay the onset of p53-mediated, transcriptionally dependent apoptosis. J Biol Chem *274*, 24263-24269.

Samuels, Y., and Velculescu, V. E. (2004). Oncogenic mutations of PIK3CA in human cancers. Cell Cycle *3*, 1221-1224.

Samuels, Y., Wang, Z., Bardelli, A., Silliman, N., Ptak, J., Szabo, S., Yan, H., Gazdar, A., Powell, S. M., Riggins, G. J., *et al.* (2004). High frequency of mutations of the PIK3CA gene in human cancers. Science *304*, 554.

Savitsky, K., Platzer, M., Uziel, T., Gilad, S., Sartiel, A., Rosenthal, A., Elroy-Stein, O., Shiloh, Y., and Rotman, G. (1997). Ataxia-telangiectasia: structural diversity of untranslated sequences suggests complex post-transcriptional regulation of ATM gene expression. Nucleic Acids Res *25*, 1678-1684.

Schlosshauer, P. W., Cohen, C. J., Penault-Llorca, F., Miranda, C. R., Bignon, Y. J., Dauplat, J., and Deligdisch, L. (2003). Prophylactic oophorectomy: a morphologic and immunohistochemical study. Cancer *98*, 2599-2606.

Scholzen, T., and Gerdes, J. (2000). The Ki-67 protein: from the known and the unknown. J Cell Physiol *182*, 311-322.

Schwartz, M. A., and Assoian, R. K. (2001). Integrins and cell proliferation: regulation of cyclin-dependent kinases via cytoplasmic signaling pathways. J Cell Sci *114*, 2553-2560.

Scully, R. E. (1995a). Early de novo ovarian cancer and cancer developing in benign ovarian lesions. Int J Gynaecol Obstet *49 Suppl*, S9-15.

Scully, R. E. (1995b). Pathology of ovarian cancer precursors. J Cell Biochem Suppl *23*, 208-218.

Seto, E., Usheva, A., Zambetti, G. P., Momand, J., Horikoshi, N., Weinmann, R., Levine, A. J., and Shenk, T. (1992). Wild-type p53 binds to the TATA-binding protein and represses transcription. Proc Natl Acad Sci U S A *89*, 12028-12032.

Shay, J. W., Wright, W. E., and Werbin, H. (1991). Defining the molecular mechanisms of human cell immortalization. Biochim Biophys Acta *1072*, 1-7.

Shayesteh, L., Lu, Y., Kuo, W. L., Baldocchi, R., Godfrey, T., Collins, C., Pinkel, D., Powell, B., Mills, G. B., and Gray, J. W. (1999). PIK3CA is implicated as an oncogene in ovarian cancer. Nat Genet *21*, 99-102.

Shieh, S. Y., Taya, Y., and Prives, C. (1999). DNA damage-inducible phosphorylation of p53 at N-terminal sites including a novel site, Ser20, requires tetramerization. Embo J *18*, 1815-1823.

Shultzaberger, R. K., and Schneider, T. D. (1999). Using sequence logos and information analysis of Lrp DNA binding sites to investigate discrepanciesbetween natural selection and SELEX. Nucleic Acids Res *27*, 882-887.

Siemens, C. H., and Auersperg, N. (1988). Serial propagation of human ovarian surface epithelium in tissue culture. J Cell Physiol *134*, 347-356.

Singh, B., Reddy, P. G., Goberdhan, A., Walsh, C., Dao, S., Ngai, I., Chou, T. C., P, O. C., Levine, A. J., Rao, P. H., and Stoffel, A. (2002). p53 regulates cell survival by inhibiting PIK3CA in squamous cell carcinomas. Genes Dev *16*, 984-993.

Sladek, T. L., Laffin, J., Lehman, J. M., and Jacobberger, J. W. (2000). A subset of cells expressing SV40 large T antigen contain elevated p53 levels and have an altered cell cycle phenotype. Cell Prolif *33*, 115-125.

Sobczak, K., and Krzyzosiak, W. J. (2002). Structural determinants of BRCA1 translational regulation. J Biol Chem *277*, 17349-17358.

Stambolic, V., MacPherson, D., Sas, D., Lin, Y., Snow, B., Jang, Y., Benchimol, S., and Mak, T. W. (2001). Regulation of PTEN transcription by p53. Mol Cell *8*, 317-325.

Stamps, A. C., Davies, S. C., Burman, J., and O'Hare, M. J. (1994). Analysis of proviral integration in human mammary epithelial cell lines immortalized by retroviral infection with a temperature-sensitive SV40 T-antigen construct. Int J Cancer *57*, 865-874.

Stokoe, D., Stephens, L. R., Copeland, T., Gaffney, P. R., Reese, C. B., Painter, G. F., Holmes, A. B., McCormick, F., and Hawkins, P. T. (1997). Dual role of phosphatidylinositol-3,4,5-trisphosphate in the activation of protein kinase B. Science *277*, 567-570.

Stommel, J. M., Marchenko, N. D., Jimenez, G. S., Moll, U. M., Hope, T. J., and Wahl, G. M. (1999). A leucine-rich nuclear export signal in the p53 tetramerization domain: regulation of subcellular localization and p53 activity by NES masking. Embo J *18*, 1660-1672.

Subbaramaiah, K., Altorki, N., Chung, W. J., Mestre, J. R., Sampat, A., and Dannenberg, A. J. (1999). Inhibition of cyclooxygenase-2 gene expression by p53. J Biol Chem *274*, 10911-10915.

Sun, Y., Wenger, L., Rutter, J. L., Brinckerhoff, C. E., and Cheung, H. S. (1999). p53 down-regulates human matrix metalloproteinase-1 (Collagenase-1) gene expression. J Biol Chem *274*, 11535-11540.

Suzuki, S., Moore, D. H., 2nd, Ginzinger, D. G., Godfrey, T. E., Barclay, J., Powell, B., Pinkel, D., Zaloudek, C., Lu, K., Mills, G., *et al.* (2000). An approach to analysis of large-scale correlations between genome changes and clinical endpoints in ovarian cancer. Cancer Res *60*, 5382-5385.

Takahashi, K., Sumimoto, H., Suzuki, K., and Ono, T. (1993). Protein synthesis-dependent cytoplasmic translocation of p53 protein after serum stimulation of growth-arrested MCF-7 cells. Mol Carcinog *8*, 58-66.

Tiemann, F., Zerrahn, J., and Deppert, W. (1995). Cooperation of simian virus 40 large and small T antigens in metabolic stabilization of tumor suppressor p53 during cellular transformation. J Virol *69*, 6115-6121.

Toker, A., and Cantley, L. C. (1997). Signalling through the lipid products of phosphoinositide-3-OH kinase. Nature *387*, 673-676.

Truant, R., Xiao, H., Ingles, C. J., and Greenblatt, J. (1993). Direct interaction between the transcriptional activation domain of human p53 and the TATA box-binding protein. J Biol Chem *268*, 2284-2287.

Tsao, S. W., Mok, S. C., Fey, E. G., Fletcher, J. A., Wan, T. S., Chew, E. C., Muto, M. G., Knapp, R. C., and Berkowitz, R. S. (1995). Characterization of human ovarian surface epithelial cells immortalized by human papilloma viral oncogenes (HPV-E6E7 ORFs). Exp Cell Res *218*, 499-507.

Unger, T., Juven-Gershon, T., Moallem, E., Berger, M., Vogt Sionov, R., Lozano, G., Oren, M., and Haupt, Y. (1999). Critical role for Ser20 of human p53 in the negative regulation of p53 by Mdm2. Embo J *18*, 1805-1814.

van Dijck, P., Schoonjans, K., Sassone-Corsi, P., Auwerx, J., and Verhoeven, G. (1993). A Fos-Jun element in the first intron of an alpha 2u-globulin gene. Mol Cell Biochem *125*, 127-136.

Vanhaesebroeck, B., and Alessi, D. R. (2000). The PI3K-PDK1 connection: more than just a road to PKB. Biochem J *346 Pt 3*, 561-576.

Vanhaesebroeck, B., Leevers, S. J., Ahmadi, K., Timms, J., Katso, R., Driscoll, P. C., Woscholski, R., Parker, P. J., and Waterfield, M. D. (2001). Synthesis and function of 3-phosphorylated inositol lipids. Annu Rev Biochem *70*, 535-602.

Vanhaesebroeck, B., Leevers, S. J., Panayotou, G., and Waterfield, M. D. (1997). Phosphoinositide 3-kinases: a conserved family of signal transducers. Trends Biochem Sci *22*, 267-272.

Viniegra, J. G., Martinez, N., Modirassari, P., Losa, J. H., Parada Cobo, C., Lobo, V. J., Luquero, C. I., Alvarez-Vallina, L., Ramon y Cajal, S., Rojas, J. M., and Sanchez-Prieto, R. (2005). Full activation of PKB/Akt in response to insulin or ionizing radiation is mediated through ATM. J Biol Chem *280*, 4029-4036.

Vivanco, I., and Sawyers, C. L. (2002). The phosphatidylinositol 3-Kinase AKT pathway in human cancer. Nat Rev Cancer *2*, 489-501.

Walker, E. H., Perisic, O., Ried, C., Stephens, L., and Williams, R. L. (1999). Structural insights into phosphoinositide 3-kinase catalysis and signalling. Nature *402*, 313-320.

Wan, T. S., Chan, L. C., Ngan, H. Y., and Tsao, S. W. (1997). t(High) frequency of telomeric associations in human ovarian surface epithelial cells transformed by human papilloma viral oncogenes. Cancer Genet Cytogenet *95*, 166-172.

Wang, Y., Helland, A., Holm, R., Kristensen, G. B., and Borresen-Dale, A. L. (2005). PIK3CA mutations in advanced ovarian carcinomas. Hum Mutat *25*, 322.

Wasserman, W. W., and Sandelin, A. (2004). Applied bioinformatics for the identification of regulatory elements. Nat Rev Genet *5*, 276-287.

Wong, A. S., and Auersperg, N. (2003). Ovarian surface epithelium: family history and early events in ovarian cancer. Reprod Biol Endocrinol *1*, 70.

Woods Ignatoski, K. M., Livant, D. L., Markwart, S., Grewal, N. K., and Ethier, S. P. (2003). The role of phosphatidylinositol 3'-kinase and its downstream signals in erbB-2-mediated transformation. Mol Cancer Res *1*, 551-560.

Wright, W. E., Pereira-Smith, O. M., and Shay, J. W. (1989). Reversible cellular senescence: implications for immortalization of normal human diploid fibroblasts. Mol Cell Biol *9*, 3088-3092.

Wu, S., and Barger, S. W. (2004). Induction of Serine Racemase by Inflammatory Stimuli Is Dependent on AP-1. Ann N Y Acad Sci *1035*, 133-146.

Wymann, M. P., and Pirola, L. (1998). Structure and function of phosphoinositide 3-kinases. Biochim Biophys Acta *1436*, 127-150.

Xu, C. F., Chambers, J. A., Nicolai, H., Brown, M. A., Hujeirat, Y., Mohammed, S., Hodgson, S., Kelsell, D. P., Spurr, N. K., Bishop, D. T., and Solomon, E. (1997). Mutations and alternative splicing of the BRCA1 gene in UK breast/ovarian cancer families. Genes Chromosomes Cancer *18*, 102-110.

Yaginuma, Y., and Westphal, H. (1992). Abnormal structure and expression of the p53 gene in human ovarian carcinoma cell lines. Cancer Res *52*, 4196-4199.

Yin, Y., Tainsky, M. A., Bischoff, F. Z., Strong, L. C., and Wahl, G. M. (1992). Wild-type p53 restores cell cycle control and inhibits gene amplification in cells with mutant p53 alleles. Cell *70*, 937-948.

Yuan, Z. Q., Feldman, R. I., Sussman, G. E., Coppola, D., Nicosia, S. V., and Cheng, J. Q. (2003). AKT2 inhibition of cisplatin-induced JNK/p38 and Bax activation by phosphorylation of ASK1: implication of AKT2 in chemoresistance. J Biol Chem *278*, 23432-23440.

Yun, J., Chae, H. D., Choy, H. E., Chung, J., Yoo, H. S., Han, M. H., and Shin, D. Y. (1999). p53 negatively regulates cdc2 transcription via the CCAAT-binding NF-Y transcription factor. J Biol Chem *274*, 29677-29682.

Zhang, W., and Liu, H. T. (2002). MAPK signal pathways in the regulation of cell proliferation in mammalian cells. Cell Res *12*, 9-18.

Zhang, Y., and Xiong, Y. (2001). A p53 amino-terminal nuclear export signal inhibited by DNA damage-induced phosphorylation. Science *292*, 1910-1915.

Zhao, J. J., Gjoerup, O. V., Subramanian, R. R., Cheng, Y., Chen, W., Roberts, T. M., and Hahn, W. C. (2003). Human mammary epithelial cell transformation through the activation of phosphatidylinositol 3-kinase. Cancer Cell *3*, 483-495.